Copper Bis(oxazoline)-Catalyzed Enantioselective Alkynylation of Quinolones

A Major Qualifying Project Proposal submitted to the Faculty of Worcester Polytechnic Institute in partial fulfillment of the requirements for the degree of Bachelor of Science

By Sean Burns & Margaret Richins

Date:

April 28, 2022

Report Submitted to:

Professor Anita E. Mattson

Worcester Polytechnic Institute

Abstract

Nitrogen heterocycles continue to be highly regarded as valuable bioactive molecules and important precursors to pharmaceuticals. A novel N-heterocycle functionalization method has been developed through the enantioselective alkynylation of substituted quinolones. This synthesis utilizes copper (I) bis(oxazoline) catalysis to selectively add phenylacetylene derivatives on the 2-position of 4-quinolones. The generated stereocenter is created with high levels of enantiocontrol, up to 96% e.e.. The mechanism of the reaction was investigated through a Linear Free Energy Relationship study to probe the effects of various functional groups on both the phenylacetylene and the aromatic ring of the quinolone. Hammett plots suggested an accumulation of negative charge at the phenylacetylene in the enantio-determining step. We hypothesize that electron-withdrawing groups, which demonstrated the highest level of enantioselectivity, stabilize the transition state through resonance and inductive effects.

Table of Contents

List of Figures

Introduction

Nitrogen Heterocycles

Nitrogen-containing heterocycles are common motifs in many natural products and pharmaceuticals, including vitamins, nucleic acids, and antibiotics.[1] Heterocycles comprise more than 85% of all biologically active molecules, and of those, nitrogen heterocycles are the most common.[2] As of 2014, 59% of all unique small-molecule pharmaceuticals on the market contained a nitrogen heterocycle.[3] Nitrogen heterocycles exhibit a wide range of biological activities like anticancer, anti-HIV, antimalaria, and more, which explains why organic chemists view these scaffolds as attractive targets for drug discovery.[1,2] The stability and efficiency of these compounds in the human body can be attributed to the ability of the nitrogen to either accept or donate a proton while also establishing weak intermolecular interactions such as hydrogen bonding, π-stacking, Van der Waals forces, and dipole-dipole interactions.[1] These properties allow nitrogen heterocycles to constructively interact with enzymes and cellular receptors which results in the enhanced biological activity of these compounds. Some examples of *N*-heterocyclic pharmaceuticals can be seen in Figure 1.

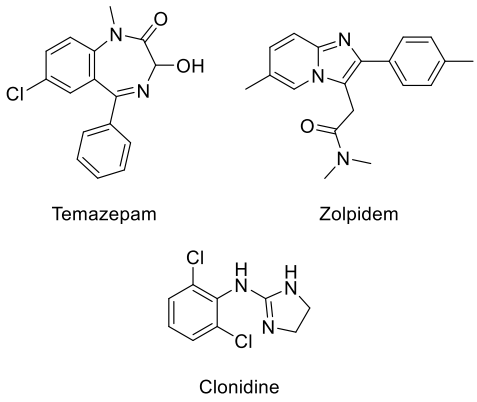

***Figure 1**: Examples of N-heterocyclic Pharmaceuticals*

Quinolones in Medicinal Chemistry

Quinolones are nitrogen-containing heterocycles with various biological activities such as antibacterial, antifungal, antitumor, antiviral, and antiparasitic.[4] Quinolones are commonly found in biologically active natural products, as well as synthesized pharmaceutical compounds, seen as attractive molecules in medicinal chemistry as they have "high bioavailability, relative low toxicity and favorable pharmacokinetics".[5] Current research on quinolones focuses on the synthesis of various quinolone derivatives with enhanced activity in different biological targets. Though these quinolone derivatives have a lot of biological potential, there are limited methods to synthesize them under mild reaction conditions.[6]

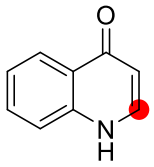

***Figure 2**: 4-Quinolone Structure*

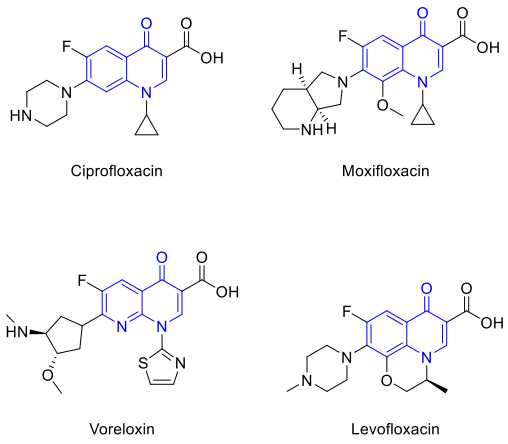

***Figure 3**: Examples of 4-Quinolone-Containing Pharmaceuticals*

This paper discusses the enantioselective alkynylation of the 2-position of 4-quinolones (Figure 2), which has only just been reported in the literature this year.[7] Quinolones are the backbone of many antibiotics (Figure 3), and reactions with these compounds to create biologically active derivatives have been a growing field in organic chemistry.[8] These 4-quinolones have also been found to act as an inhibitor to multiple enzymes, specifically topoisomerase I, topoisomerase II, farnesyltransferase, and casein kinase 2.[9] Some existing non-asymmetric reactions involving substitution at this 2-position include Sonogashira Coupling, Ullmann Coupling, Decarboxylative Coupling, C-H bond functionalization, and Lewis-Acid-Catalyzed Synthesis. Asymmetric syntheses of 2-substituted 4-quinolones have also been reported (Figure 4). The Shintani method achieved high enantioselectivity with the addition of a phenyl group at the 2-position of the quinolone but presented a limited substrate scope.[10] The Guo & Harutyunyan method boasts a large substrate scope but is limited to alkyl groups at the R' position.[11] The Cheng method requires high catalyst loading.[12] Our novel method aims to expand on these asymmetric methods through insertion of a substituted alkyne utilizing a commercially available ligand, ultimately leading to greater synthetic potential in the molecule.

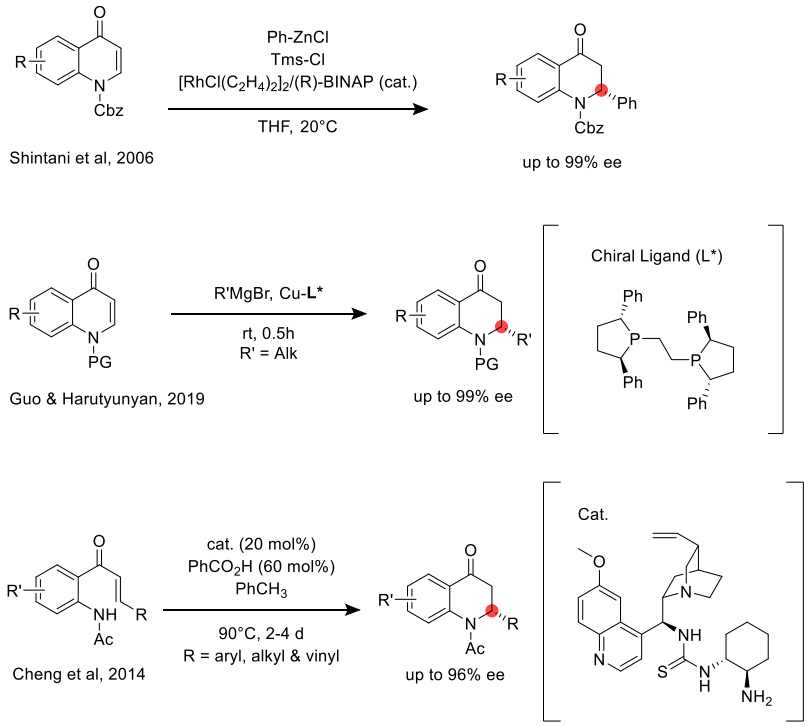

***Figure 4**: Existing Asymmetric Functionalization Methods of 4-Quinolones*

Copper (I) Bis(oxazoline) Catalysis

Asymmetric catalysis utilizes a chiral catalyst, often in low molar quantities, to direct a reaction in favor of one enantiomer product versus another. A common method of asymmetric catalysis involves using chiral Lewis acid catalysts with substrates that can chelate through five or six-membered rings, such as cycloadditions, conjugate additions, and aldol additions.[13] When subjected to these chiral Lewis acid catalysts, these types of reactions can experience rate acceleration and greater enantioselectivity. Bis(oxazoline) ligands, abbreviated BOX, are commonly used bidentate ligands that can coordinate with a metal, such as manganese, zinc, iron, cobalt, nickel, and copper (Figure 5).[14] BOX ligands are commonly coordinated with Cu(I), as copper is an effective Lewis acidic center and forms a relatively stable ligand-metal complex compared to other metals.[13] These Cu(I) bis(oxazoline) complexes are typically formed *in situ* by reacting the chiral BOX ligand with the appropriate copper salt prior to catalysis.[15] A drawback to using these copper bis(oxazoline) catalyst systems is that they are in the homogeneous phase, so it is difficult to isolate and recycle these costly and/or time-consuming complexes after the reaction.[14]

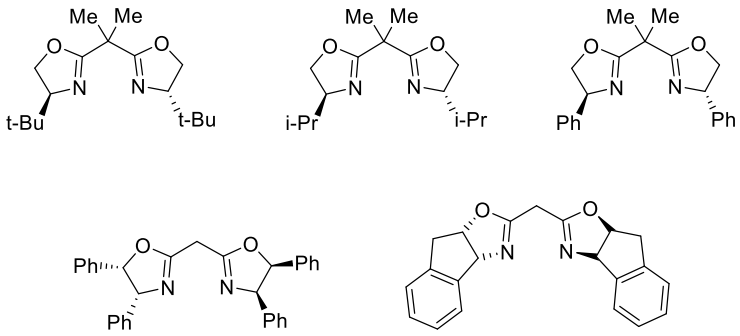

***Figure 5**: Common BOX Ligands*

The choice of a counterion for the chiral BOX complex, as well as the choice of solvent, can have a significant effect on the enantioselectivity of a reaction, so researchers should determine the best conditions for their specific reaction before moving forward with their investigation. The counterion helps to modulate the catalytic activity and "can affect the nature of the reaction mechanism, leading to undesired side reactions that are non-asymmetric".[15] When correctly optimized, copper (I) bis(oxazoline) catalysts can afford products in up to 99% e.e..

Linear Free Energy Relationships & Hammett Plots

In many reactions, the reactivity/reaction mechanism of a molecule can change as substituents with different electronic profiles are introduced. Linear free energy relationship (LFER) studies investigate the bond formation and bond breakage occurring at the transition state of a reaction through a specified chemical or physical property. LFER studies typically compare the change in rate or equilibrium constants of a substituted reaction with those of a reference reaction.[16]

The most common LFER study is the Hammett plot, which is characterized by the Hammett equation:

$$log\frac{k_i}{k_0} = \rho\sigma$$

Hammett utilized the dissociation of benzoic acid as the reference reaction to determine a scale of substituent constants (σ) and demonstrate the ability of different substituents to affect the acidity of benzoic acid.[16] Electron-donating substituents have a σ value less than zero, electron-withdrawing substituents have a σ value greater than zero, and hydrogen is used as the reference standard with a σ value of exactly zero. In the Hammett equation, k_i is the rate/equilibrium constant of the substituted reaction, k_0 is the rate/equilibrium constant of benzoic acid, σ is the substituent constant of the substituent being investigated, and ρ is the slope of the line generated by the Hammett plot, also called the proportionality constant. The values of ρ can be used to determine a buildup of charge, which can uncover information about a reaction mechanism (Figure 6).[17] The magnitude of ρ also reflects how sensitive the reaction is to changes in substituents compared to the reference reaction. Larger ρ values correlate to a greater reaction sensitivity in response to change in reagent structure. Sometimes, a reaction is not significantly impacted by the electronics of substituents. In this case, a Hammett plot would have a very low R^2 value for the trendline which shows low or no correlation between the data points.

Interpretations of Hammett Plot ρ-values [17]	
ρ > 1	Significant negative charge buildup
0 < ρ < 1	Weak negative charge buildup *or* loss of positive charge
ρ = 0	No charge buildup or loss
-1 < ρ < 0	Weak positive charge buildup *or* loss of negative charge
-1 < ρ	Significant positive charge buildup

***Figure 6**: Interpretations of Hammett Plot ρ-values*

Enantiomeric ratio (e.r.) can also be utilized in the Hammett equation if dealing with an enantioselective reaction, replacing the equilibrium constant as the property under examination. The enantiomeric ratio is the ratio of one enantiomer to its counterpart; e.r. can be thought of as the rate of the reaction producing one enantiomer compared to the rate of the reaction producing the opposing enantiomer.

If a reaction is fundamentally different from the dissociation of benzoic acid, chemists have developed alternative reference reactions with their own sets of substituent constants to better describe how substituents behave under different conditions. Examples of these include the Brown & Okamoto constants and Jaffe's constants.[18] In this paper we will utilize both the Hammett and the Brown & Okamoto references, which are shown in Figure 7 below.

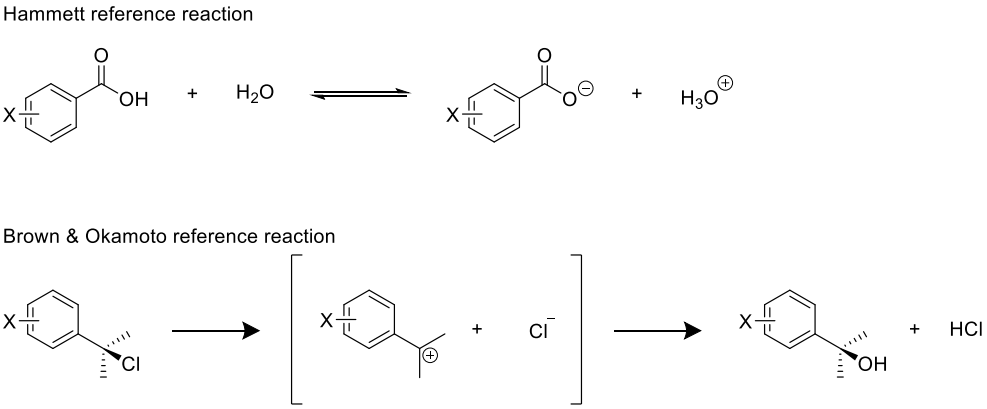

***Figure 7**: Hammett and Brown & Okamoto Reference Reactions*

Prior Work

The Mattson group has been interested in anion-binding catalysis for several years. They initially found success with silanediols as hydrogen-bond donors for the functionalization of nitrogen-based heterocycles in 2018. The first reported instance of a silanediol and copper system allowed for an enhanced Lewis acid catalyst capable of enantioselectivity.[19] Mattson demonstrated high yield and high enantiomeric excess in the addition of indoles to alkylidene malonates, discovering a useful reaction along the way. This work was continued in a comparison of a silanediol's catalytic ability to that of thioureas and squaramides, other anion-binding catalysts. It not only accomplished enantioselective synthesis using quinoline and chromenone bodies but uncovered valuable information about these catalyst systems that expanded a relatively new field.[20] Interest in thiourea enantioselective catalysis was continued into 2020, where Mattson published work on S-H insertions of sulfoxonium ylides, again demonstrating high yields and high enantiomeric excess.[21]

In 2019, a different catalyst system gained the attention of the group: copper bis(oxazoline) complexes. Returning to functionalization of chromenone bodies as the studied reaction, the group explored stereocontrol with a methodology that could see use in the synthesis of biologically relevant tetrahydroxanthones.[22] Further research was carried out on the alkynylation of chromenones to create tertiary ether stereocenters, again with applications in natural product synthesis.[23] With success using the copper-bis(oxazoline) system, Mattson branched off onto quinolones, which is the basis of this project. Recently, while our own investigations were underway, the Harutyunyan group reported the copper-catalyzed alkynylation of quinolones (using a different ligand than ours) and showed the possibility for enantioselective applications (Figure 8).[7] While the timing of this publication is unfortunate for the Mattson group, our project still holds valuable discoveries that were not addressed in the Harutyunyan paper and more comprehensively addresses the stereocontrol aspect of the reaction.

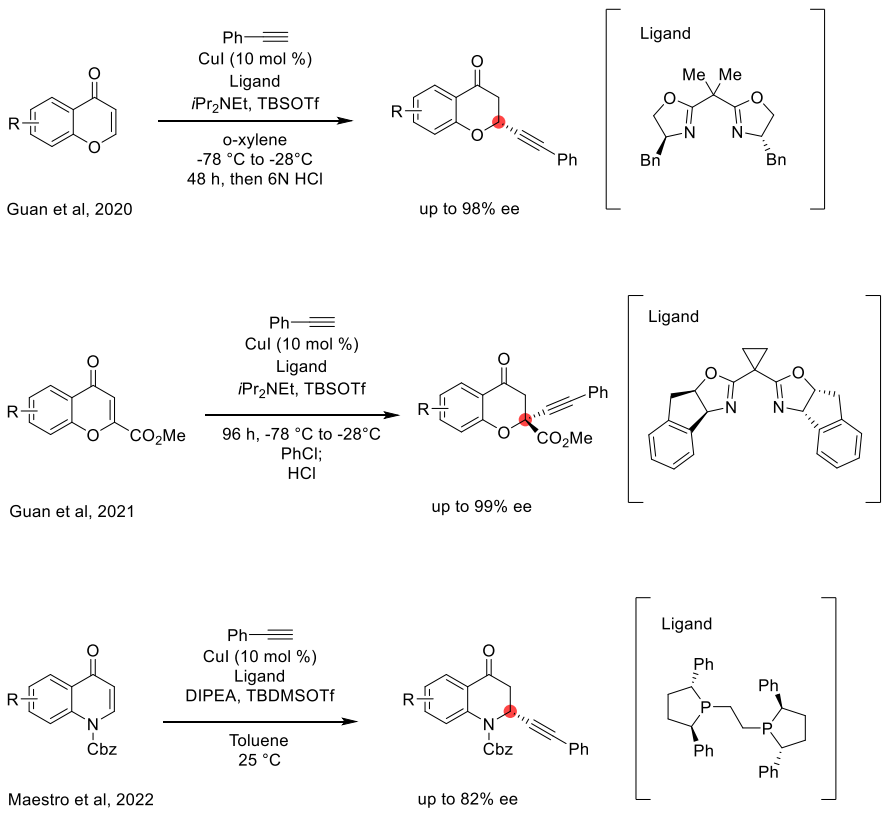

***Figure 8**: Mattson Group Previous Work & Related Reactions*

Project Goal

The goal of this Major Qualifying Project (MQP) was to investigate the reaction mechanism of our novel asymmetric alkynylation method through a Linear Free Energy Relationship study, particularly at the enantio-determining step. Previous work by Harutyunyan and coworkers showed that the asymmetric insertion of phenylacetylene onto 2- position of 4-quinolones was possible but lacked mechanistic insight of the Cu(I)-catalyzed system and demonstrated such on a limited substrate scope. Recent work within the Mattson group showed promising enantiocontrol using a copper catalyst with a chiral BOX ligand. With this in mind, the enantioselective alkynylation of quinolones was explored to yield product in high enantiomeric excess. Our investigation took a bilateral approach based on a comprehensive substrate scope for each the quinolone body and the phenylacetylene involved in the reaction. This focused on the optimization of enantioenriched yields and substrate tolerability as well as a mechanistic investigation via Hammett plot analysis.

Results and Discussion

Quinolone Starting Materials

Synthesis of Quinolones

The 4-quinolones were first synthesized through a two-step route shown in Figure 9. 2-aminobenzonitrile was first converted into 2-aminoacetophenone through cooled methyl magnesium bromide. The acetyl group in the 3-position of the ring allowed for treatment with sodium hydride to facilitate a condensation to close the ring, yielding the 4-quinolone product.

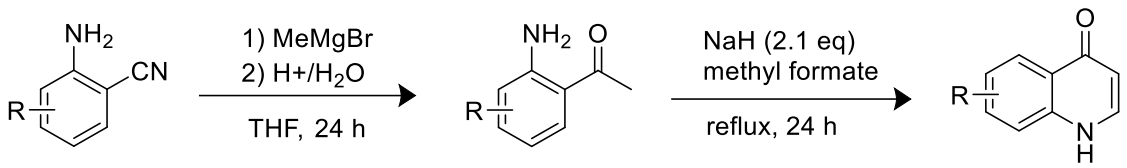

***Figure 9**: Previous Synthesis Route to 4-Quinolones*

While the presence of product was confirmed through TLC standards and ^{1}H-NMR spectroscopy, several experimental problems arose. Firstly, there was difficulty maintaining dry conditions, especially with the reaction solvent. The lab's solvent-still experienced issues that led to wet solvent, forcing us to distill our own THF. Yet, even after fresh distillation and storage over molecular sieves, the hygroscopic nature of THF remained troublesome. Similar issues were faced using an alternative solvent, diethyl ether. Secondly, purification of crude products proved messy, with the observation of several undesired side products. With the scaled-up manner these reactions were run, column chromatography made the most sense for purification. However, the poor separation and number of spots by TLC led to difficult columns that in some cases had to be run multiple times. In addition to this, the Grignard reaction also had relatively low yields. The combination of these issues led the group to search for a more efficient synthesis route, which is described in Figure 10.

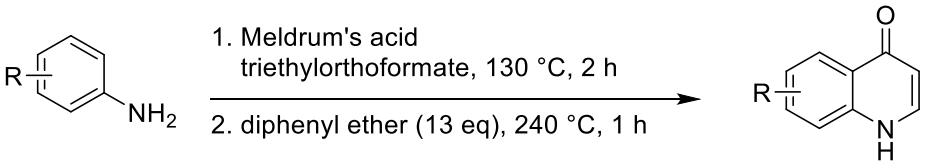

***Figure 10**: Improved Synthesis Route to 4-Quinolones*

This two-step reaction was less particular about dry conditions and afforded product in higher yield with fewer impurities. Meldrum's acid was first activated by triethyl orthoformate at 130°C, then exposed to aniline to form a stable solid intermediate which could be easily filtered out of solution. This filtered compound was then treated with diphenyl ether at 250°C to yield the 4-quinolone product. Crude material still required purification by column chromatography, and it was hypothesized that side-product generation was partly due to the high temperatures of the reaction. Intermediate formation was still run at 130°C, but the diphenyl ether thermolysis was run at 240°C instead of 250°C. From this we saw no significant change in product yield yet

observed cleaner TLCs with more distinct spot separation. This reaction worked for several substituted anilines, all of which were commercially available.

Troc Protections

Before the alkynylation reaction, the vulnerable nitrogen of quinolone required protection. The substituted quinolones were protected using Troc chloride according to the scheme shown in Figure 11.

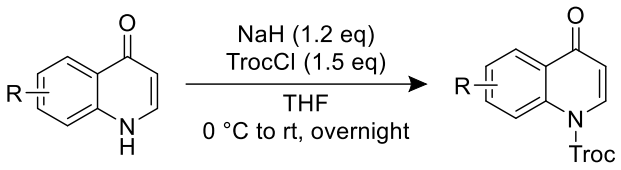

***Figure 11**: Insertion of Troc Protecting Group*

This protection reaction used the same hygroscopic THF as the Grignard procedures, which could be an explanation of their tendency to have low yields. However, at this point, the faulty solvent-still had been fixed and we were unable pinpoint solvent wetness as a significant problem on its own. The leading reason for this was the observation of higher yields in larger amounts of solvent. It is believed that this is due to the formation of a slurry post-addition of sodium hydride and starting material, where the addition of more solvent leads to a more homogenous solution with better stirring in preparation for dropwise-addition of TrocCl. We also observed low yields following a room temperature quench using aqueous acid, presumably due to a vigorous reaction between water and excess NaH. To combat this, the quench took place at 0ºC in an ice bath over several minutes to limit decomposition of product.

The crude products afforded from this reaction proved troublesome to purify. It was found that protected quinolone rapidly decomposed on silica, eliminating column chromatography as a possible method. In turn, a series of solvent washes was developed to either extract impurities or forcibly crash the product out of solution. In either case, the aim was to obtain solid product for recrystallization, as the crudes often took the form of an oil.

Enantioselective Alkynylations

Optimization of Reaction Conditions

The key reaction of our project involves the generation of a stereocenter through an asymmetric alkynylation of our protected quinolone starting materials (Figure 12). The inserted phenylacetylene and any substituted derivatives were commercially available and required no further preparation. The reaction conditions were optimized by other members of the Mattson group, including optimization of ligand, base, protecting group, solvent, temperature, and reaction time (Appendix 4). The reaction ran for 96 hours before facing an aqueous acid quench, where it then was left to stir at room temperature overnight, before its workup. Product was

confirmed by ^{1}H-NMR before being purified via preparatory TLC and characterized via HPLC, where enantiomeric excess was obtained.

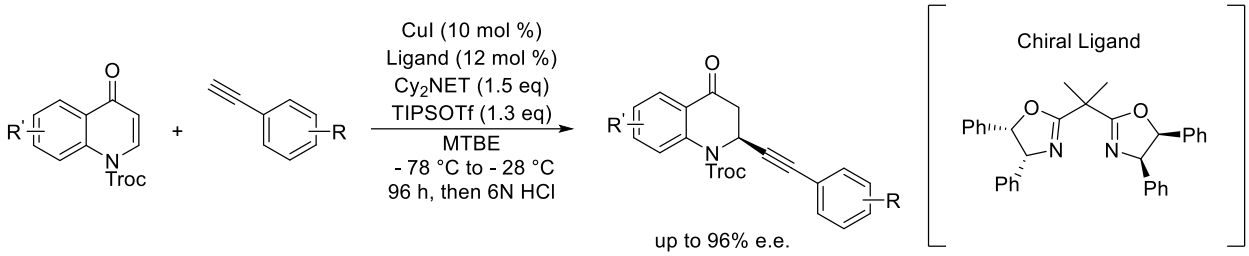

***Figure 12**: Reaction Scheme to Alkynylated 4-Quinolones*

Substrate Scope

Due to the ringed nature of each main reagent (quinolone and phenylacetylene), we were able to carry out two separate LFER investigations. The first focused on using substituted phenylacetylene and analyzing the effect of functional groups on yield and enantiomeric excess, keeping all other reaction conditions constant. The second study was identical except that 4-quinolone would be modified and held against an unsubstituted phenylacetylene. The complete substrate scopes for each study can be seen in Figures 13 and 14.

The first sets of substrates were selected with Hammett plots in mind; substrates with substituent position and identity that had corresponding σ values were required to create the foundation of a Hammett plot. We made sure to include a range of σ values, including both electron withdrawing and donating groups. Once these base datapoints were obtained, new substrates were chosen based on optimizing enantiomeric excess. For example, it was observed that electron withdrawing groups led to higher e.e. in the para-position on both the quinolone and phenylacetylene, so this trend was further explored.

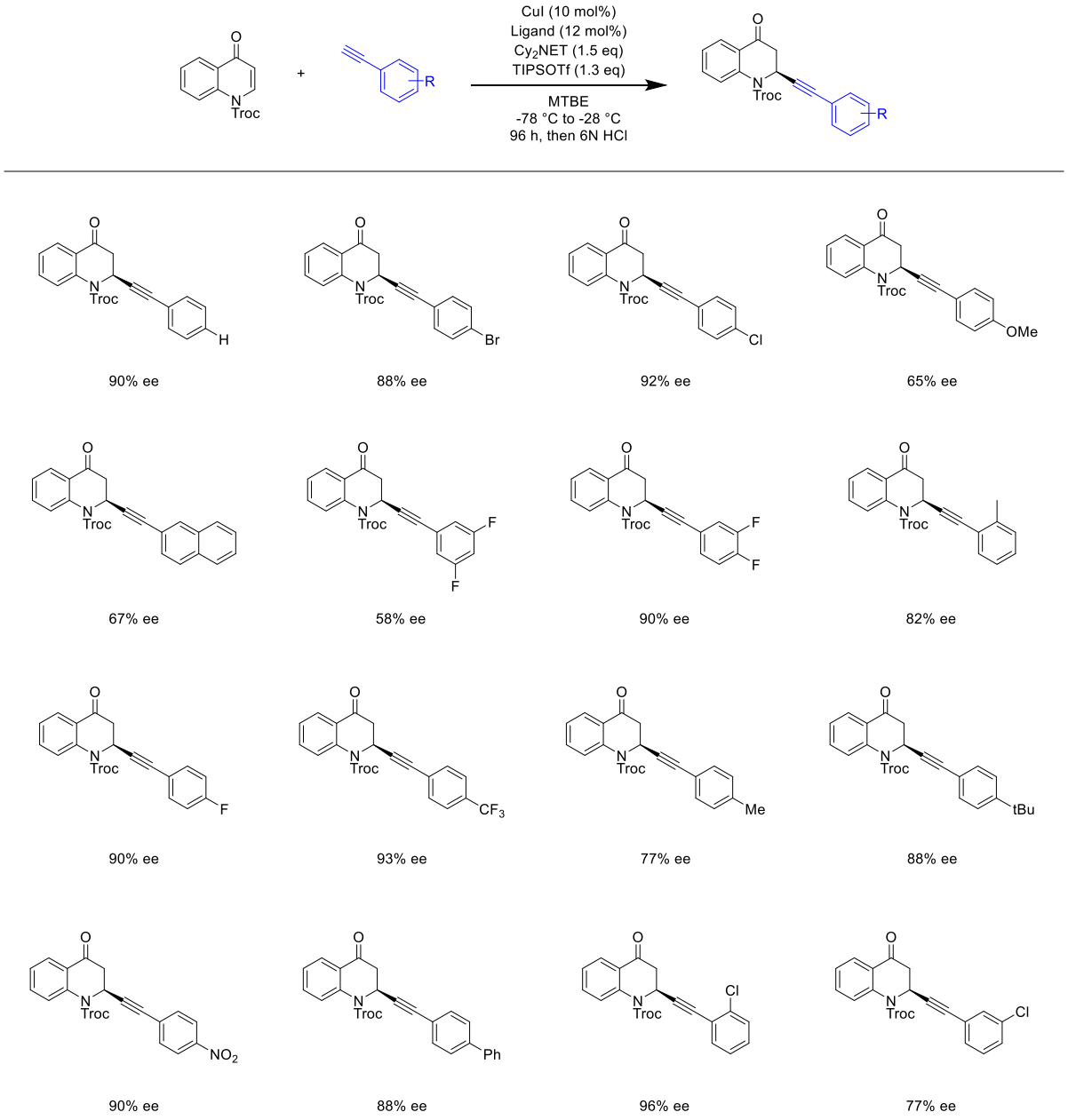

***Figure 13**: Alkynylation Substrate Scope of Substituted Phenylacetylene (see Appendices 5a and 6a)*

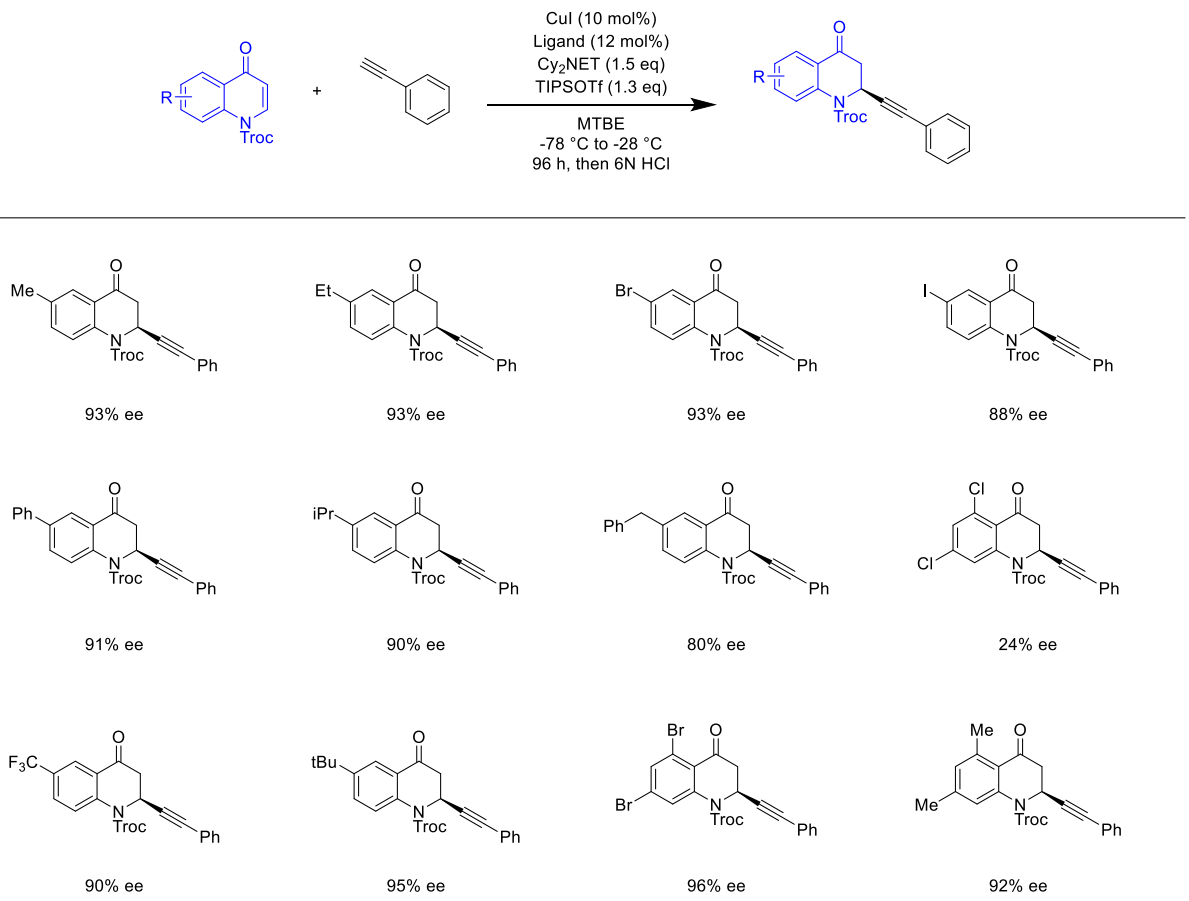

***Figure 14**: Alkynylation Substrate Scope of Substituted 4-Quinolone (see Appendices 5b and 6b)*

Hammett Plot Analysis

Substitutions on Phenylacetylene

Hammett parameters focused mainly on σ_{para} values. Four plots in total were made, one for each study (phenylacetylenes and quinolones), and an optimized plot for each case using the modified Brown & Okamoto σ^{+} values. All Hammett and Brown & Okamoto parameters can be found in Appendix A. Each relationship plotted the log of enantiomeric ratio (e.r.) against σ values. Product yield was not used to describe any relationships as we found no correlation between it and substituent effects.

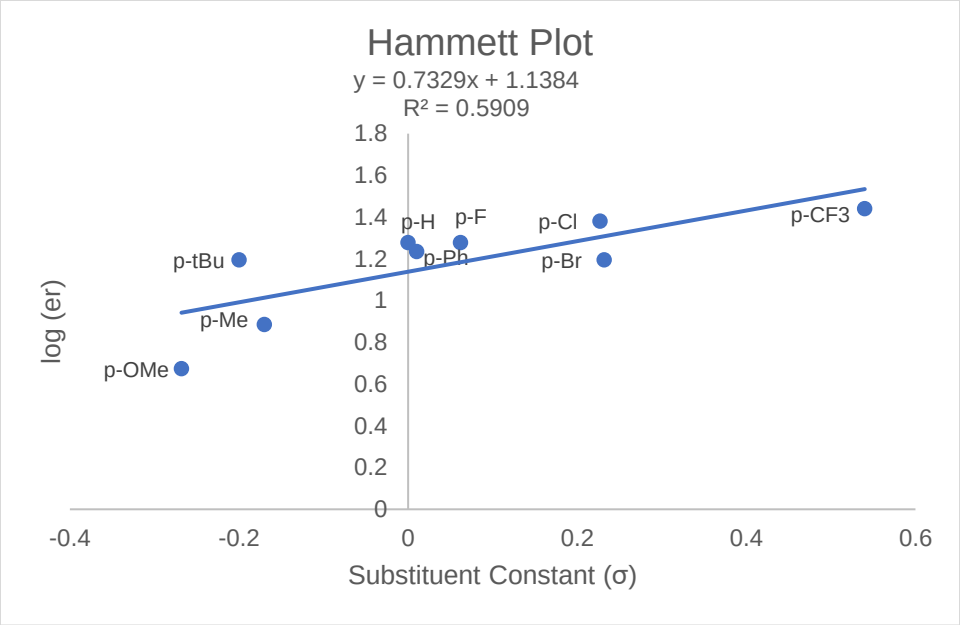

***Figure 15**: Hammett Plot of Substituted Phenylacetylene*

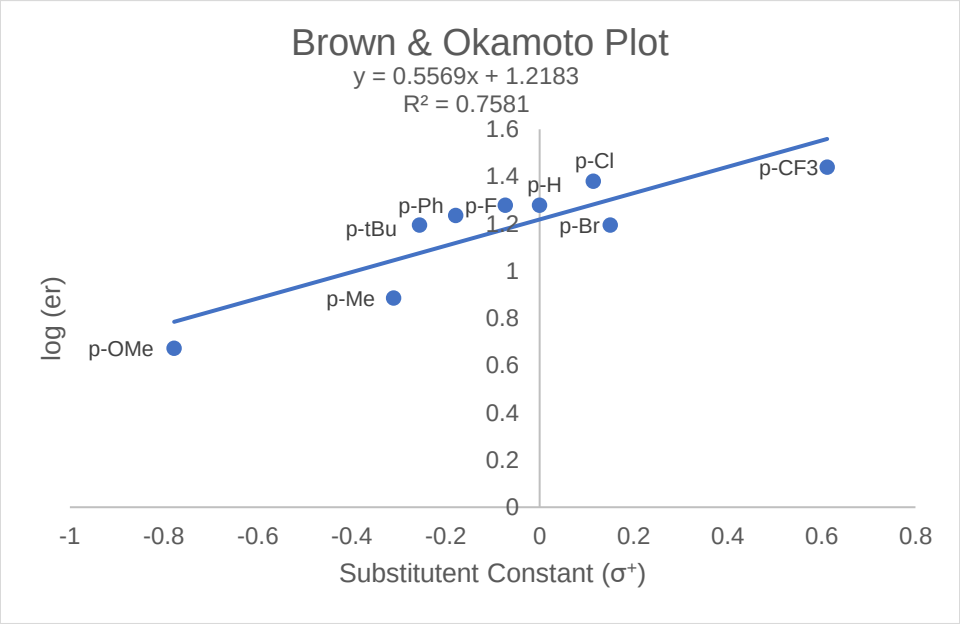

***Figure 16**: Brown & Okamoto Plot of Substituted Phenylacetylene*

Both plots for the phenylacetylene investigation show clear trends. Figure 15 utilizes Hammett's original σ values from the benzoic acid reaction standard. It owns an R^2 of 0.6216, showing a moderate correlation between the Hammett parameters and enantiomeric ratio. A positive ρ value of 0.707 suggests a weak buildup of negative charge or loss of a weak positive charge. It

also suggests that the reaction is slightly less sensitive to changes in substituent effects than the benzoic acid standard, since $\rho < 1$. It became clear that strong electron withdrawing groups had a beneficial impact on e.e., with $-NO_2$, $-CF_3$, and halogen substituents having the most promising results (Figure 13). We hypothesized that these EWG's played an important role in the transition state of the enantio-determining step of the mechanism through resonance stabilization. We probed at this idea by moving the -Cl substituent around the ring of phenylacetylene. We observed the para- and ortho- positions to have significantly higher e.e. (92% and 96% respectively) than the meta- position (77%). Additionally, difluoro substitutions in the 3- and 4- positions (meta and para) afford 90% e.e., while difluoro substitutions in the 3- and 5- positions (both meta) only affords 58% e.e.. This compares to a single fluorine at the 4-position (para) with an e.e. of 90%, suggesting that a meta-substituent is tolerated so long as an able resonance participant is present. This supported our hypothesis and led us to search for different LFER standards in hopes of increasing the correlation between our data and σ values. Our search ended at the work of Brown & Okamoto, who created the σ^+ parameters for the cumyl chloride reaction standard, one shown to be a better reference for resonance effects.

We replotted our data in Figure 16 using the σ^+ parameters and saw a much stronger correlation with log (e.r.), with an R^2 value of 0.7769. A positive ρ value was still observed at 0.5475, slightly less than that of the Hammett parameters. This would suggest our reaction is less sensitive to substituent effects of this new reference than the previous, yet the increased R^2 makes the slight decrease in ρ relatively insignificant. Even so, we are inclined to believe the enantio-determining step involves the generation of negative charge or a loss of positive charge at the phenylacetylene.

We also believe that inductive effects are present at the phenylacetylene. This is based on the observation of higher e.e.'s when substituents are moved around the ring closer towards the alkyne. This is seen with the -Cl substituent, where e.e. increases from 92% in the 4-position to 96% in the 2-position. We also see an increase in e.e. with -methyl from 77% in the 4-position to 82% in the 2-position. With carbon and chlorine owning higher electronegativities, they may be able draw electron density away from the alkyne (which supposedly sees a small buildup in negative charge) towards themselves, delocalizing the charge and stabilizing the transition state. This is further supported by correlating the increase in e.e. to the increase in electronegativity from carbon to chlorine.

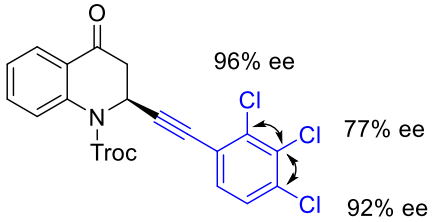

***Figure 17**: Resonance & Inductive Effects on Substituted Phenylacetylene*

No steric hindrances were observed with bulky substituents. Functional groups like -tert-butyl and -phenyl were still able to obtain high e.e. (both 88%) despite their size. Both groups would

also be considered electron-donating groups, so it is assumed that they have a larger contribution to inductive effects than resonance to justify their e.e.'s.

Substitutions on the Quinolone

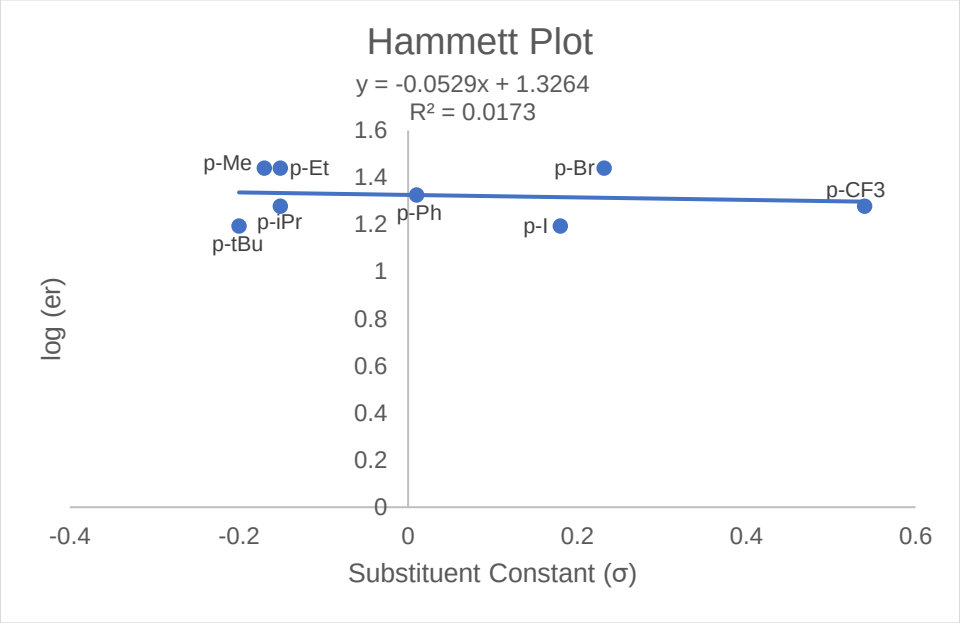

***Figure 18**: Hammett Plot of Substituted 4-Quinolone*

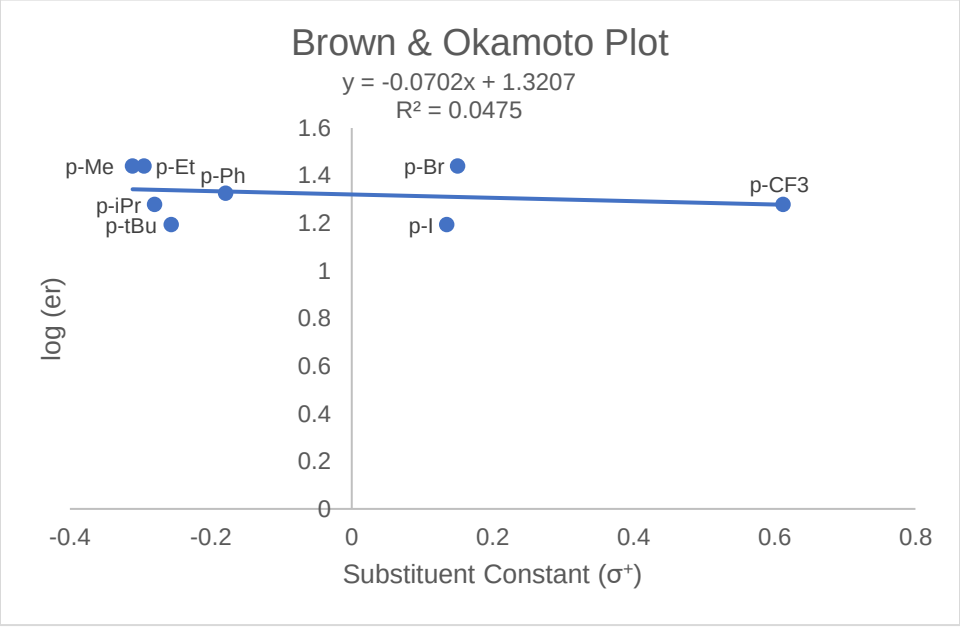

***Figure 19**: Brown & Okamoto Plot of Substituted 4-Quinolone*

Neither of the LFER studies, the Hammett nor the Brown & Okamoto, showed a strong correlation between substitutions on the aromatic ring of the quinolone and the enantiomeric ratio. Both studies show a very slight negative ρ value, with the Hammett ρ value equal to -0.0529 and the Brown & Okamoto ρ value equal to -0.0702. While the R^2 values for both plots are below 0.1 (indicating very poor correlations), the ρ values between the two plots are consistent. Strictly utilizing the information in Figures 18 and 19, these ρ values that are so close to zero would seemingly indicate that there is no charge buildup in the transition state of the enantio-determining step of the reaction. When we replotted the data using substituent constants derived from Brown & Okamoto, we saw a slightly improved R^2 value of 0.0475, versus the Hammett plot's R^2 value of 0.0173, with a similar ρ value shared between the plots. This suggests that the mechanism of our reaction responds to variations in substituents more like the Brown & Okamoto reference reaction than the Hammett reference reaction.

Based on this data and the other substrates we tested (Figure 14), the reaction is not especially sensitive to electron-withdrawing or electron-donating groups on the aromatic ring of the quinolone. Apart from a para benzyl substituent (e.e. of 80%), which seems to be an outlier in the data, all the e.e.'s were greater than 88%. No steric hindrance effects on the enantiomeric ratio were observed in this investigation—larger groups such as *tert*-butyl and phenyl had e.e.'s greater than 90% just like the smaller substituents.

While we can draw some theories about the reaction mechanism from these LFER studies on substitutions on the aromatic ring of the quinolone, it is important to note the poor R^2 values of this investigation. Due to the poor correlation, it is likely that the electronic property of the substituents on the aromatic ring of the quinolone have little effect on the reaction's transition state, in which case LFER studies would provide little evidence to help elucidate the reaction mechanism.

Proposed Mechanism

Our proposed mechanism is shown in Figure 20. The ligand coordinates to CuI to form a complex, which in the presence of base reacts with phenylacetylene to create the copper acetylide. The quinolone is protected *in situ* with TIPSOTf, which then reacts with the copper acetylide through the enantio-determining step to afford an alkynylated product. This is then treated with HCl to yield the final product.

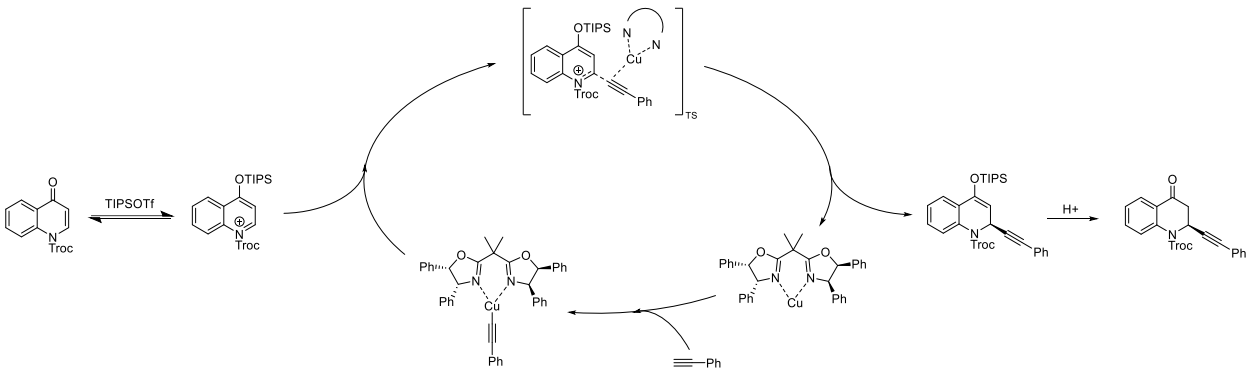

***Figure 20**: Proposed Mechanism & Catalytic Cycle*

The phenylacetylene substrate investigation suggested the substituents on the aryl ring had a notable impact on enantioselectivity. Electron-withdrawing groups owned the greatest e.e.'s, likely due to resonance and inductive effects that stabilized the transition state. We propose that since EWG's can pull electron density away from the terminal carbon of the alkyne, this creates an unequal sharing of electrons between the alkyne and the copper in the acetylide. This disproportionality makes it more likely for the alkyne to move away from the copper and form a bond with the carbon of quinolone. This is also supported by the positive ρ value in the Hammett and Brown & Okamoto plots, which suggest a buildup of negative charge on the phenylacetylene. The magnitude of ρ being between 0 and 1 also suggests that this charge is relatively weak, not having fully ionic character. This coincides with the movement of electrons through the carbon of phenylacetylene as it forms a bond with quinolone and dissociates from copper.

The 4-quinolone substrate investigation demonstrated that the reaction was not very sensitive to electronic changes on the quinolone, since we observed equally high e.e.'s with both EWG and EDG groups. While this linear free energy relationship study was not able to tell us much about the reaction mechanism, the results do make sense with the proposed mechanism. It could be hypothesized, given the proposed mechanism, that the enantioselectivity of the reaction would not be affected much by changes in substituents at the para-position of the quinolone. While these investigations were helpful in drawing some conclusions about our reaction mechanism, more evidence would need to be collected to support the proposed mechanism.

Conclusions

Nitrogen-containing heterocycles are a common motif in many natural products and pharmaceuticals and comprise over half of all current FDA-approved drugs. Quinolones are a common type of nitrogen heterocycle and are found in many natural products and pharmaceuticals, specifically anti-cancer and antibiotic drugs. Current methods of asymmetric functionalization of the 2-position of a 4-quinolone exist, with drawbacks such as limited substrate scopes, sensitive procedures, and high catalyst loadings. The Mattson group has successfully demonstrated an asymmetric functionalization method to insert a phenylacetylene derivative onto this position on a 4-quinolone derivative with relatively mild reaction conditions and up to 96% e.e. with 28 substrates.

Linear free energy relationship (LFER) studies investigating various phenylacetylene derivatives showed a ρ value of 0.7329 and 0.5569 and an R^2 correlation value of 0.5909 and 0.7581 for Hammett values and Brown & Okamoto values respectively. These suggest the buildup of weak negative charge at the phenylacetylene during the transition state, which appears to support the proposed mechanism. These substrates were most sensitive towards electron-withdrawing groups. We believe that the reason behind this is due to resonance and inductive effects that stabilize the enantio-determining step. LFER studies investigating substitutions on the 4-quinolone indicated that the reaction was not sensitive to electron-withdrawing or electron-donating groups on the para position of the quinolone, with ρ values of -0.0529 and -0.0702 and R^2 values of 0.0173 and 0.0475 for Hammett values and Brown & Okamoto values, respectively. The low correlations make it difficult to draw conclusions from these plots, but we argue the results could make sense in terms of the plausible mechanism in that 4-quinolone is not very susceptible to changes in electronic properties and is a minor contributor to the transition state. While this method demonstrates highly selective insertion of an alkyne, further studies are required to comprehensively support our proposed mechanism.

References

1. Kerru, N., Gummidi, L., Maddila, S., Gangu, K. K., & Jonnalagadda, S. B. (2020). A review on recent advances in nitrogen-containing molecules and their biological applications. *Molecules (Basel, Switzerland)*, *25*(8), 1909. https://doi.org/10.3390/molecules25081909
2. Heravi, M. & Zadsirjan, V. (2020). Prescribed drugs containing nitrogen heterocycles: an overview. *RSC Advances*, *1*(72), 44247–44311. https://doi.org/10.1039/d0ra09198g
3. Vitaku, E., Smith, D. T., & Njardarson, J. T. (2014). Analysis of the structural diversity, substitution patterns, and frequency of nitrogen heterocycles among U.S. FDA approved pharmaceuticals. *Journal of Medicinal Chemistry*, *57*(24), 10257–10274. https://doi.org/10.1021/jm501100b
4. Senerovic, L., Opsenica, D., Moric, I., Aleksic, I., Spasić, M., & Vasiljevic, B. (2019). Quinolines and quinolones as antibacterial, antifungal, anti-virulence, antiviral and anti-parasitic agents. *Advances in Experimental Medicine and Biology*, *1282*, 37–69. https://doi.org/10.1007/5584_2019_428
5. Naeem, A., Badshah, S. L., Muska, M., Ahmad, N., & Khan, K. (2016). The current case of quinolones: Synthetic approaches and antibacterial activity. *Molecules (Basel, Switzerland)*, *21*(4), 268–268. https://doi.org/10.3390/molecules21040268
6. Shen, C., Wang, A., Xu, J., An, Z., Loh, K. Y., Zhang, P., & Liu, X. (2019). Recent Advances in the Catalytic Synthesis of 4-Quinolones. *Chem*, *5*(5), 1059–1107. https://doi.org/10.1016/j.chempr.2019.01.006
7. Maestro, A., Lemaire, S., & Harutyunyan, S. R. (2022). Cu(I)-Catalyzed Alkynylation of Quinolones. *Organic Letters*, *24*(5), 1228–1231. https://doi.org/10.1021/acs.orglett.2c00020
8. Kise, N., Yoshimura, Y., Manto, T., & Sakurai, T. (2019). Electroreductive Intermolecular Coupling of 4-Quinolones with Benzophenones: Synthesis of 2-Substituted 4-Quinolones. *ACS Omega*, *4*(22), 20080–20093. https://doi.org/10.1021/acsomega.9b03342
9. Hasan, P., Aneja, B., Masood, M. M., Ahmad, M. B., Yadava, U., Daniliuc, C. G., & Abid, M. (2017). Efficient synthesis of novel N-substituted 2-carboxy-4-quinolones via lithium bis(trimethylsilyl)amide (LiHMDS)-induced in situ cyclocondensation reaction. *RSC Advances*, *7*(19), 11367–11372. https://doi.org/10.1039/c6ra28631c
10. Shintani, R., Yamagame, T., Kimura, T., & Hayashi, T. (2006). Asymmetric Synthesis of 2-Aryl-2,3-dihydro-4-quinolones by Rhodium-Catalyzed 1,4-Addition of Arylzinc Reagents in the Presence of Chlorotrimethylsilane. *ChemInform.*, *37*(13). https://doi.org/10.1002/chin.200613150
11. Guo, Y., & Harutyunyan, S. R. (2019). Highly Enantioselective Catalytic Addition of Grignard Reagents to N-Heterocyclic Acceptors. *Angewandte Chemie (International Ed.)*, *58*(37), 12950–12954. https://doi.org/10.1002/ange.201906237
12. Cheng, S., Zhao, L., & Yu, S. (2014). Enantioselective Synthesis of Azaflavanones Using Organocatalytic 6-endo Aza-Michael Addition. *Advanced Synthesis & Catalysis*, *356*(8), 982–986. https://doi.org/10.1002/adsc.201300920

13. Johnson, J.S. & Evans, D.A. (2000). Chiral Bis(oxazoline) Copper(II) Complexes: Versatile Catalysts for Enantioselective Cycloaddition, Aldol, Michael, and Carbonyl Ene Reactions. *Accounts of Chemical Research*, *33*(6), 325–335. https://doi.org/10.1021/ar960062n
14. Carneiro, L., Silva, A. R., Lourenço, M. A. O., Mayoral, A., Diaz, I., & Ferreira, P. (2016). Chiral Copper(II) Bis(oxazoline) Complexes Directly Coordinated to Amine-Functionalized Phenylene/Biphenylene Periodic Mesoporous Organosilicas as Heterogeneous Catalysts. *European Journal of Inorganic Chemistry*, *2016*(3), 413–421. https://doi.org/10.1002/ejic.201501196
15. Owen, M., Carter, E., Hutchings, G. J., Ward, B. D., & Murphy, D. M. (2012). Influence of counterions on the structure of bis(oxazoline)copper(ii) complexes; An EPR and ENDOR investigation. *Dalton Transactions : an International Journal of Inorganic Chemistry*, *41*(36), 11085–11092. https://doi.org/10.1039/c2dt31273e
16. Wells, Peter. (1963). Linear Free Energy Relationships. *Chemical Reviews*, *63*(2), 171–219. https://doi.org/10.1021/cr60222a005
17. Noel, J. (2021). *Synthesis of Tetrahydroxanthones via Formal [4+2] Cycloadditions*. Worcester Polytechnic Institute.
18. Brown, H. & Okamoto, Y. (1958). Electrophilic Substituent Constants. *Journal of the American Chemical Society*, *80*(18), 4979–4987. https://doi.org/10.1021/ja01551a055
19. Guan, Y., Attard, J. W., Visco, M. D., Fisher, T. J., & Mattson, A. E. (2018). Enantioselective Catalyst Systems from Copper(II) Triflate and BINOL–Silanediol. *Chemistry: a European Journal*, *24*(28), 7123–7127. https://doi.org/10.1002/chem.201801304
20. Attard, J. W., Osawa, K., Guan, Y., Hatt, J., Kondo, S. I., & Mattson, A. (2019). Silanediol Anion Binding and Enantioselective Catalysis. *Synthesis*, *51*(10), 2107–2115. https://doi.org/10.1055/s-0037-1612217
21. Momo, P.B., Leveille, A. N., Farrar, E. H. E., Grayson, M. N., Mattson, A. E., & Burtoloso, A. C. B. (2020). Enantioselective S−H Insertion Reactions of α-Carbonyl Sulfoxonium Ylides. *Angewandte Chemie (International Ed.)*, *59*(36), 15554–15559. https://doi.org/10.1002/anie.202005563
22. Guan, Y., Attard, J. W., & Mattson, A. E. (2020). Copper Bis(oxazoline)-Catalyzed Enantioselective Alkynylation of Benzopyrylium Ions. *Chemistry: a European Journal*, *26*(8), 1742–1747. https://doi.org/10.1002/chem.201904822
23. Guan, Y., Buivydas, T. A., Lalisse, R. F., Attard, J. W., Ali, R., Stern, C., Hadad, C. M., & Mattson, A. E. (2021). Robust, Enantioselective Construction of Challenging, Biologically Relevant Tertiary Ether Stereocenters. *ACS Catalysis*, *11*(10), 6325–6333. https://doi.org/10.1021/acscatal.1c01095

Appendices

Appendix 1: Substituent Constants

Hammett Substituent Constants	
Substituent	σ Value
p-OPh	-0.320
p-OMe	-0.268
p-tBu	-0.200
p-Me	-0.170
p-H	0.000
p-Ph	0.010
p-F	0.062
p-Cl	0.227
p-Br	0.232
p-CF_3	0.540
p-NO_2	0.778

Brown & Okamoto Substituent Constants	
Substituent	σ^+ Value
p-OMe	-0.778
p-OPh	-0.530
p-Me	-0.311
p-tBu	-0.256
p-Ph	-0.179
p-F	-0.073
p-H	0.000
p-Cl	0.114
p-Br	0.150
p-CF_3	0.612
p-NO_2	0.790

Appendix 2: General Information

Anhydrous toluene, dichloromethane, diethyl ether and THF were dried using a pure process technologies solvent system. Anhydrous DCE, chlorobenzene, m-xylene, and o-xylene were used as received. CuI was used as received and stored in a desiccator under ambient lab conditions. TIPSOTf was vacuum distilled and stored under dry nitrogen. Cy2NET was used as received. Alkynes were used as received or prepared according to literature. 1 All bis(oxazoline) ligands were used as received from Sigma Aldrich or TCl or prepared according to literature. 1, 3-9 All other reagents were used directly as received from the manufacturer unless otherwise noted. Preparative silica gel chromatography was performed using SiliaFlash F60 silica gel (40 - 63 µm). Analytical thin layer chromatography was performed using Analtech 250 µm silica gel HLF plates and visualized under UV 254nm or 365nm. All 1H NMR spectra were acquired using a Bruker BioSpin 500 MHz Avance III Digital NMR spectrometer and calibrated using the solvent signal (CDCl3 7.26 ppm). J Coupling constants are reported in Hz. Multiplicities are reported as follows: s, singlet; d, doublet; t, triplet; q, quartet; p, pentet; hept, heptet; m, multiplet; b, broad; dd, doublet of doublets; ddd, doublet of doublet of doublets; td, triplet of doublets; ddt, doublet of doublet of triplets; dtd, doublet of triplet of doublets. All 13C NMR spectra were acquired using a Bruker BioSpin 126MHz Avance III Digital NMR spectrometer and calibrated using the solvent signal (CDCl3 77.16 ppm). Infrared spectra were acquired using a Bruker Vertex 70 with an ATR accessory. High resolution mass spectra were acquired using an Agilent 6520 Q-TOF mass spectrometer. Chiral HPLC analysis was performed using an Agilent 1260 equip with a diode array detector using Chiralcel OD-H or AD-H columns.

Appendix 3: General Procedures

Quinolone Formation

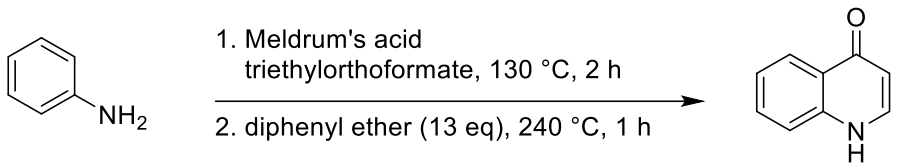

To a dried 100 mL round bottom flask was added 2,2-dimethyl-1,3-dioxane-4,6-dione (2.32 g, 16.1 mol, 1.5 eq) at room temperature. The flask was purged with dry N_2 and triethyl orthoformate (39.8 mL, 25 eq) was then added via syringe. The reaction was then refluxed for 2 hours under dry N_2 at 130 ºC. The reaction was allowed to cool to room temperature before the addition of aniline (1.0 g, 10.7 mol). The reaction was refluxed under dry N_2 at 130 ºC for 2 hours. The reaction was again allowed to cool to room temperature before a precipitate was filtered off and washed with hexanes (5 mL) and dried. The dried precipitate was added to a dried 100 mL round bottom flask along with diphenyl ether (22.1 mL, 13 eq). The flask was purged with dry N_2 and the reaction refluxed at 240 ºC for 1 hour. The reaction was allowed to cool to room temperature. A precipitate was drawn out by addition of hexanes (5 mL). This precipitate was filtered off and washed with hexanes (5 mL) then dried as pure product to afford a brown solid (65% yield).

Troc Protection

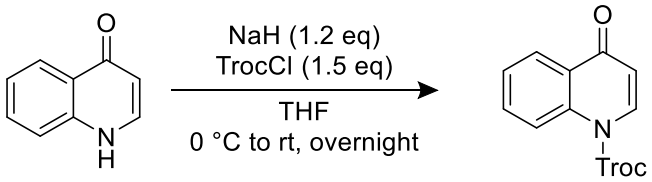

To a dried 100 mL round bottom flask was added 4-oxoquinoline (1.0 g, 6.9 mmol) and dried THF (25 mL). The flask was purged with dry N_2 and cooled to 0 ºC before addition of 60% NaH in oil (0.34 g, 8.6 mmol, 1.25 eq). The reaction was allowed to stir for 1 hour. 2,2,2-Trichloroethyl carbonochloridate (1.4 mL, 10.3 mmol, 1.5 eq) was added dropwise over 30 minutes at 0 ºC. The reaction was allowed to run for 12 hours at room temperature before facing a quench by the addition of distilled water (20 mL). The reaction mixture was extracted with DCM (3 x 30 mL), washed with distilled water (3 x 30 mL), dried over anhydrous Na2SO4, and the solvent removed under vacuum to obtain the crude product. The crude product was purified by recrystallization in acetone to afford a white solid (28% yield).

Alkynylation

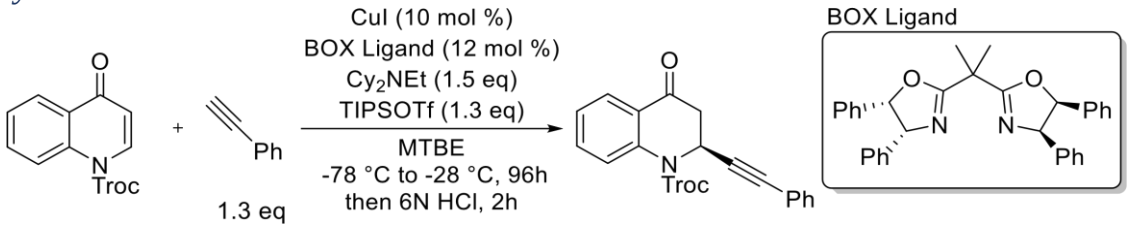

To an 8 mL screw top vial was added 2,2,2-trichloroethyl 4-oxoquinoline-1(4H)-carboxylate (64.1 mg, 0.2 mmol), CuI (1.9 mg, 10 mol%), BOX Ligand (5.8 mg, 0.024 mmol, 12 mol%), MTBE (2 mL), Cy_2NEt (69 µL, 1.5 eq), and phenyl acetylene (28.6 µL, 1.3 eq) in that order at room temperature. This mixture was allowed to stir for 30 minutes. The vial was purged with dry N_2 and then cooled to -78 ºC. TIPSOTf (70 µL, 0.26 mmol, 1.3 eq) was added at -78 ºC, then the reaction was transferred to the lab freezer at -28 ºC and allowed to react for 96h. The reaction was quenched by the addition of 6N HCl (2 mL) and stirred for 2 hours. The reaction mixture was extracted with EtOAc (3 x 2 mL), washed with saturated $NaHCO_3$ solution, dried over anhydrous $NaSO_4$, and the solvent removed under vacuum to obtain the crude product. The crude product was purified by column chromatography on silica gel with Hexane:EtOAc (4:1) to afford a white solid (74% yield, 91% ee).

Racemic substrates were prepared using the general procedure without ligand or using achiral-box ligand which was prepared according to literature[2].

achiral-Box:

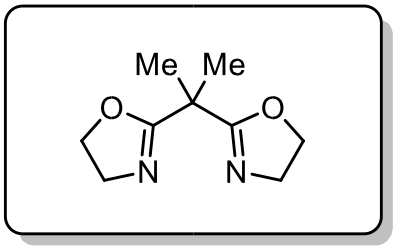

Appendix 4: Optimization

All optimization experiments were performed using the general procedure unless otherwise noted.

Protecting Group Screen

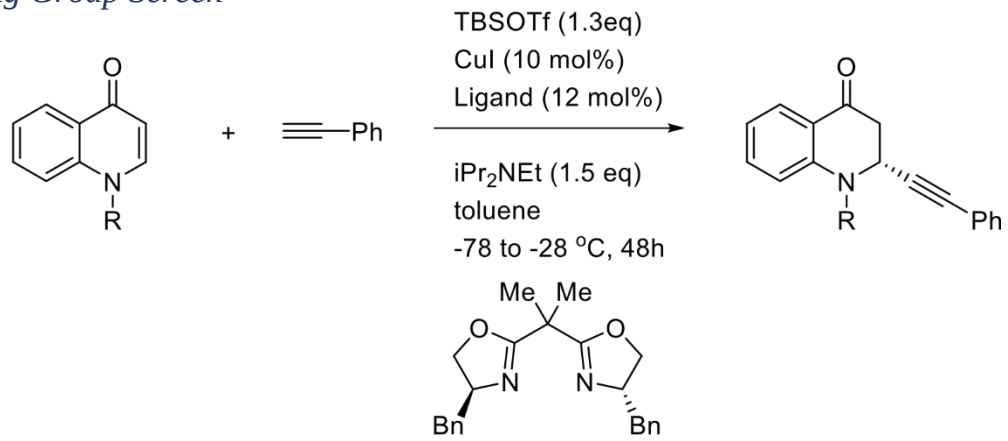

Entry	R	yield (%)	ee (%)
1	Troc	15	13
2	CO_2Me	26	4
3	CO_2Bn	24	3
4	Boc	n.d.	n.d.
5	Me	n.d.	n.d.

Copper Salt Screen

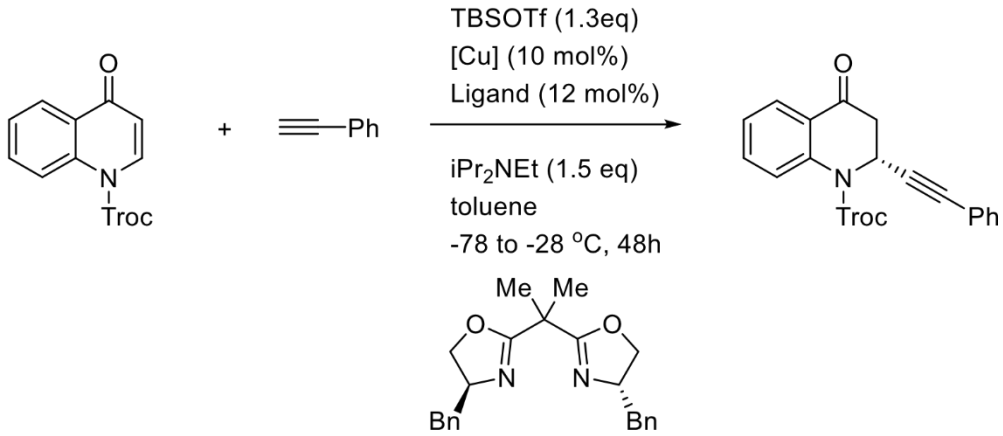

Entry	[Cu]	yield (%)	ee (%)
1	CuI	15	13
2	$Cu(OTf)_2$	n.d.	n.d.
3	CuOTf	n.d.	n.d.
4	CuCl	n.d.	n.d.
5	CuOAc	n.d.	n.d.
6	CuBr	n.d.	n.d.

7	CuSPh	n.d.	n.d.
8	$Cu(MeCN)_4BF_4$	n.d.	n.d.
9	$Cu(MeCN)_4PF_6$	n.d.	n.d.
10	CuMeSal	n.d.	n.d.

Silyl Triflate Screen

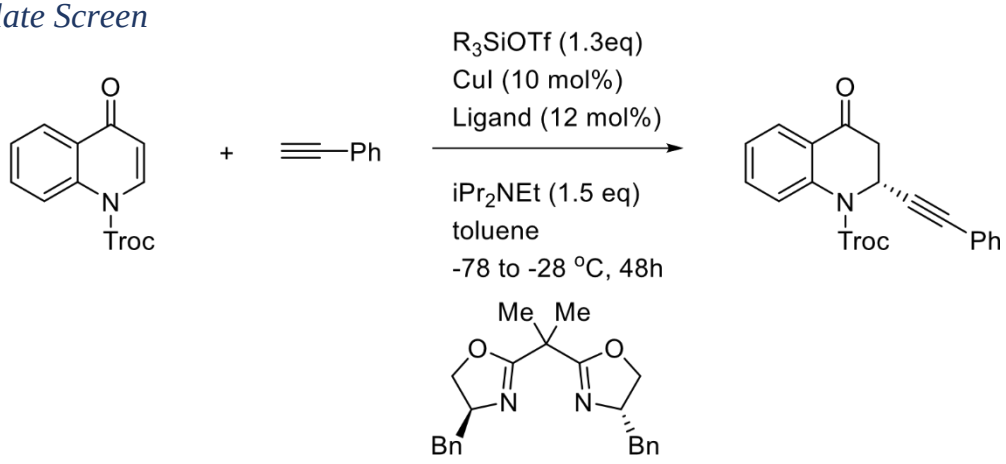

Entry	R_3SiOTf	yield (%)	ee (%)
1	TBSOTf	15	13
2	TIPSOTf	40	22
3	TMSOTf	30	9

Base Screening

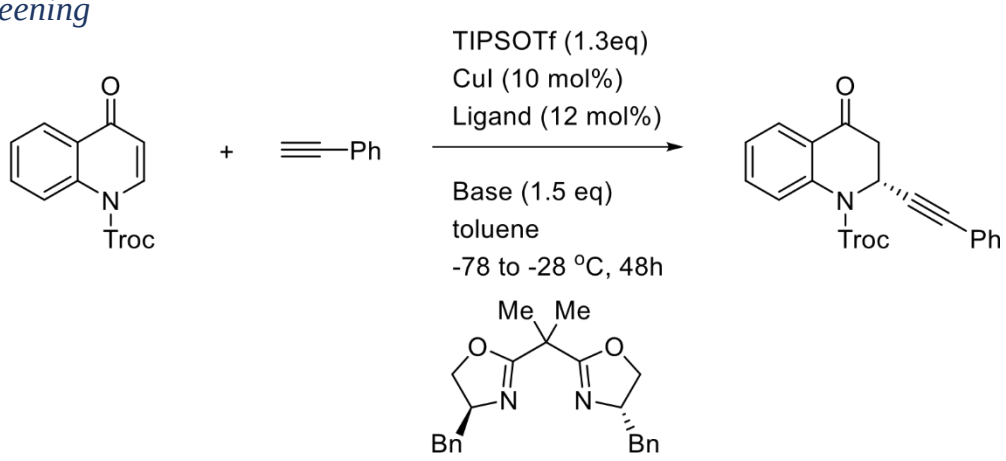

Entry	Base	yield (%)	ee (%)
1	*i*-Pr_2NEt	40	22
2	Cy_2NEt	82	26
3	Et_3N	19	24
4	DBU	n.d.	n.d.
5	MTBD	n.d.	n.d.
6	2,6-lutidine	n.d.	n.d.

Solvent Screen

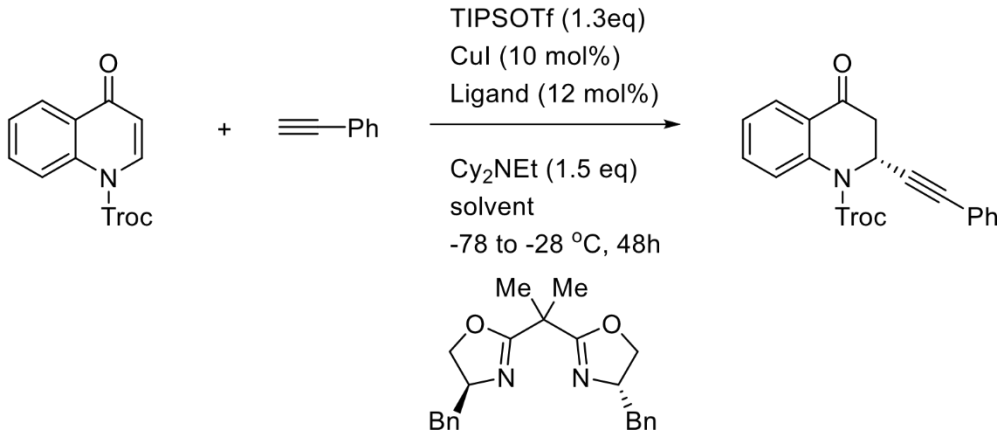

Entry	Solvent	yield (%)	ee (%)
1	toluene	82	26
2	PhCl	71	25
3	m-xylene	19	25
4	o-xylene	34	24
5	THF	59	19
6	DCM	82	19
7	DCE	85	19
8	$CHCl_3$	n.d.	n.d.
9	ether	27	28

Ligand Screen

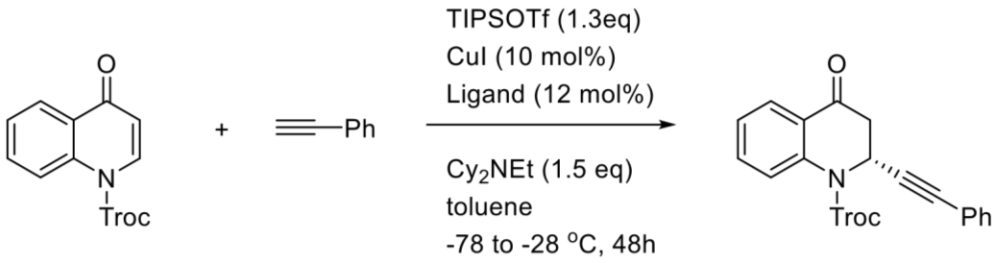

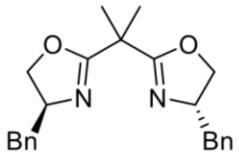

82% yield
26% ee

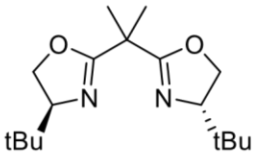

12% yield
6% ee

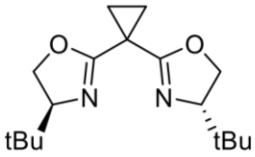

60% yield
rac

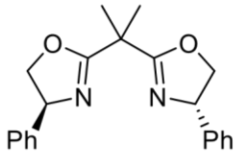

57% yield
35% ee

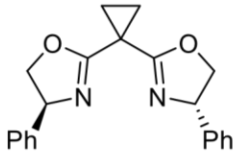

7% yield
36% ee

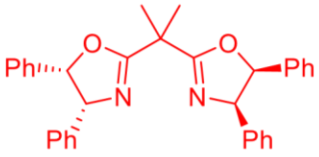

80% yield
-82% ee

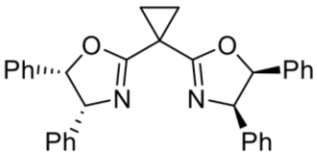

57% yield
-76% ee

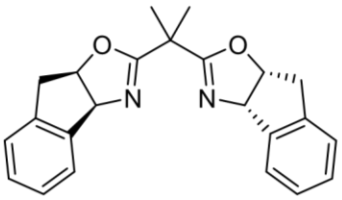

65% yield
-13% ee

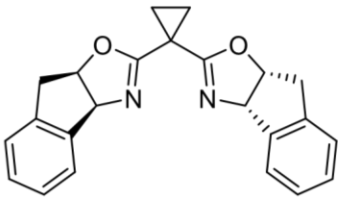

n.d.

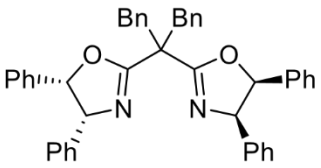

67% yield
-54% ee

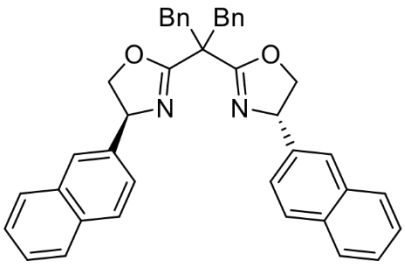

60% yield
7% ee

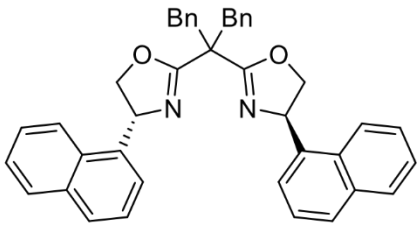

65% yield
-35% ee

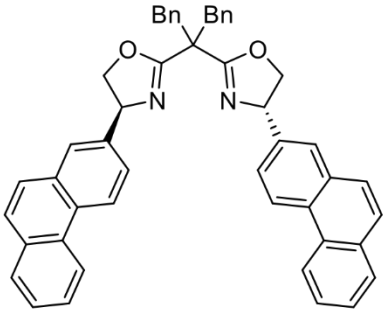

56% yield
19% ee

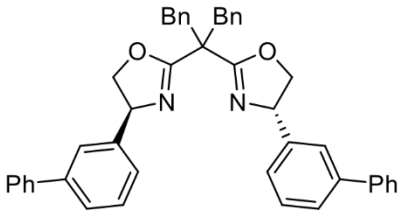

82% yield
-58% ee

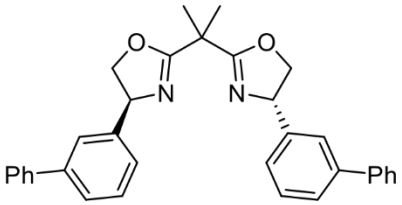

>99% yield
73% ee

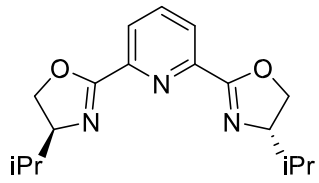

n.d.

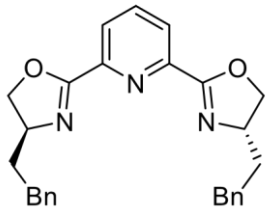

n.d.

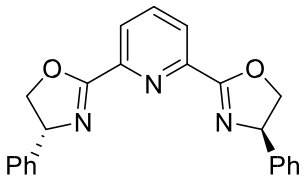

n.d.

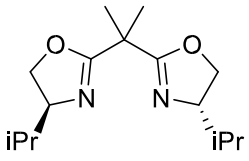

89% yield
11% ee

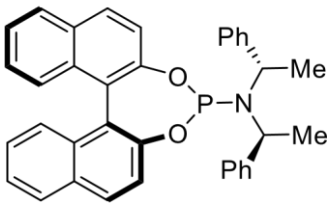

16% yield
-5% ee

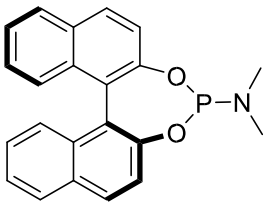

62% yield
13% ee

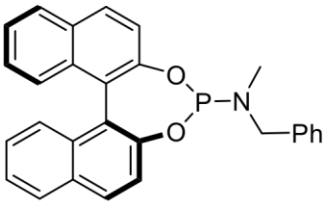

n.d.

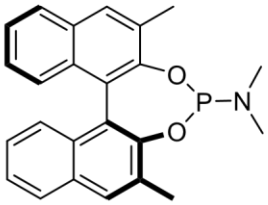

17% yield
10% ee

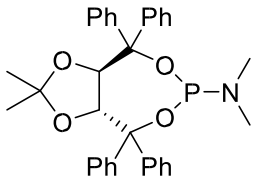

55% yield
-34% ee

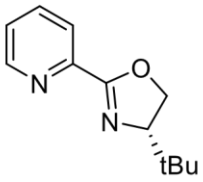

85% yield
52% ee

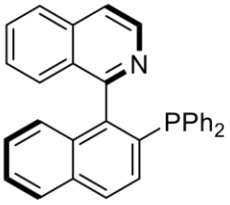

14% yield
23% ee

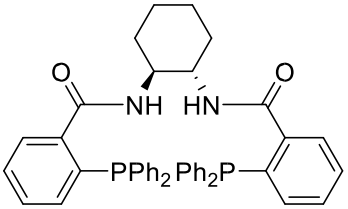

n.d.

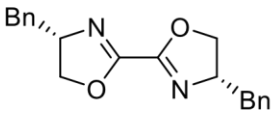

56% yield
9% ee

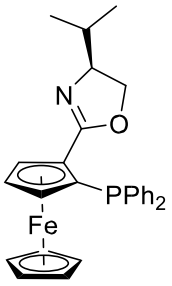

n.d.

Further Optimization

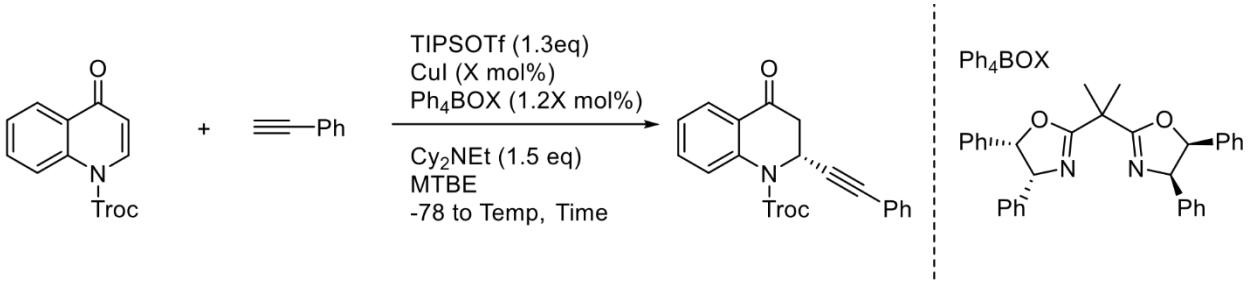

Entry	X	Conc. (M)	Temp (°C)	Time (h)	Yield (%)	ee (%)
1	10	0.1	-28	48	86	-84
2	10	0.1	-35	48	76	-48
3	10	0.05	-28	48	40	-87

4	10	0.05	-28	72	67	-87
5	10	0.05	-28	96	71	-87
6	5	0.05	-28	96	74	-91

Appendix 5: Synthesis of 2,2,2-trichloroethyl (S)-4-oxo-2-(phenylethynyl)-3,4-dihydroquinoline-1(2H)-carboxylates

Appendix 5A: Phenylacetylene Substitutions

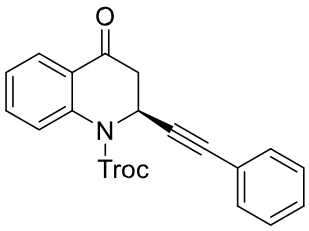

2,2,2-trichloroethyl (S)-4-oxo-2-(phenylethynyl)-3,4-dihydroquinoline-1(2H)-carboxylate (1a): Prepared according to the general procedure, using MTBE, BOX ligand, quinolone (66.1 mg, 0.20 mmol) and phenyl acetylene (0.26 mmol). **1a** was isolated as a white solid, 74% yield. R_f = 0.51 (4:1, Hexanes:EtOAc), $[\alpha]^{23}_D$ = +90.7 (c = 0.9, $CHCl_3$), ^{1}H NMR (500 MHz, Chloroform-*d*) δ 8.08 (ddd, *J* = 7.8, 1.7, 0.5 Hz, 1H), 7.90 (d, *J* = 8.4 Hz, 1H), 7.59 (ddd, *J* =

8.4, 7.3, 1.7 Hz, 1H), 7.31 – 7.24 (m, 2H), 7.23 – 7.15 (m, 4H), 6.12 (dd, *J* = 5.5, 2.1 Hz, 1H), 5.12 (d, *J* = 11.9 Hz, 1H), 4.78 (d, *J* = 11.9 Hz, 1H), 3.19 (dd, *J* = 17.2, 5.6 Hz, 1H), 3.02 (dd, *J* = 17.2, 2.1 Hz, 1H).^{13}C NMR (126 MHz, $CDCl_3$) δ 191.69, 151.62, 140.43, 134.68, 131.96, 128.94, 128.34, 127.35, 125.48, 125.32, 124.62, 121.73, 94.94, 85.45, 84.96, 75.99, 47.87, 44.79. Chiral HPLC: 95.0:4.9 e.r., 91% ee, Chiralcel AD-H column (2% *i*PrOH/Hexanes, 1 mL/min, 254 nm); t_R (minor) = 15.7 min, t_R (major) = 17.1 min.

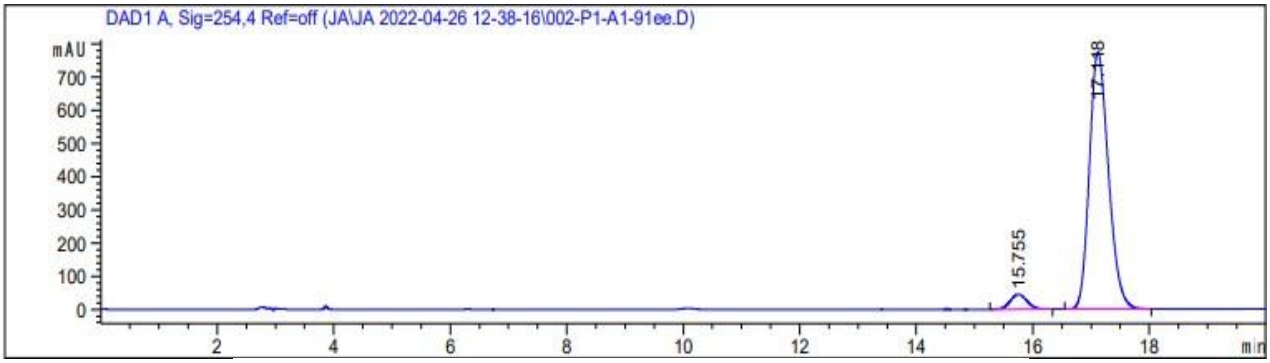

Signal 1: DAD1 A, Sig=254,4 Ref=off

Peak #	RetTime [min]	Type	Width [min]	Area [mAU*s]	Height [mAU]	Area %
1	15.755	VB R	0.2949	910.10480	45.20191	4.9004
2	17.118	BB	0.3535	1.76621e4	774.55219	95.0996
Totals :				1.85722e4	819.75409	

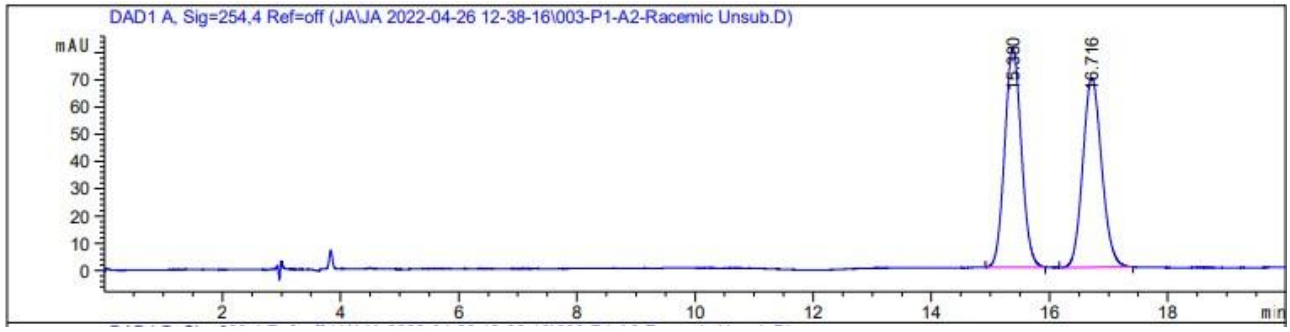

Signal 1: DAD1 A, Sig=254,4 Ref=off

Peak #	RetTime [min]	Type	Width [min]	Area [mAU*s]	Height [mAU]	Area %
1	15.380	BB	0.2986	1577.22217	80.66135	50.4250
2	16.716	BB	0.3304	1550.63306	69.75237	49.5750
Totals :				3127.85522	150.41371	

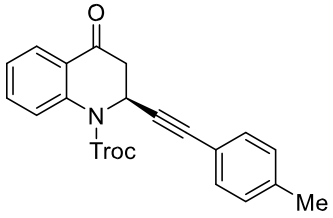

2,2,2-trichloroethyl (S)-4-oxo-2-(p-tolylethynyl)-3,4-dihydroquinoline-1(2H)-carboxylate (1b): Prepared according to the general procedure, using MTBE, BOX ligand, quinolone (66.1 mg, 0.20 mmol) and phenyl acetylene (0.26 mmol). **1b** was isolated as a white solid, 77% yield. R_f = 0.50 (4:1, Hexanes:EtOAc), $[\alpha]^{23}_D$ = +90.7 (c = 0.9, $CHCl_3$), ^{1}H NMR (500 MHz, Chloroform-*d*) δ 8.07 (ddd, *J* = 7.9, 1.7, 0.5 Hz, 1H), 7.90 (d, *J* = 8.4 Hz, 1H), 7.58 (ddd, *J* =

8.4, 7.3, 1.7 Hz, 1H), 7.31 – 7.25 (m, 1H), 7.07 (d, *J* = 8.2 Hz, 2H), 7.01 (d, *J* = 7.9 Hz, 2H), 6.11 (dd, *J* = 5.5, 2.1 Hz, 1H), 5.12 (d, *J* = 11.9 Hz, 1H), 4.77 (d, *J* = 11.9 Hz, 1H), 3.18 (dd, *J* = 17.2, 5.5 Hz, 1H), 3.01 (dd, *J* = 17.2, 2.1 Hz, 1H), 2.28 (s, 3H). ^{13}C NMR (126 MHz, $CDCl_3$) δ 191.77, 151.62, 140.45, 139.15, 134.63, 131.83, 129.08, 127.31, 125.42, 125.33, 124.61, 118.64, 94.95, 85.62, 84.28, 75.96, 47.91, 44.84, 21.57. Chiral HPLC: 87.1:12.8 e.r., 74% ee, Chiralcel AD-H column (2% iPrOH/Hexanes, 1 mL/min, 254 nm); t_R (minor) = 16.0 min, t_R (major) = 12.1 min.

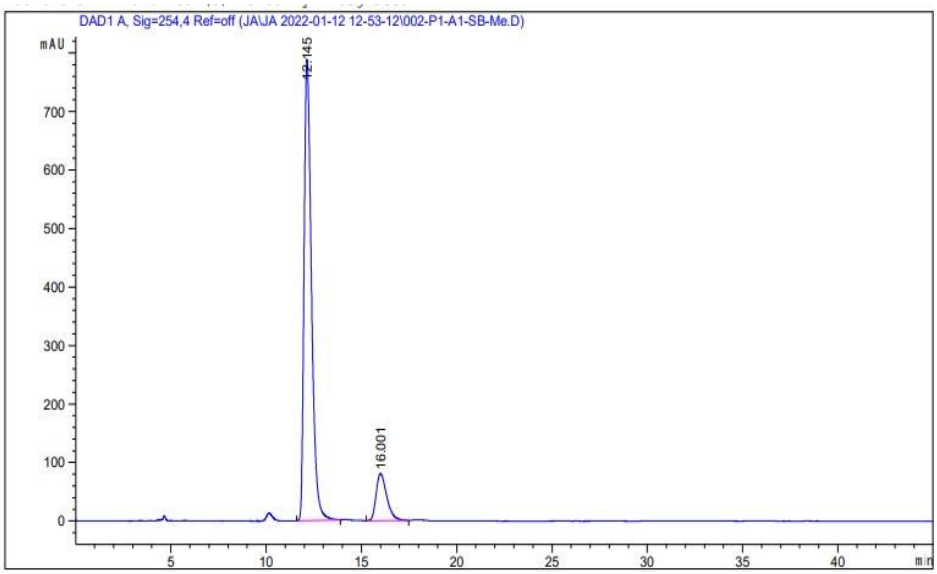

Signal 1: DAD1 A, Sig=254,4 Ref=off

Peak #	RetTime [min]	Type	Width [min]	Area [mAU*s]	Height [mAU]	Area %
1	12.145	BB	0.4133	2.11638e4	788.04279	87.1773
2	16.001	BB	0.5930	3112.95093	80.52009	12.8227
Totals :				2.42768e4	868.56287	

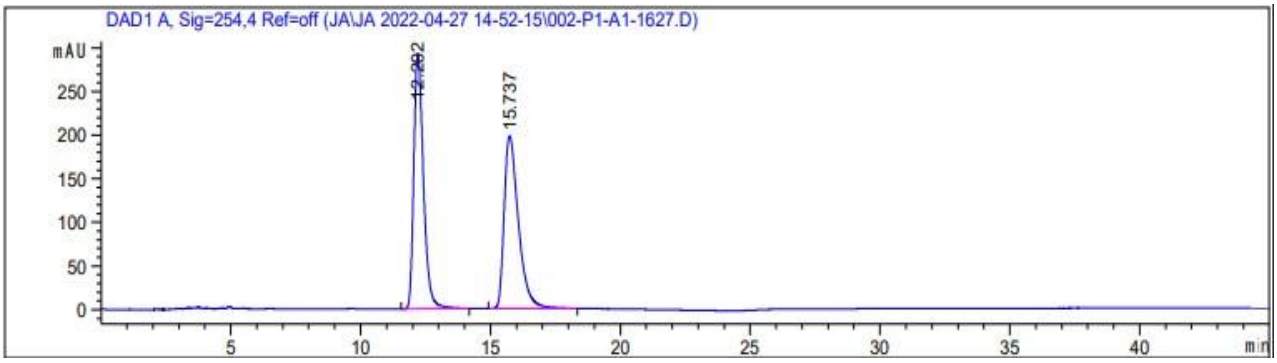

Signal 1: DAD1 A, Sig=254,4 Ref=off

Peak #	RetTime [min]	Type	Width [min]	Area [mAU*s]	Height [mAU]	Area %
1	12.202	BB	0.3959	7558.97852	292.09201	50.0503
2	15.737	BB	0.5766	7543.78516	197.96948	49.9497
Totals :				1.51028e4	490.06149	

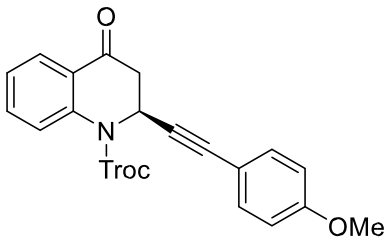

2,2,2-trichloroethyl (S)-2-((4-methoxyphenyl)ethynyl)-4-oxo-3,4-dihydroquinoline-1(2H)carboxylate (1c): Prepared according to the general procedure, using MTBE, BOX ligand, quinolone (66.1 mg, 0.20 mmol) and phenyl acetylene (0.26 mmol). **1c** was isolated as a white solid, 82% yield. R_f = 0.38 (4:1, Hexanes:EtOAc), $[\alpha]^{23}_D$ = +90.7 (c = 0.9, $CHCl_3$), ^{1}H NMR (500 MHz, Chloroform-*d*) δ 8.07 (dd, *J* = 7.8, 1.7 Hz, 1H), 7.90 (d, *J* = 8.4 Hz, 1H), 7.59 (ddd, *J* = 8.6, 7.3, 1.7 Hz, 1H), 7.31 – 7.23 (m, 1H), 7.15 – 7.08 (m, 2H), 6.76 – 6.69 (m, 2H), 6.10 (dd, *J* = 5.5, 2.0 Hz, 1H), 5.12 (d, *J* = 11.9 Hz, 1H), 4.77 (d, *J* = 11.9 Hz, 1H), 3.75 (s, 3H), 3.18 (dd, *J* = 17.1, 5.5 Hz, 1H), 3.01 (dd, *J* = 17.2, 2.1 Hz, 1H).^{13}C NMR (126 MHz, CDCl3) δ 191.82, 160.09, 151.62, 140.47, 134.62, 133.44, 127.29, 125.39, 125.33, 124.61,

113.96, 113.78, 94.95, 85.46, 83.61, 75.95, 55.39, 47.95, 44.89. Chiral HPLC: 62.0:37.9 e.r., 24% ee, Chiralcel OD-H column (2% iPrOH/Hexanes, 1 mL/min, 254 nm); t_R (minor) = 26.0 min, t_R (major) = 20.3 min.

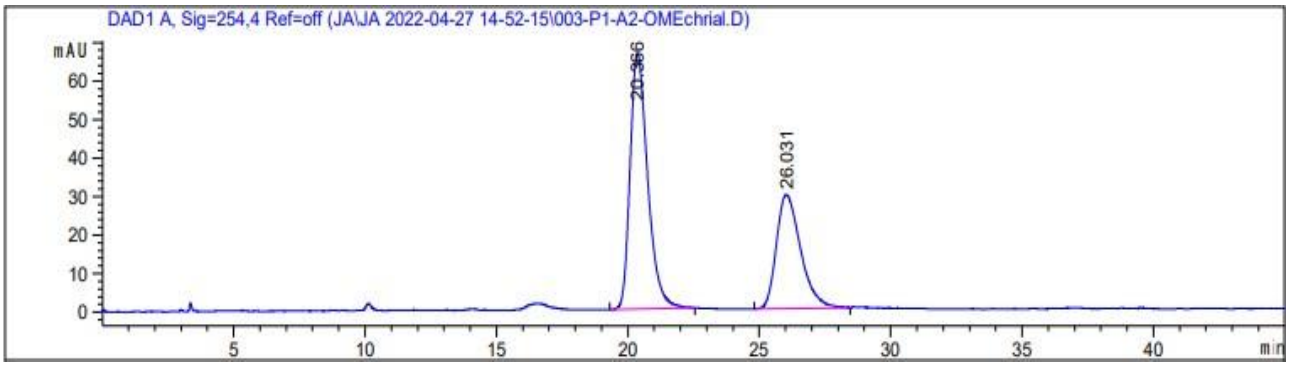

Signal 1: DAD1 A, Sig=254,4 Ref=off

Peak #	RetTime [min]	Type	Width [min]	Area [mAU*s]	Height [mAU]	Area %
1	20.366	BB	0.6816	3092.20117	66.36452	62.0023
2	26.031	BB	0.9027	1895.03333	29.52752	37.9977
Totals :				4987.23450	95.89204	

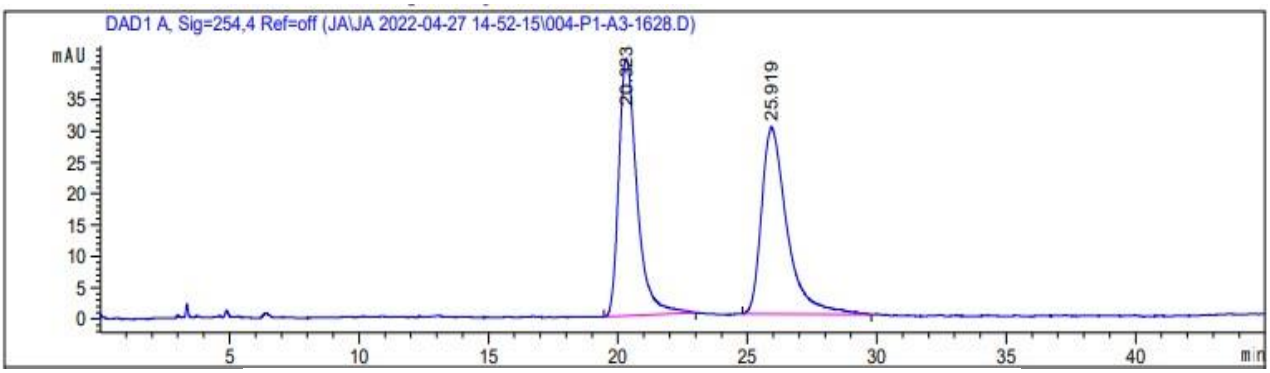

Signal 1: DAD1 A, Sig=254,4 Ref=off

Peak #	RetTime [min]	Type	Width [min]	Area [mAU*s]	Height [mAU]	Area %
1	20.323	BB	0.7309	2004.06067	41.09513	49.4200
2	25.919	BB	0.8536	2051.10229	29.85390	50.5800
Totals :				4055.16296	70.94903	

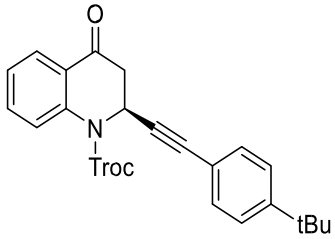

2,2,2-trichloroethyl (S)-2-((4-(tert-butyl)phenyl)ethynyl)-4-oxo-3,4-dihydroquinoline1(2H)-carboxylate (1d): Prepared according to the general procedure, using MTBE, BOX ligand, quinolone (66.1 mg, 0.20 mmol) and phenyl acetylene (0.26 mmol). **1d** was isolated as a white solid, 67% yield. R_f = 0.52 (4:1, Hexanes:EtOAc), $[\alpha]^{23}_D$ = +90.7 (c = 0.9, $CHCl_3$), ^{1}H NMR (500 MHz, Chloroform-*d*) δ 8.07 (dd, *J* = 7.8, 1.7 Hz, 1H), 7.90 (d, *J* = 8.4 Hz, 1H), 7.59 (ddd, *J* = 8.6, 7.3, 1.7 Hz, 1H), 7.31 – 7.23 (m, 1H), 7.15 – 7.08 (m, 2H), 6.76 – 6.69 (m, 2H), 6.10 (dd, *J* = 5.5, 2.0 Hz, 1H), 5.12 (d, *J* = 11.9 Hz, 1H), 4.77 (d, *J* = 11.9 Hz, 1H), 3.75 (s, 3H), 3.18 (dd, *J* = 17.1, 5.5 Hz, 1H), 3.01 (dd, *J* = 17.2, 2.1 Hz, 1H). ^{13}C NMR (126 MHz, CDCl3) δ 191.82, 160.09, 151.62, 140.47, 134.62, 133.44, 127.29, 125.39, 125.33, 124.61,

113.96, 113.78, 94.95, 85.46, 83.61, 75.95, 55.39, 47.95, 44.89.Chiral HPLC: 91.7:8.2 e.r., 87% ee, Chiralcel OD-H column (2% iPrOH/Hexanes, 1 mL/min, 254 nm); t_R (minor) = 16.2 min, t_R (major) = 12.3 min.

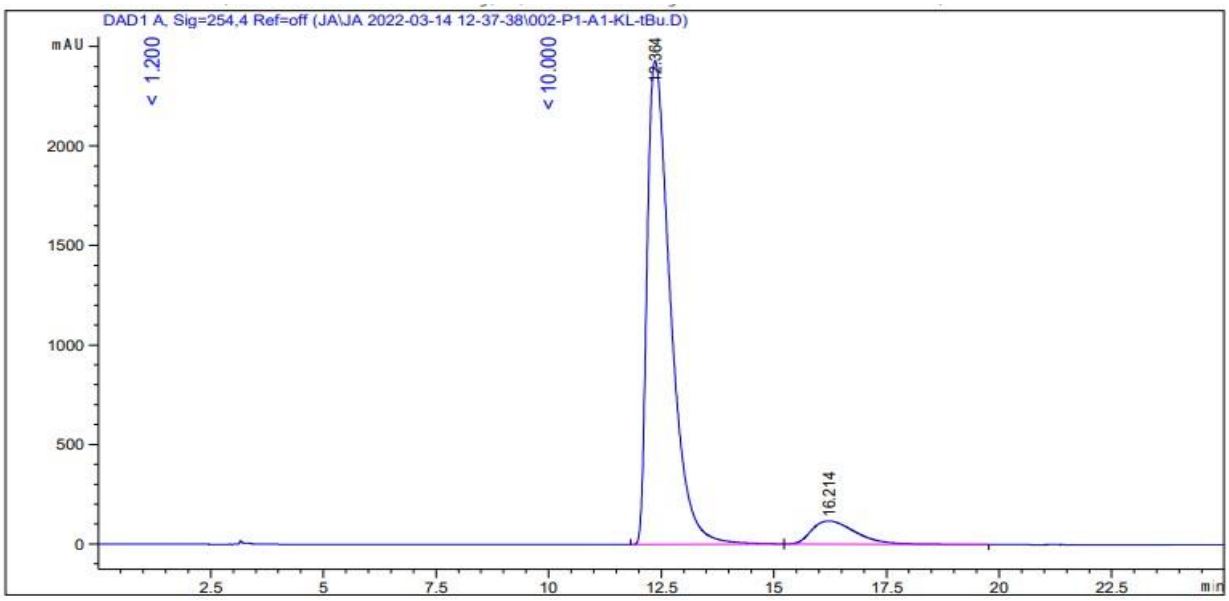

Signal 1: DAD1 A, Sig=254,4 Ref=off

Peak #	RetTime [min]	Type	Width [min]	Area [mAU*s]	Height [mAU]	Area %
1	12.364	BB	0.5466	8.72236e4	2430.85767	91.7345
2	16.214	BB	1.0359	7859.10693	116.07418	8.2655
Totals :				9.50827e4	2546.93185	

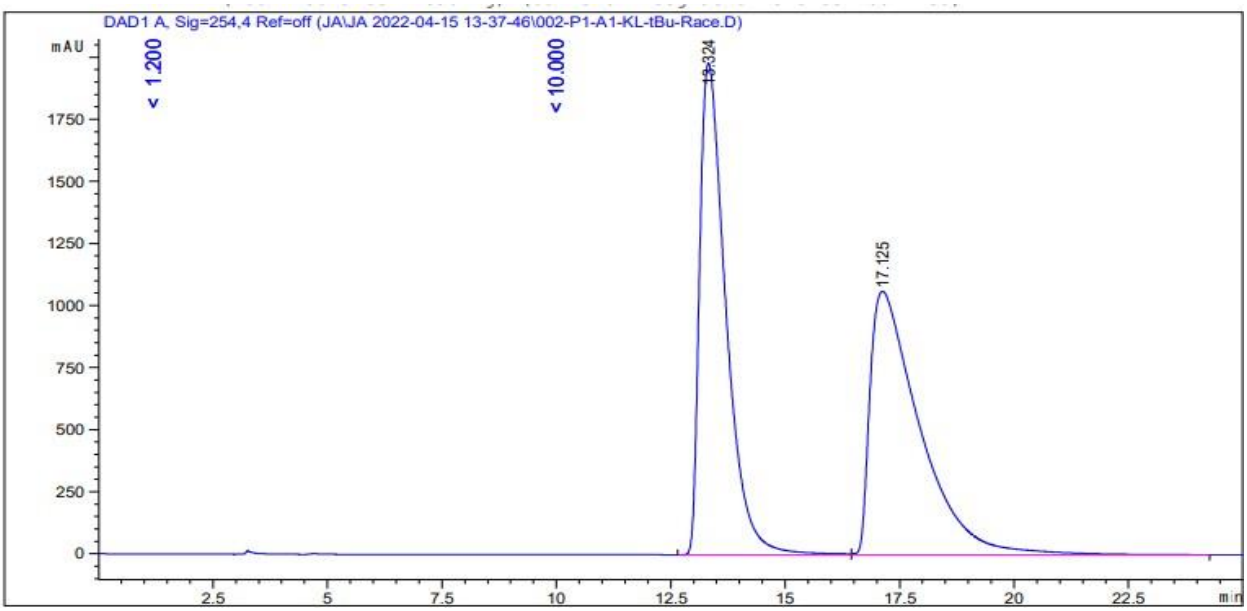

Signal 1: DAD1 A, Sig=254,4 Ref=off

Peak #	RetTime [min]	Type	Width [min]	Area [mAU*s]	Height [mAU]	Area %
1	13.324	BV	0.6078	7.90920e4	1980.91040	49.6854
2	17.125	VB	1.0883	8.00935e4	1061.47498	50.3146
Totals :				1.59185e5	3042.38538	

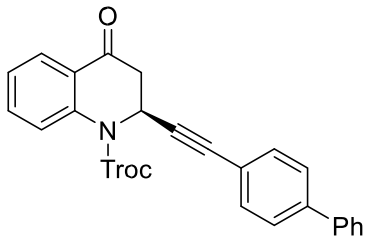

2,2,2-trichloroethyl (S)-2-([1,1'-biphenyl]-4-ylethynyl)-4-oxo-3,4-dihydroquinoline-1(2H)carboxylate (1e): Prepared according to the general procedure, using MTBE, BOX ligand, quinolone (66.1 mg, 0.20 mmol) and phenyl acetylene (0.26 mmol). **1e** was isolated as a white solid, 36% yield. R_f = 0.48 (4:1, Hexanes:EtOAc), $[\alpha]^{23}_D$ = +90.7 (c = 0.9, $CHCl_3$), ^{1}H NMR (500 MHz, Chloroform-*d*) δ 8.09 (dd, *J* = 7.9, 1.7 Hz, 1H), 7.92 (d, *J* = 8.4 Hz, 1H), 7.60 (ddd, *J* = 8.4, 7.3, 1.8 Hz, 1H), 7.54 – 7.48 (m, 2H), 7.48 – 7.38 (m, 4H), 7.38 – 7.23 (m, 4H), 6.14 (dd, *J* = 5.6, 2.1 Hz, 1H), 5.13 (d, *J* = 11.9 Hz, 1H), 4.79 (d, *J* = 11.9 Hz, 1H), 3.21 (dd, *J* = 17.2, 5.5 Hz, 1H), 3.04 (dd, *J* = 17.2, 2.1 Hz, 1H).

^{13}C NMR (126 MHz, $CDCl_3$) δ 191.69, 151.62, 141.74, 140.44, 140.25, 134.69, 132.37, 128.98, 127.88, 127.35, 127.13, 127.02, 125.48, 125.31, 124.61, 120.56, 94.94, 85.59, 85.34, 75.99, 47.94, 44.80. Chiral HPLC: 93.5:6.4 e.r., 88% ee, Chiralcel OD-H column (2% iPrOH/Hexanes, 1 mL/min, 254 nm); t_R (minor) = 42.6 min, t_R (major) = 28.9 min.

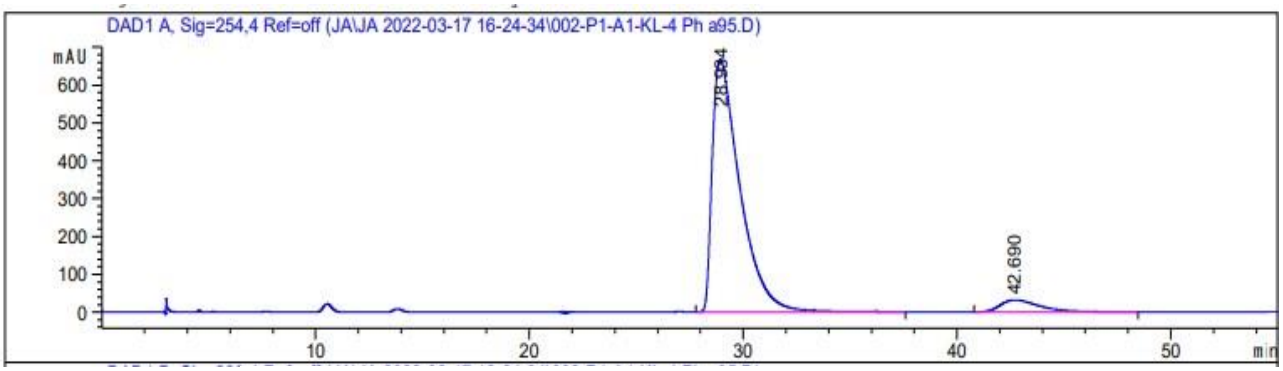

Signal 1: DAD1 A, Sig=254,4 Ref=off

Peak #	RetTime [min]	Type	Width [min]	Area [mAU*s]	Height [mAU]	Area %
1	28.934	BB	1.3623	6.00878e4	667.42188	93.5009
2	42.690	BB	1.6698	4176.63867	32.10321	6.4991
Totals :				6.42644e4	699.52509	

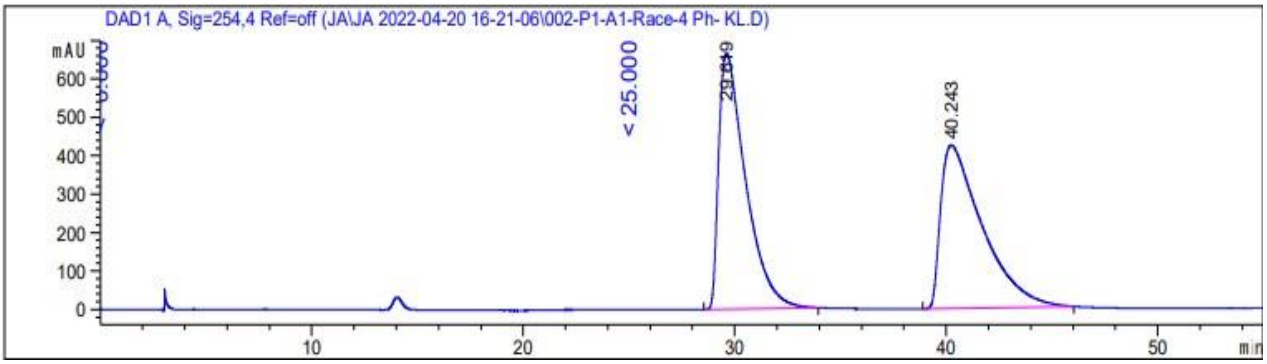

Signal 1: DAD1 A, Sig=254,4 Ref=off

Peak #	RetTime [min]	Type	Width [min]	Area [mAU*s]	Height [mAU]	Area %
1	29.619	BB	1.0538	5.89762e4	665.87250	50.3900
2	40.243	VB R	1.5986	5.80632e4	424.95569	49.6100
Totals :				1.17039e5	1090.82819	

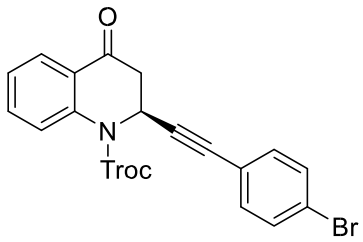

2,2,2-trichloroethyl (S)-2-((4-bromophenyl)ethynyl)-4-oxo-3,4-dihydroquinoline-1(2H)carboxylate (1f): Prepared according to the general procedure, using MTBE, BOX ligand, quinolone (66.1 mg, 0.20 mmol) and phenyl acetylene (0.26 mmol). **1f** was isolated as a white solid, 80% yield. R_f = 0.46 (4:1, Hexanes:EtOAc), $[\alpha]^{23}_D$ = +90.7 (c = 0.9, $CHCl_3$), ^{1}H NMR (500 MHz, Chloroform-*d*) δ 8.07 (ddd, *J* = 7.9, 1.8, 0.5 Hz, 1H), 7.90 (d, *J* = 8.4 Hz, 1H),

7.60 (ddd, *J* = 8.4, 7.3, 1.7 Hz, 1H), 7.38 – 7.32 (m, 2H), 7.29 (ddd, *J* = 8.3, 7.4, 1.1 Hz, 1H), 7.07 – 7.00 (m, 2H), 6.10 (dd, *J* = 5.6, 2.0 Hz, 1H), 5.11 (d, *J* = 11.9 Hz, 1H), 4.78 (d, *J* = 11.9 Hz, 1H), 3.19 (dd, *J* = 17.2, 5.6 Hz, 1H), 3.01 (dd, *J* = 17.2, 2.1 Hz, 1H).

^{13}C NMR (126 MHz, $CDCl_3$) δ 191.53, 151.59, 140.36, 134.75, 133.37, 131.65, 127.37, 125.53, 125.21, 124.57, 123.34, 120.63, 94.90, 86.16, 84.38, 76.01, 47.84, 44.63. Chiral HPLC: 94.0:5.9 e.r., 88% ee, Chiralcel OD-H column (2% iPrOH/Hexanes, 1 mL/min, 254 nm); t_R (minor) = 18.3 min, t_R (major) = 14.6 min.

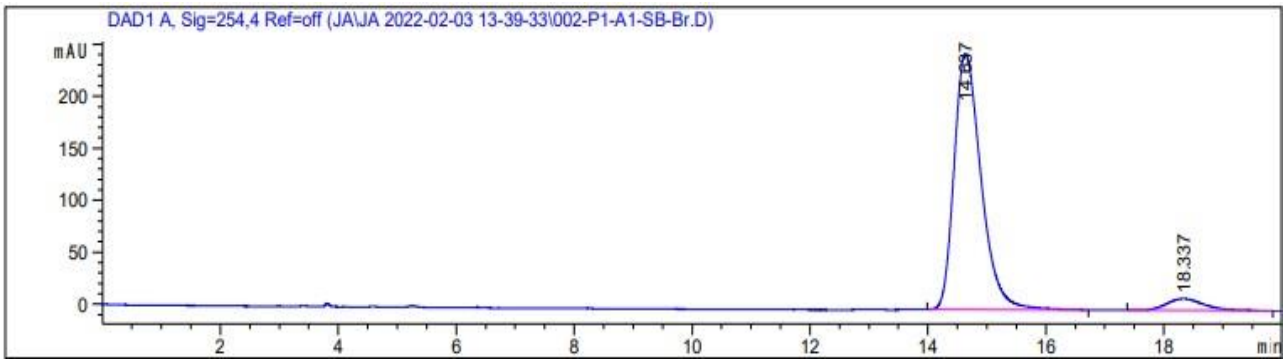

Signal 1: DAD1 A, Sig=254,4 Ref=off

Peak #	RetTime [min]	Type	Width [min]	Area [mAU*s]	Height [mAU]	Area %
1	14.637	BB	0.4840	7843.97803	245.99385	94.0725
2	18.337	BB	0.5191	494.24631	11.23771	5.9275
Totals :				8338.22433	257.23156	

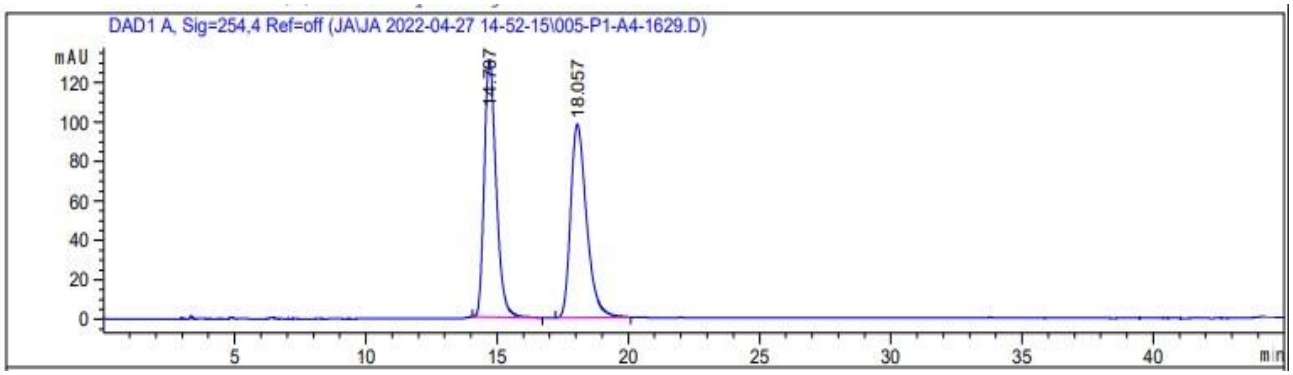

Signal 1: DAD1 A, Sig=254,4 Ref=off

Peak #	RetTime [min]	Type	Width [min]	Area [mAU*s]	Height [mAU]	Area %
1	14.707	BB	0.4871	4121.79736	130.27281	49.8967
2	18.057	BB	0.6440	4138.86523	98.14156	50.1033
Totals :				8260.66260	228.41438	

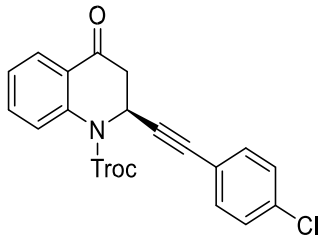

2,2,2-trichloroethyl (S)-2-((4-chlorophenyl)ethynyl)-4-oxo-3,4-dihydroquinoline-1(2H)carboxylate (**1g**): Prepared according to the general procedure, using MTBE, BOX ligand, quinolone (66.1 mg, 0.20 mmol) and phenyl acetylene (0.26 mmol). **1g** was isolated as a white solid, 56% yield. R_f = 0.47 (4:1, Hexanes:EtOAc), $[\alpha]^{23}_D$ = +90.7 (c = 0.9, $CHCl_3$), ^{1}H NMR (500 MHz, Chloroform-*d*) δ 8.07 (ddd, *J* = 7.8, 1.7, 0.5 Hz, 1H), 7.90 (d, *J* = 8.4 Hz, 1H), 7.60 (ddd, *J* = 8.4, 7.3, 1.7 Hz, 1H), 7.29 (ddd, *J* = 7.8, 7.3, 1.1 Hz, 1H), 7.22 – 7.16 (m, 2H), 7.14 – 7.07 (m, 2H), 6.11 (dd, *J* = 5.6, 2.0 Hz, 1H), 5.11 (d, *J* = 11.9 Hz, 1H), 4.78 (d, *J* = 11.9 Hz, 1H), 3.19 (dd, *J* = 17.2, 5.6 Hz, 1H), 3.01 (dd, *J* = 17.2, 2.0 Hz, 1H).

^{13}C NMR (126 MHz, $CDCl_3$) δ 191.54, 151.59, 140.36, 135.09, 134.73, 133.18, 128.71, 127.36, 125.51, 125.20, 124.57, 120.16, 94.89, 85.97, 84.32, 76.00, 47.82, 44.64. Chiral HPLC: 95.9:4.0 e.r., 92% ee, Chiralcel OD-H column (2% iPrOH/Hexanes, 1 mL/min, 254 nm); t_R (minor) = 17.3 min, t_R (major) = 13.6 min

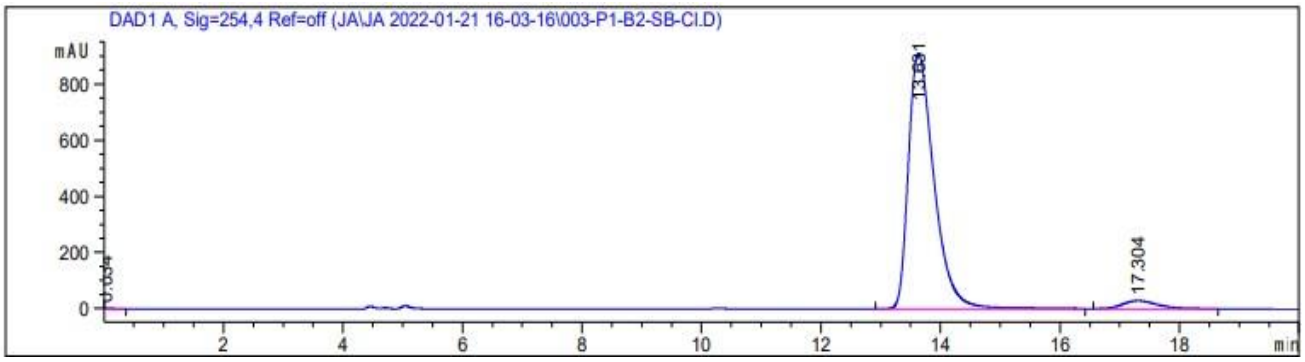

Signal 1: DAD1 A, Sig=254,4 Ref=off

Peak #	RetTime [min]	Type	Width [min]	Area [mAU*s]	Height [mAU]	Area %
1	0.034	BB	0.0902	9.26423	1.34804	0.0328
2	13.631	BB	0.4569	2.71188e4	909.42816	95.9451
3	17.304	BB	0.4741	1136.85315	28.51901	4.0221
Totals :				2.82649e4	939.29522	

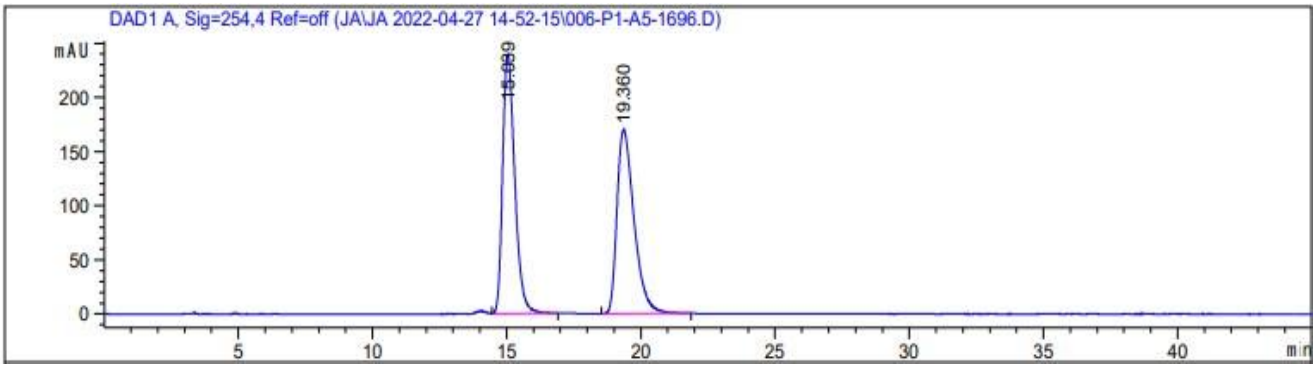

Signal 1: DAD1 A, Sig=254,4 Ref=off

Peak #	RetTime [min]	Type	Width [min]	Area [mAU*s]	Height [mAU]	Area %
1	15.039	BB	0.4825	7488.26563	239.67830	49.9155
2	19.360	BB	0.6777	7513.61768	169.96693	50.0845
Totals :				1.50019e4	409.64523	

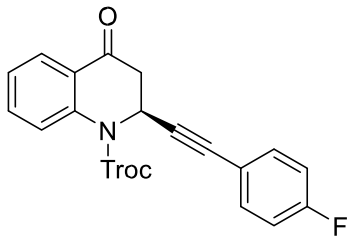

2,2,2-trichloroethyl (S)-2-((4-fluorophenyl)ethynyl)-4-oxo-3,4-dihydroquinoline-1(2H)carboxylate (**1h**): Prepared according to the general procedure, using MTBE, BOX ligand, quinolone (66.1 mg, 0.20 mmol) and phenyl acetylene (0.26 mmol). **1h** was isolated as a white solid, 36% yield. R_f = 0.48 (4:1, Hexanes:EtOAc), $[\alpha]^{23}_D$ = +90.7 (c = 0.9, $CHCl_3$), ^{1}H NMR (500 MHz, Chloroform-*d*) δ 8.08 (dd, *J* = 7.9, 1.7 Hz, 1H), 7.93 – 7.88 (m, 1H), 7.60 (ddd, *J* = 8.4, 7.3, 1.8 Hz, 1H), 7.32 – 7.22 (m, 1H), 7.20 – 7.11 (m, 2H), 6.94 – 6.86 (m, 2H), 6.11 (dd, *J* = 5.6, 2.1 Hz, 1H), 5.12 (d, *J* = 11.9 Hz, 1H), 4.78 (d, *J* = 11.9 Hz, 1H), 3.19 (dd, *J* = 17.2, 5.6 Hz, 1H), 3.01 (dd, *J* = 17.2, 2.1 Hz, 1H).

^{13}C NMR (126 MHz, $CDCl_3$) δ 191.62, 163.88, 161.89, 151.60, 140.39, 134.71, 133.93 (d, *J* = 7.6 Hz), 127.34, 125.48, 125.23, 124.58, 117.78 (d, *J* = 2.5 Hz), 115.68 (d, *J* = 21.4 Hz), 94.91, 84.72, 84.40, 75.99, 47.82, 44.71. Chiral HPLC: 96.6:3.3 e.r., 93% ee, Chiralcel OD-H column (2% iPrOH/Hexanes, 1 mL/min, 254 nm); t_R (minor) = 17.3 min, t_R (major) = 13.5 min.

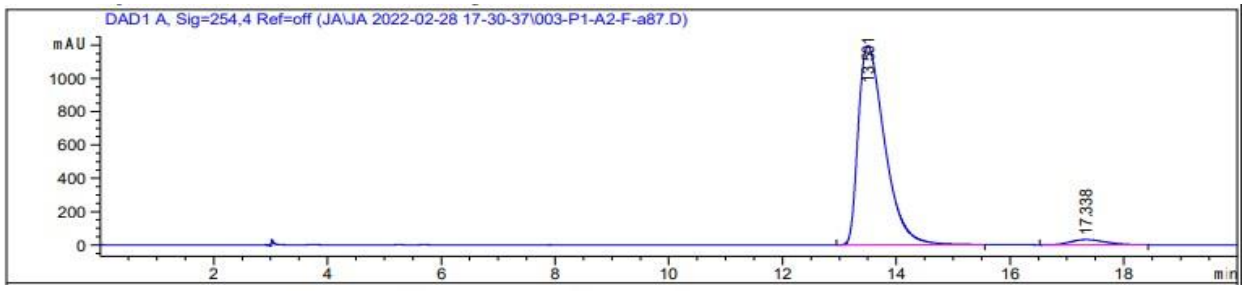

Signal 1: DAD1 A, Sig=254,4 Ref=off

Peak #	RetTime [min]	Type	Width [min]	Area [mAU*s]	Height [mAU]	Area %
1	13.501	BB	0.4900	3.85796e4	1193.81750	96.6395
2	17.338	VB R	0.5046	1341.57007	31.45226	3.3605
Totals :				3.99212e4	1225.26977	

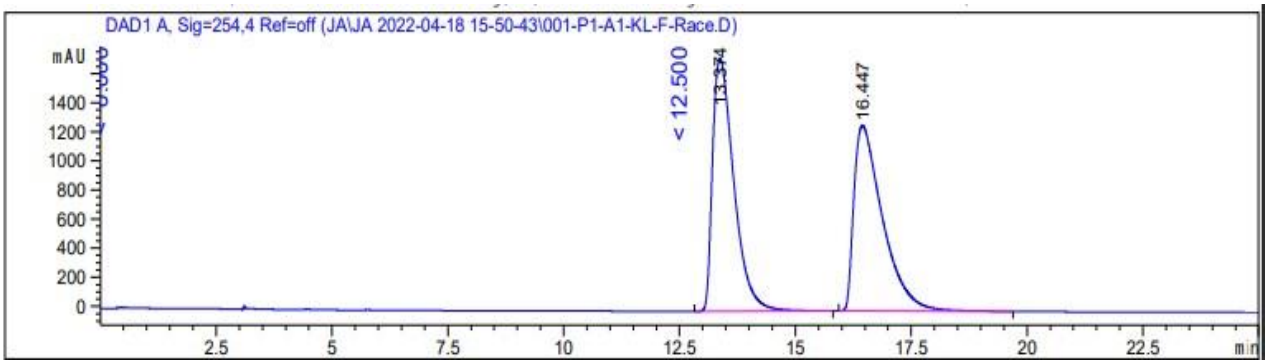

Signal 1: DAD1 A, Sig=254,4 Ref=off

Peak #	RetTime [min]	Type	Width [min]	Area [mAU*s]	Height [mAU]	Area %
1	13.374	BB	0.4735	5.57584e4	1736.94507	50.2363
2	16.447	BB	0.6124	5.52338e4	1277.42847	49.7637
Totals :				1.10992e5	3014.37354	

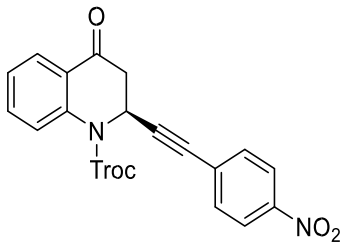

2,2,2-trichloroethyl (S)-2-((4-nitrophenyl)ethynyl)-4-oxo-3,4-dihydroquinoline-1(2H)carboxylate (**1i**): Prepared according to the general procedure, using MTBE, BOX ligand, quinolone (66.1 mg, 0.20 mmol) and phenyl acetylene (0.26 mmol). **1i** was isolated as a yellow solid, 71% yield. R_f = 0.35 (4:1, Hexanes:EtOAc), $[\alpha]^{23}_D$ = +90.7 (c = 0.9, $CHCl_3$), ^{1}H NMR (500 MHz, Chloroform-*d*) δ 8.14 – 8.07 (m, 3H), 7.94 (d, *J* = 8.4 Hz, 1H), 7.64 (ddd, *J* = 8.4, 7.3, 1.7 Hz, 1H), 7.38 – 7.31 (m, 3H), 6.19 (dd, *J* = 5.6, 2.1 Hz, 1H), 5.14 (d, *J* = 11.9 Hz, 1H), 4.82 (d, *J* = 11.9 Hz, 1H), 3.25 (dd, *J* = 17.3, 5.7 Hz, 1H), 3.06 (dd, *J* = 17.3, 2.0 Hz, 1H). ^{13}C NMR (126 MHz, $CDCl_3$) δ 191.19, 151.56, 147.59, 140.25, 134.90, 132.79, 128.42, 127.46, 125.68, 125.07, 124.54, 123.59, 94.83, 90.18, 83.40, 76.07, 47.78, 44.37. Chiral HPLC: 95.6:4.3 e.r., 91% ee, Chiralcel OD-H column (2% iPrOH/Hexanes, 1 mL/min, 254 nm); t_R (minor) = 15.9 min, t_R (major) = 19.7 min.

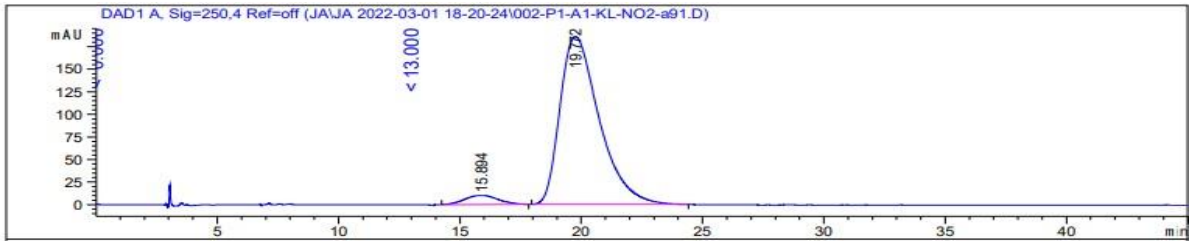

Signal 1: DAD1 A, Sig=250,4 Ref=off

Peak #	RetTime [min]	Type	Width [min]	Area [mAU*s]	Height [mAU]	Area %
1	15.894	BB	1.1267	960.76740	10.11010	4.3911
2	19.772	BB	1.6534	2.09191e4	185.81703	95.6089
Totals :				2.18798e4	195.92713	

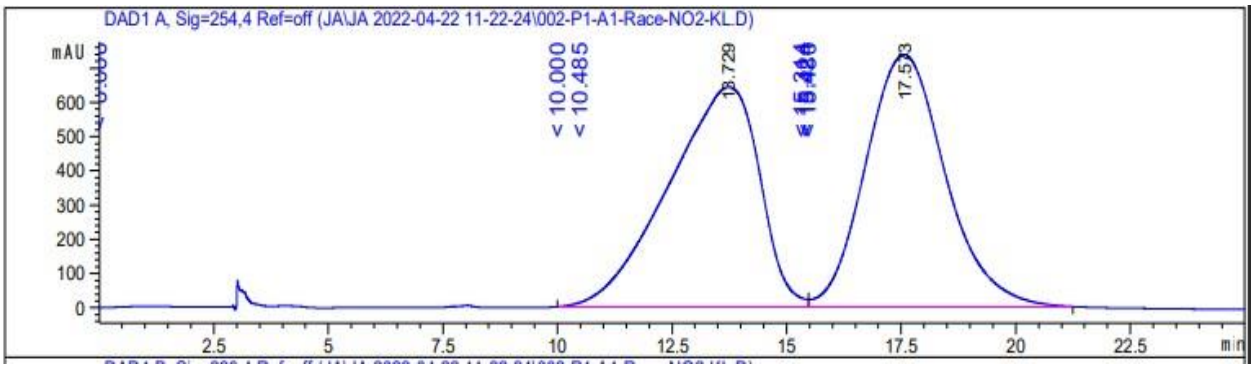

Signal 1: DAD1 A, Sig=254,4 Ref=off

Peak #	RetTime [min]	Type	Width [min]	Area [mAU*s]	Height [mAU]	Area %
1	13.729	BV S	1.6139	8.86125e4	641.77881	49.8510
2	17.573	VB S	1.4183	8.91422e4	736.40808	50.1490
Totals :				1.77755e5	1378.18689	

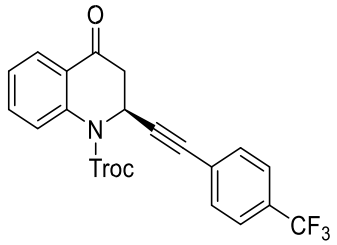

2,2,2-trichloroethyl (S)-2-((4-trifluoromethylphenyl)ethynyl)-4-oxo-3,4-dihydroquinoline1(2H)-carboxylate (**1j**): Prepared according to the general procedure, using MTBE, BOX ligand, quinolone (66.1 mg, 0.20 mmol) and phenyl acetylene (0.26 mmol). **1j** was isolated as a white solid, 67% yield. R_f = 0.53 (4:1, Hexanes:EtOAc), $[\alpha]^{23}_D$ = +90.7 (c = 0.9, $CHCl_3$), ^{1}H NMR (500 MHz, Chloroform-*d*) δ 8.08 (ddd, *J* = 7.9, 1.7, 0.5 Hz, 1H), 7.91 (d, *J* = 8.4 Hz, 1H), 7.61 (ddd, *J* = 8.4, 7.3, 1.7 Hz, 1H), 7.47 (dt, *J* = 8.0, 0.7 Hz, 2H), 7.32 – 7.27 (m, 3H), 6.14 (dd, *J* = 5.6, 2.0 Hz, 1H), 5.12 (d, *J* = 11.9 Hz, 1H), 4.79 (d, *J* = 11.9 Hz, 1H), 3.21 (dd, *J* = 17.3, 5.6 Hz, 1H), 3.03 (dd, *J* = 17.3, 2.0 Hz, 1H).

^{13}C NMR (126 MHz, $CDCl_3$) δ 191.38, 151.57, 140.32, 134.79, 132.23, 130.72 (q, *J* = 32.8 Hz), 127.42, 127.37, 125.59, 125.47, 125.29 (q, *J* = 3.8 Hz), 125.17, 124.56, 123.83 (q, *J* = 272 Hz), 94.87, 87.44, 84.00, 76.03, 47.78 (q, *J* = 3.8 Hz), 44.54.

^{19}F NMR (471 MHz, $CDCl_3$) δ -63.02.Chiral HPLC: 96.2:3.7 e.r., 93% ee, Chiralcel OD-H column (2% iPrOH/Hexanes, 1 mL/min, 254 nm); t_R (minor) = 15.0 min, t_R (major) = 12.3 min.

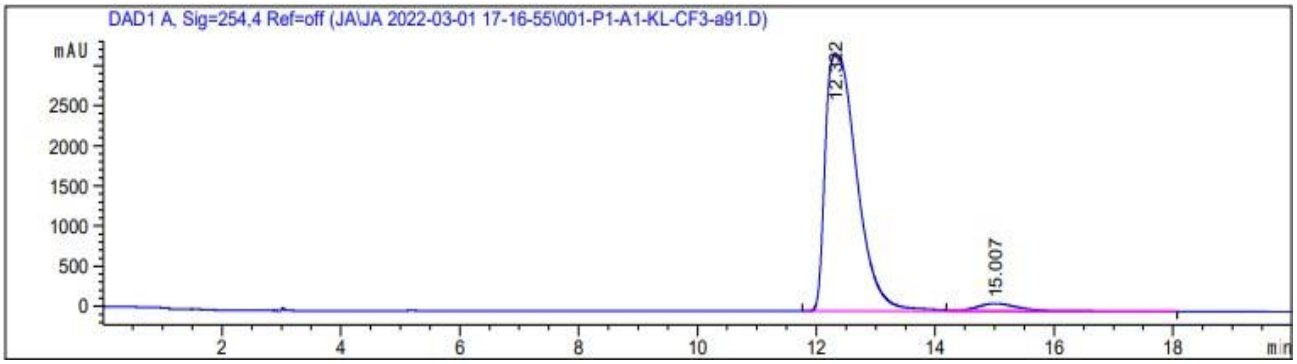

Signal 1: DAD1 A, Sig=254,4 Ref=off

Peak #	RetTime [min]	Type	Width [min]	Area [mAU*s]	Height [mAU]	Area %
1	12.322	BV R	0.4412	1.18638e5	3209.60059	96.2857
2	15.007	VB E	0.6796	4576.55176	94.07646	3.7143
Totals :				1.23215e5	3303.67705	

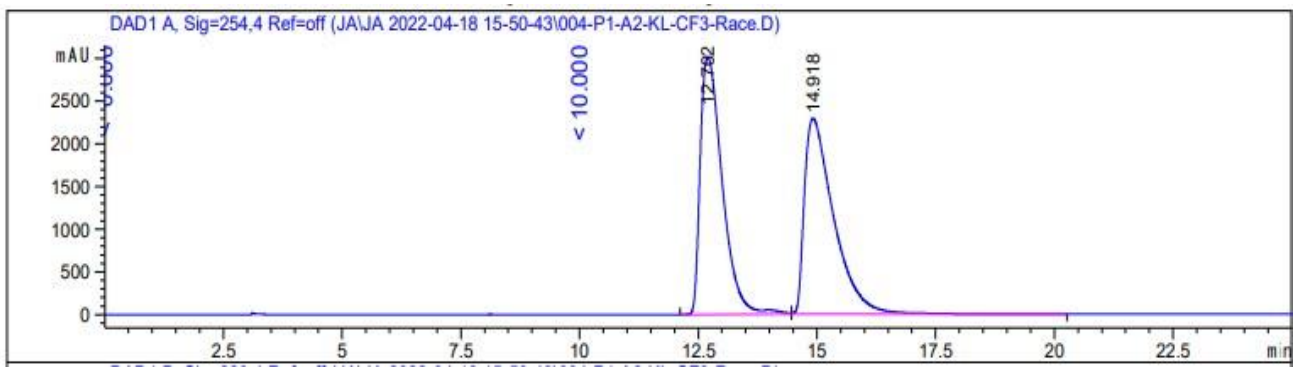

Signal 1: DAD1 A, Sig=254,4 Ref=off

Peak #	RetTime [min]	Type	Width [min]	Area [mAU*s]	Height [mAU]	Area %
1	12.702	BV R	0.5022	9.74912e4	3007.39087	49.5536
2	14.918	VB	0.6422	9.92477e4	2296.66089	50.4464
Totals :				1.96739e5	5304.05176	

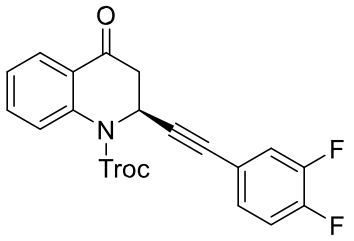

2,2,2-trichloroethyl (S)-2-((3,4-difluorophenyl)ethynyl)-4-oxo-3,4-dihydroquinoline1(2H)-carboxylate (**1k**): Prepared according to the general procedure, using MTBE, BOX ligand, quinolone (66.1 mg, 0.20 mmol) and phenyl acetylene (0.26 mmol). **1k** was isolated as a white solid, 64% yield. R_f = 0.40 (4:1, Hexanes:EtOAc), $[\alpha]^{23}_D$ = +90.7 (c = 0.9, $CHCl_3$), ^{1}H NMR (500 MHz, Chloroform-*d*) δ 8.08 (ddd, *J* = 7.8, 1.7, 0.5 Hz, 1H), 7.90 (d, *J* = 8.4 Hz, 1H), 7.61 (ddd, *J* = 8.4, 7.3, 1.7 Hz, 1H), 7.30 (ddd, *J* = 7.8, 7.3, 1.1 Hz, 1H), 7.05 – 6.96 (m, 2H), 6.96 – 6.89 (m, 1H), 6.10 (dd, *J* = 5.6, 2.0 Hz, 1H), 5.11 (d, *J* = 11.9 Hz, 1H), 4.78 (d, *J* = 11.9 Hz, 1H), 3.19 (dd, *J* = 17.2, 5.6 Hz, 1H), 3.00 (dd, *J* = 17.2, 2.1 Hz, 1H).

^{13}C NMR (126 MHz, $CDCl_3$) δ 191.40, 152.04, 151.94, 151.56, 150.96, 150.86, 150.03, 149.93, 148.98, 148.87, 140.31, 134.78, 128.73, 128.69, 128.67, 128.65, 127.37, 125.56, 125.14, 124.54, 121.02, 120.88, 118.50, 118.47, 118.44, 118.41, 117.62, 117.48, 94.87, 85.61, 85.59, 83.27, 76.01, 47.72, 44.54. Chiral HPLC: 94.9:5.0 e.r., 90% ee, Chiralcel OD-H column (2% iPrOH/Hexanes, 1 mL/min, 254 nm); t_R (minor) = 18.7 min, t_R (major) = 14.2 min.

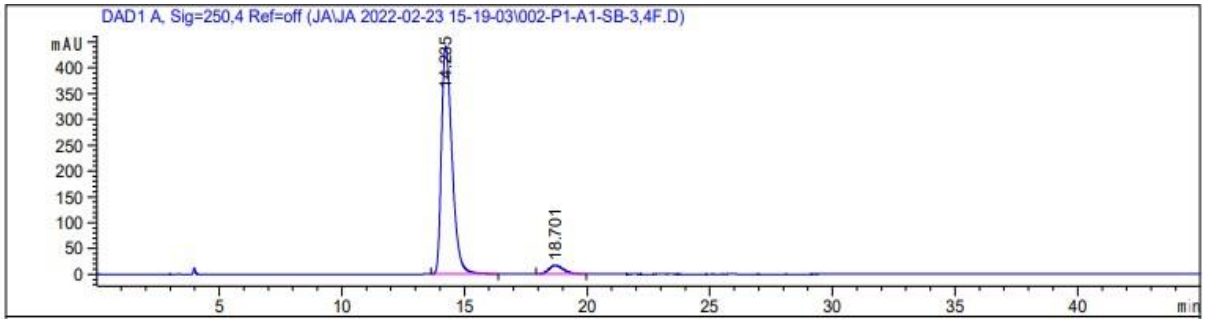

Signal 1: DAD1 A, Sig=250,4 Ref=off

Peak #	RetTime [min]	Type	Width [min]	Area [mAU*s]	Height [mAU]	Area %
1	14.235	BB	0.4602	1.31283e4	439.86429	94.9512
2	18.701	BB	0.6080	698.06732	16.75762	5.0488
Totals :				1.38264e4	456.62191	

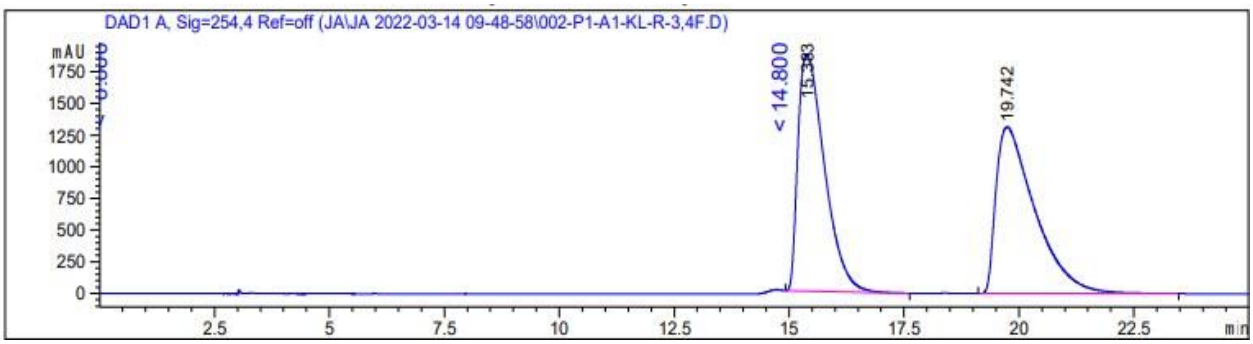

Signal 1: DAD1 A, Sig=254,4 Ref=off

Peak #	RetTime [min]	Type	Width [min]	Area [mAU*s]	Height [mAU]	Area %
1	15.383	BB	0.4900	7.53782e4	1871.00964	49.2470
2	19.742	BB	0.7139	7.76833e4	1315.52185	50.7530
Totals :				1.53062e5	3186.53149	

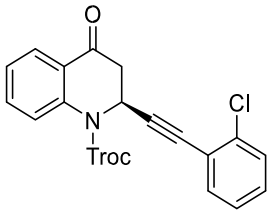

2,2,2-trichloroethyl (S)-2-((2-chlorophenyl)ethynyl)-4-oxo-3,4-dihydroquinoline-1(2H)carboxylate (**1l**): Prepared according to the general procedure, using MTBE, BOX ligand, quinolone (66.1 mg, 0.20 mmol) and phenyl acetylene (0.26 mmol). **XX** was isolated as a white solid, 92% yield. R_f = 0.46 (4:1,

Hexanes:EtOAc), $[\alpha]^{23}_D$ = +90.7 (c = 0.9, $CHCl_3$), ^{1}H NMR (500 MHz, Chloroform-*d*) δ 8.08 (dd, *J* = 7.9, 1.7 Hz, 1H), 7.89 (d, *J* = 8.4 Hz, 1H), 7.59 (ddd, *J* = 8.3, 7.3, 1.7 Hz, 1H), 7.31 – 7.21 (m, 3H), 7.18 (td, *J* = 7.7, 1.7 Hz, 1H), 7.11 (td, *J* = 7.5, 1.3 Hz, 1H), 6.15 (dd, *J* = 5.5, 2.0 Hz, 1H), 5.12 (d, *J* = 11.9 Hz, 1H), 4.77 (d, *J* = 11.9 Hz, 1H), 3.22 (dd, *J* = 17.3, 5.6 Hz, 1H), 3.05 (dd, *J* = 17.3, 2.0 Hz, 1H).

^{13}C NMR (126 MHz, $CDCl_3$) δ 191.54, 151.58, 140.44, 136.47, 134.63, 133.32, 129.96, 129.30, 127.45, 126.41, 125.54, 125.52, 124.75, 121.75, 94.91, 90.31, 82.26, 76.00, 47.97, 44.76. Chiral HPLC: 97.8:2.1 e.r., 95% ee, Chiralcel OD-H column (2% iPrOH/Hexanes, 1 mL/min, 254 nm); t_R (minor) = 21.3 min, t_R (major) = 17.2 min.

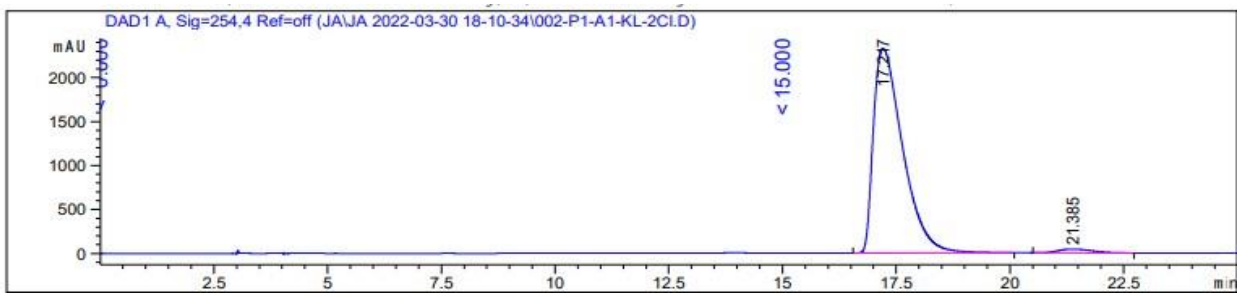

Signal 1: DAD1 A, Sig=254,4 Ref=off

Peak #	RetTime [min]	Type	Width [min]	Area [mAU*s]	Height [mAU]	Area %
1	17.217	BV R	0.5265	1.04366e5	2327.91992	97.8341
2	21.385	BB	0.6160	2310.49536	44.33838	2.1659
Totals :				1.06677e5	2372.25830	

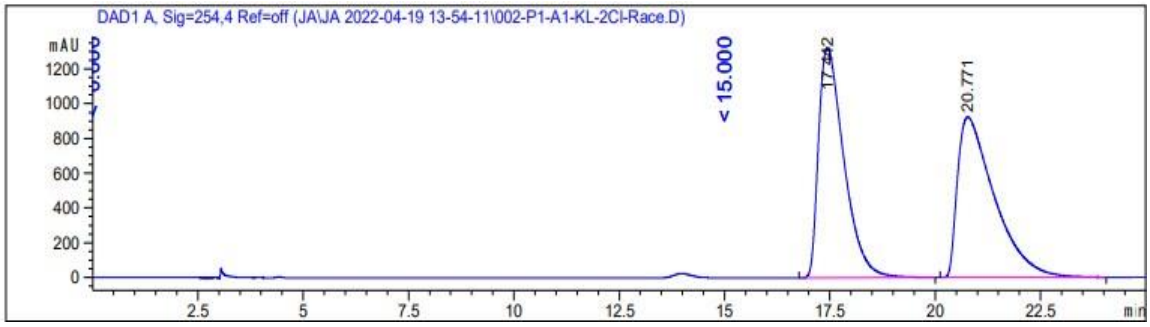

Signal 1: DAD1 A, Sig=254,4 Ref=off

Peak #	RetTime [min]	Type	Width [min]	Area [mAU*s]	Height [mAU]	Area %
1	17.442	BB	0.6031	5.55982e4	1324.91309	49.6783
2	20.771	BB	0.8352	5.63182e4	924.44714	50.3217
Totals :				1.11916e5	2249.36023	

Appendix 5B: Quinolone Substitutions

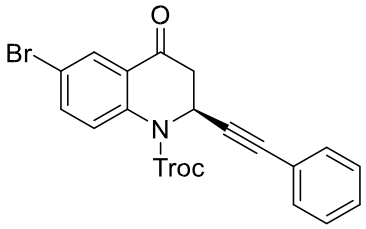

2,2,2-trichloroethyl (S)-6-bromo-4-oxo-2-(phenylethynyl)-3,4-dihydroquinoline-1(2H)carboxylate (**2a**): Prepared according to the general procedure, using MTBE, BOX ligand, quinolone (66.1 mg, 0.20 mmol) and phenyl acetylene (, 0.26 mmol). **2a** was isolated as a white solid, 50% yield. R_f = 0.58 (4:1, Hexanes:EtOAc), $[\alpha]^{23}_D$ = +90.7 (c = 0.9, $CHCl_3$ ^{1}H NMR (500 MHz, Chloroform-*d*) δ 8.19 (d, *J* = 2.5 Hz, 1H), 7.83 (d, *J* = 8.9 Hz, 1H), 7.68 (dd, *J* =

8.9, 2.5 Hz, 1H), 7.32 – 7.18 (m, 5H), 6.12 (dd, *J* = 5.5, 2.1 Hz, 1H), 5.10 (d, *J* = 11.9 Hz, 1H),

4.79 (d, *J* = 11.9 Hz, 1H), 3.17 (dd, *J* = 17.2, 5.5 Hz, 1H), 3.03 (dd, *J* = 17.2, 2.1 Hz, 1H).

^{13}C NMR (126 MHz, $CDCl_3$) δ 190.38, 151.36, 139.35, 137.35, 131.99, 130.04, 129.10, 128.39, 126.41, 126.27, 121.47, 118.89, 94.77, 85.78, 84.42, 76.06, 47.75, 44.49. Chiral HPLC: 95.3:4.6 e.r., 93% ee,

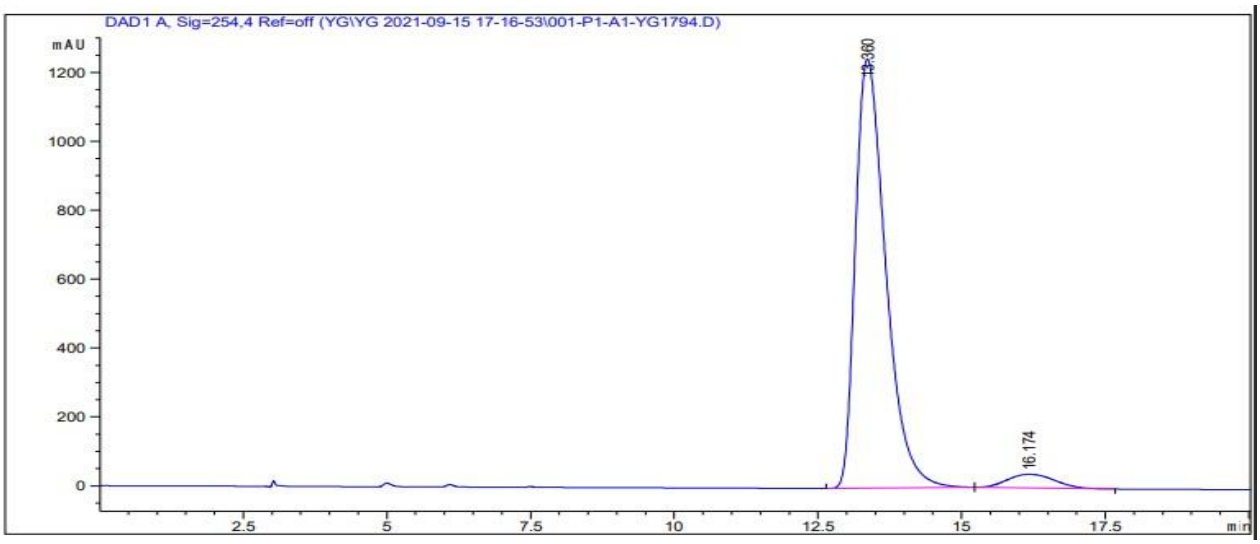

Signal 1: DAD1 A, Sig=254,4 Ref=off

Peak #	RetTime [min]	Type	Width [min]	Area [mAU*s]	Height [mAU]	Area %
1	13.360	BB	0.5678	4.56518e4	1245.05530	95.3131
2	16.174	BB	0.9074	2244.86890	39.48029	4.6869
Totals :				4.78967e4	1284.53558	

Chiralcel OD-H column (2% iPrOH/Hexanes, 1 mL/min, 254 nm); t_R (minor) = 16.1 min, t_R (major) = 13.3 min.

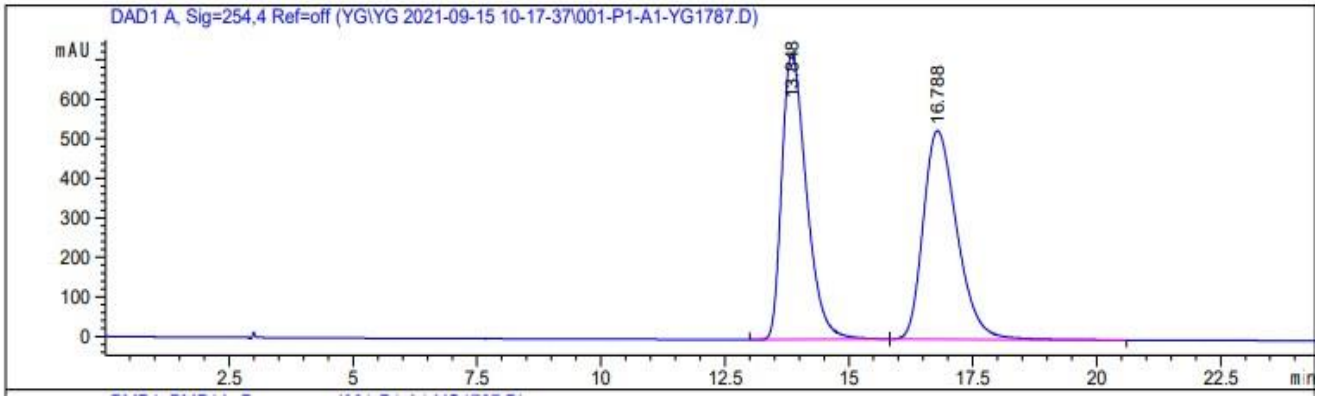

Signal 1: DAD1 A, Sig=254,4 Ref=off

Peak #	RetTime [min]	Type	Width [min]	Area [mAU*s]	Height [mAU]	Area %
1	13.848	BB	0.5330	2.49661e4	722.75922	50.0065
2	16.788	BB	0.7316	2.49596e4	527.94995	49.9935
Totals :				4.99257e4	1250.70917	

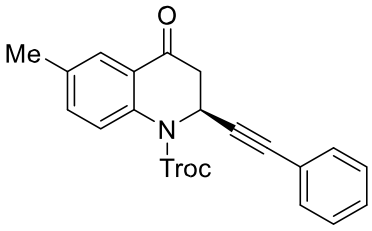

2,2,2-trichloroethyl (S)-6-methyl-4-oxo-2-(phenylethynyl)-3,4-dihydroquinoline-1(2H)carboxylate (**2b**): Prepared according to the general procedure, using MTBE, BOX ligand, quinolone (66.1 mg, 0.20 mmol) and phenyl acetylene (0.26 mmol). **2b** was isolated as a white solid, 42% yield. R_f = 0.52 (4:1, Hexanes:EtOAc), $[\alpha]^{23}_D$ = +90.7 (c = 0.9, $CHCl_3$ ^{1}H NMR (500 MHz, Chloroform-*d*) δ 7.89 – 7.84 (m, 1H), 7.78 (d, *J* = 8.5 Hz, 1H), 7.40 (ddd, *J* = 8.5, 2.3, 0.7 Hz, 1H), 7.30 – 7.17 (m, 5H), 6.10 (dd, *J* = 5.6, 2.0 Hz, 1H), 5.11 (d, *J* = 11.9 Hz, 1H), 4.76 (d, *J* = 11.9 Hz, 1H), 3.17 (dd, *J* = 17.2, 5.6 Hz, 1H), 3.00 (dd, *J* = 17.2, 2.0 Hz, 1H), 2.38 (s, 3H).

^{13}C NMR (126 MHz, $CDCl_3$) δ 191.93, 151.66, 138.03, 135.58, 135.28, 131.97, 128.88, 128.32, 127.31, 124.99, 124.48, 121.81, 94.98, 85.23, 85.11, 75.95, 47.81, 44.76, 20.89. Chiral HPLC: 96.5:3.4 e.r., 93%

ee, Chiralcel OD-H column (2% iPrOH/Hexanes, 1 mL/min, 254 nm); t_R (minor) = 21.0 min, t_R (major) = 12.8 min.

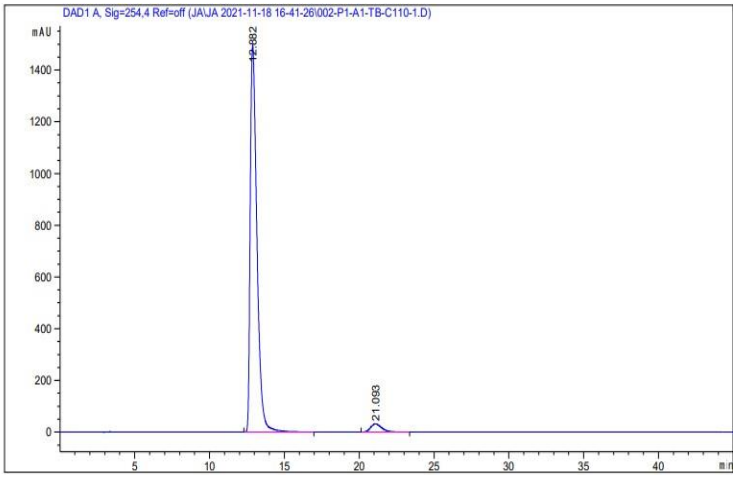

Signal 1: DAD1 A, Sig=254,4 Ref=off

Peak #	RetTime [min]	Type	Width [min]	Area [mAU*s]	Height [mAU]	Area %
1	12.882	BB	0.4761	4.64379e4	1496.20056	96.5994
2	21.093	BB	0.7705	1634.77844	31.55271	3.4006
Totals :				4.80726e4	1527.75327	

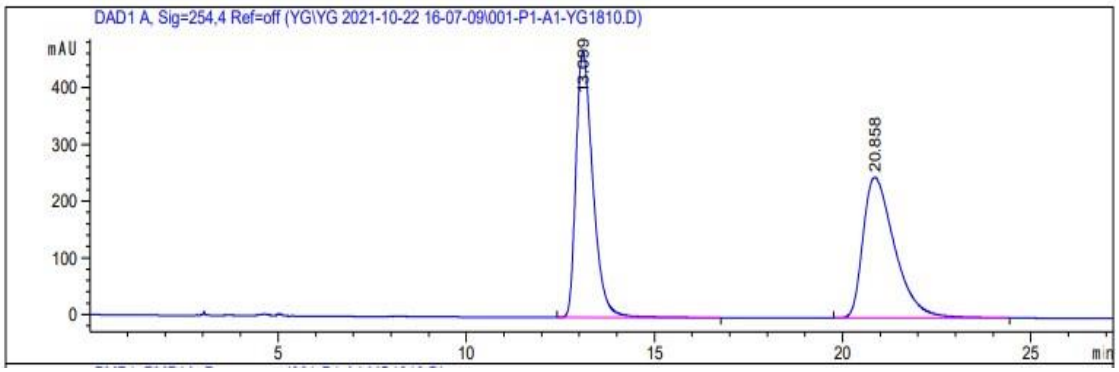

Signal 1: DAD1 A, Sig=254,4 Ref=off

Peak #	RetTime [min]	Type	Width [min]	Area [mAU*s]	Height [mAU]	Area %
1	13.099	BB	0.4797	1.45938e4	468.09033	50.1782
2	20.858	BB	0.9014	1.44901e4	248.10376	49.8218
Totals :				2.90839e4	716.19409	

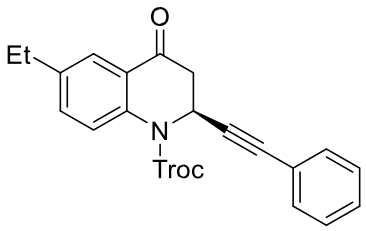

2,2,2-trichloroethyl (S)-6-ethyl-4-oxo-2-(phenylethynyl)-3,4-dihydroquinoline-1(2H)carboxylate (**2c**): Prepared according to the general procedure, using MTBE, BOX ligand, quinolone (66.1 mg, 0.20 mmol) and phenyl acetylene (0.26 mmol). **2c** was isolated as a white solid, 80% yield. R_f = 0.55 (4:1, Hexanes:EtOAc), $[\alpha]^{23}_D$ = +90.7 (c = 0.9, $CHCl_3$ ^{1}H NMR (500 MHz, Chloroform-*d*) δ 7.89 (d, *J* = 2.3 Hz, 1H), 7.81 (d, *J* = 8.5 Hz, 1H), 7.43 (dd, *J* =

8.5, 2.3 Hz, 1H), 7.29 – 7.17 (m, 5H), 6.10 (dd, *J* = 5.6, 2.0 Hz, 1H), 5.12 (d, *J* = 11.9 Hz, 1H), 4.76 (d, *J* = 11.9 Hz, 1H), 3.17 (dd, *J* = 17.2, 5.6 Hz, 1H), 3.00 (dd, *J* = 17.2, 2.1 Hz, 1H), 2.69 (q, *J* = 7.6 Hz, 2H), 1.26 (t, *J* = 7.6 Hz, 3H).
^{13}C NMR (126 MHz, $CDCl_3$) δ 191.97, 151.67, 141.52, 138.21, 134.50, 131.97, 128.88, 128.31, 126.11, 125.08, 124.51, 121.84, 95.00, 85.26, 85.16, 75.93, 47.83, 44.77, 28.26, 15.29. Chiral HPLC: 96.4:3.5 e.r., 93% ee, Chiralcel OD-H column (2% iPrOH/Hexanes, 1 mL/min, 254 nm); t_R (minor) = 16.2 min, t_R (major) = 11.1 min.

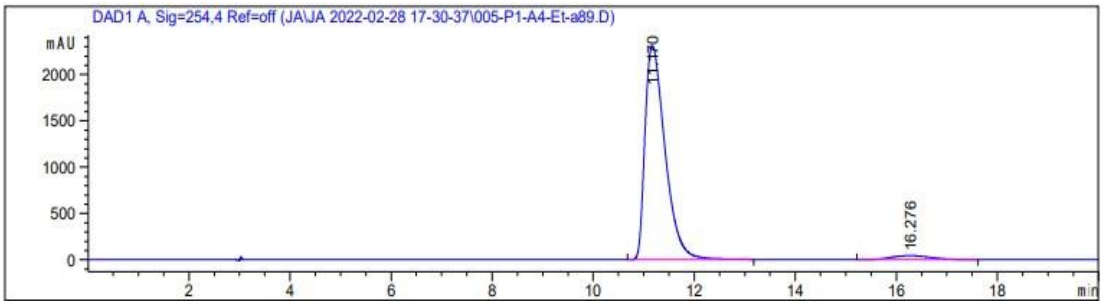

Signal 1: DAD1 A, Sig=254,4 Ref=off

Peak #	RetTime [min]	Type	Width [min]	Area [mAU*s]	Height [mAU]	Area %
1	11.170	BB	0.3729	6.38113e4	2312.74170	96.4090
2	16.276	BV R	0.6389	2376.78076	43.77721	3.5910
Totals :				6.61880e4	2356.51891	

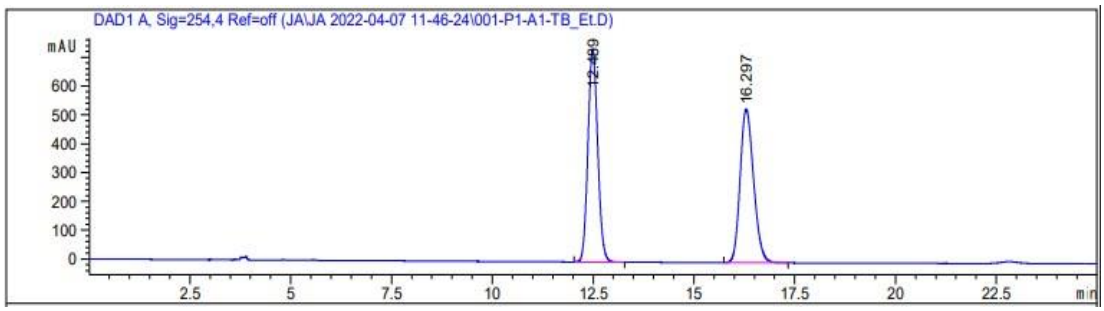

Signal 1: DAD1 A, Sig=254,4 Ref=off

Peak #	RetTime [min]	Type	Width [min]	Area [mAU*s]	Height [mAU]	Area %
1	12.489	BB	0.2615	1.24284e4	739.91943	50.0416
2	16.297	BB	0.3625	1.24078e4	533.20587	49.9584
Totals :				2.48362e4	1273.12531	

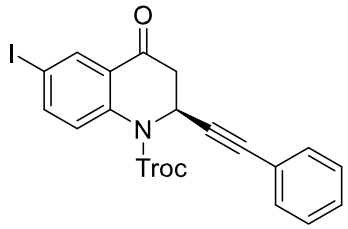

2,2,2-trichloroethyl (S)-6-iodo-4-oxo-2-(phenylethynyl)-3,4-dihydroquinoline-1(2H)carboxylate (**2d**): Prepared according to the general procedure, using MTBE, BOX ligand, quinolone (66.1 mg, 0.20 mmol) and phenyl acetylene (, 0.26 mmol). **2d** was isolated as a white solid, 35% yield. R_f = 0.47 (4:1, Hexanes:EtOAc), $[\alpha]^{23}_D$ = +90.7 (c = 0.9, $CHCl_3$ ^{1}H NMR (500 MHz, Chloroform-*d*) δ 8.37 (d, *J* = 2.2 Hz, 1H), 7.87 (dd, *J* = 8.8, 2.2 Hz, 1H), 7.70 (d, *J* = 8.7 Hz, 1H), 7.31 – 7.20 (m, 5H), 6.12 (dd, *J* = 5.5, 2.1 Hz, 1H), 5.10 (d, *J* = 11.9 Hz, 1H), 4.79 (d, *J* = 11.9 Hz, 1H), 3.17 (dd, *J* = 17.2, 5.5 Hz, 1H), 3.02 (dd, *J* = 17.2, 2.1 Hz, 1H).

^{13}C NMR (126 MHz, $CDCl_3$) δ 190.29, 151.34, 143.15, 140.05, 136.13, 132.01, 129.11, 128.40, 126.47, 126.33, 121.49, 94.77, 89.41, 85.76, 84.44, 76.07, 47.71, 44.42.

Chiral HPLC: 93.8:6.1 e.r., 85% ee, Chiralcel OD-H column (2% iPrOH/Hexanes, 1 mL/min, 254 nm); t_R (minor) = 14.4 min, t_R (major) = 16.8 min.

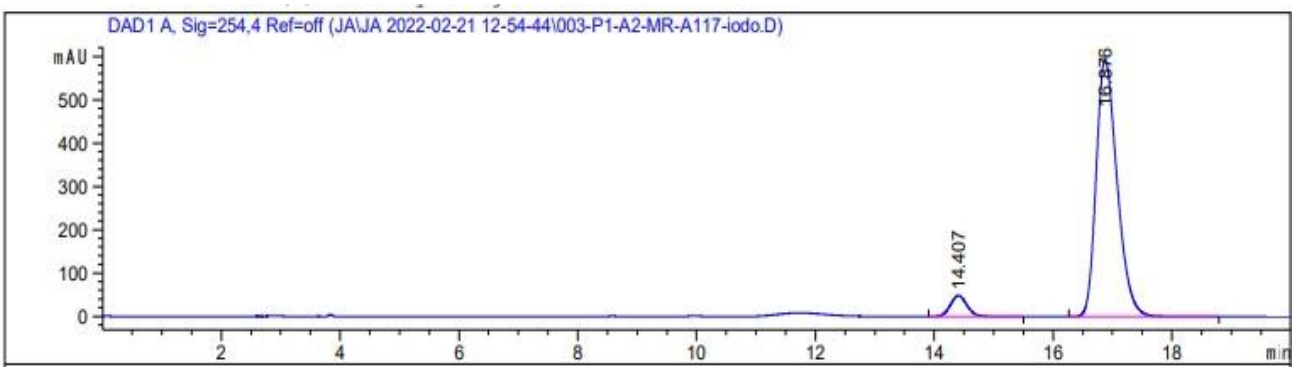

Signal 1: DAD1 A, Sig=254,4 Ref=off

Peak #	RetTime [min]	Type	Width [min]	Area [mAU*s]	Height [mAU]	Area %
1	14.407	BB	0.3029	949.62964	48.82121	6.1548
2	16.876	BB	0.3768	1.44795e4	593.16699	93.8452
Totals :				1.54291e4	641.98820	

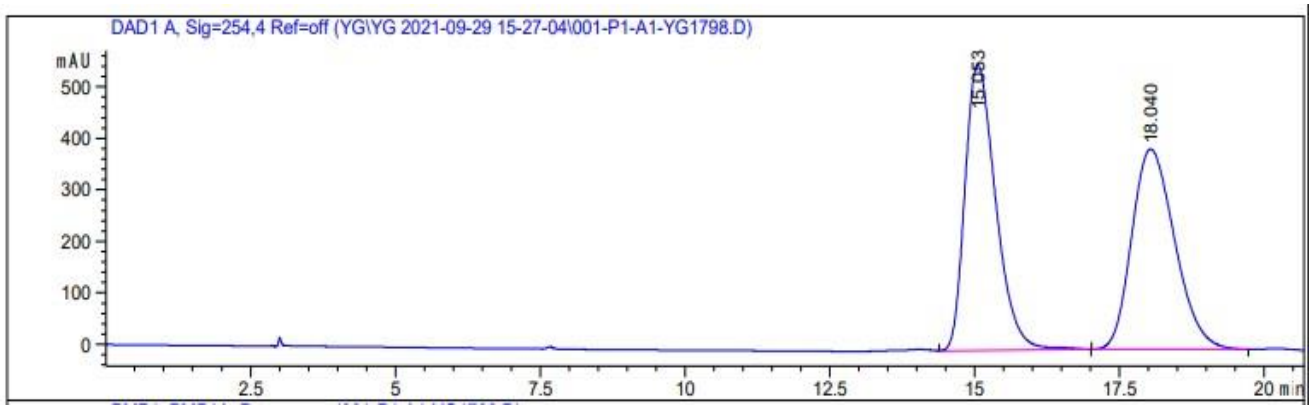

Signal 1: DAD1 A, Sig=254,4 Ref=off

Peak #	RetTime [min]	Type	Width [min]	Area [mAU*s]	Height [mAU]	Area %
1	15.053	BB	0.5710	2.04971e4	554.88739	50.5836
2	18.040	BB	0.8129	2.00242e4	388.77057	49.4164
Totals :				4.05213e4	943.65796	

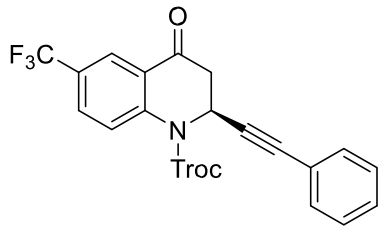

2,2,2-trichloroethyl (S)-6-trifluoromethyl-4-oxo-2-(phenylethynyl)-3,4-dihydroquinoline1(2H)-carboxylate (**2e**): Prepared according to the general procedure, using MTBE, BOX ligand, quinolone (66.1 mg, 0.20 mmol) and phenyl acetylene (0.26 mmol). **2e** was isolated as a white solid, 60% yield. R_f = 0.49 (4:1, Hexanes:EtOAc), $[\alpha]^{23}_D$ = +90.7 (c = 0.9, $CHCl_3$ ^{1}H NMR (500 MHz, Chloroform-*d*) δ 8.36 (d, *J* = 2.3 Hz, 1H), 8.12 (d, *J* = 8.7 Hz, 1H), 7.85 – 7.79 (m, 1H), 7.32 – 7.25 (m, 2H), 7.25 – 7.17 (m, 3H),

6.16 (dd, *J* = 5.4, 2.2 Hz, 1H), 5.13 (d, *J* = 11.9 Hz, 1H), 4.83 (d, *J* = 11.9 Hz, 1H), 3.21 (dd, *J* = 17.2, 5.5 Hz, 1H), 3.09 (dd, *J* = 17.2, 2.2 Hz, 1H).

^{13}C NMR (126 MHz, $CDCl_3$) δ 190.30, 151.39, 143.11, 131.99, 131.04 (q, *J* = 3.8 Hz), 129.20, 128.42, 127.51 (q, *J* = 32.8 Hz), 124.90, 124.86, 123.61 (q, *J* = 272 Hz), 121.35, 94.68, 85.99, 84.13, 76.16, 47.87, 44.43 (*1 aromatic signal overlapped*).
^{19}F NMR (471 MHz, $CDCl_3$) δ -62.72. Chiral HPLC: 94.8:5.1 e.r., 90% ee, Chiralcel OD-H column (2% iPrOH/Hexanes, 1 mL/min, 254 nm); t_R (minor) = 13.1 min, t_R (major) = 10.9 min.

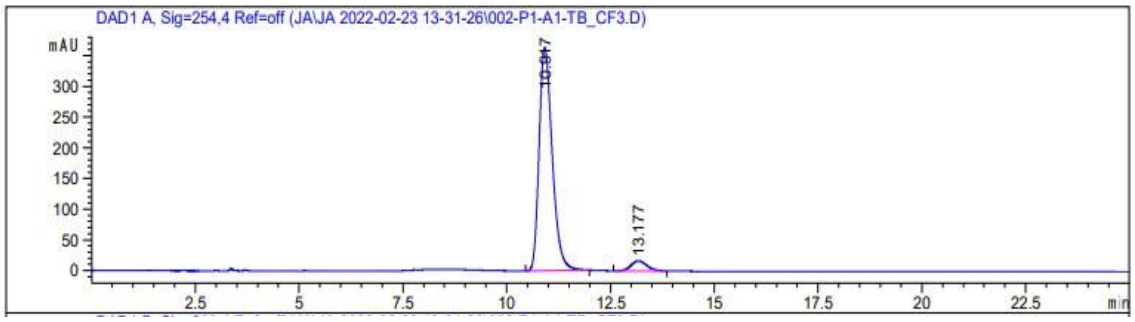

Signal 1: DAD1 A, Sig=254,4 Ref=off

Peak #	RetTime [min]	Type	Width [min]	Area [mAU*s]	Height [mAU]	Area %
1	10.917	BB	0.3357	7958.23193	363.16977	94.8688
2	13.177	VB R	0.3133	430.43542	16.31531	5.1312
Totals :				8388.66736	379.48508	

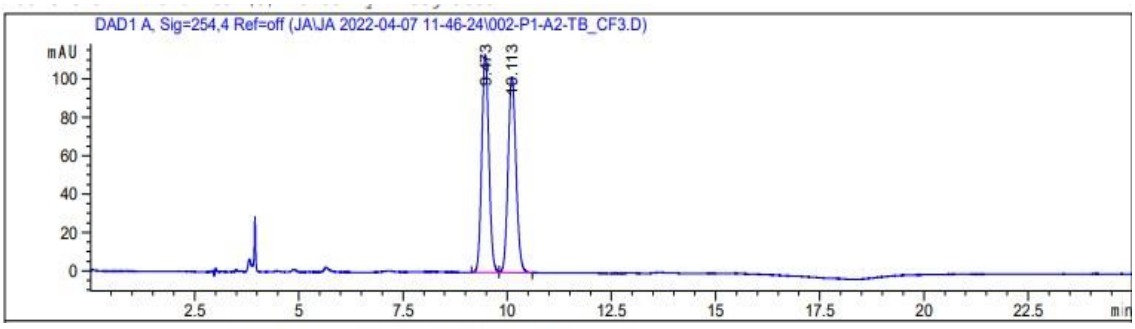

Signal 1: DAD1 A, Sig=254,4 Ref=off

Peak #	RetTime [min]	Type	Width [min]	Area [mAU*s]	Height [mAU]	Area %
1	9.473	VV R	0.1870	1357.48877	113.53748	50.0928
2	10.113	VV R	0.2057	1352.45911	102.00962	49.9072
Totals :				2709.94788	215.54710	

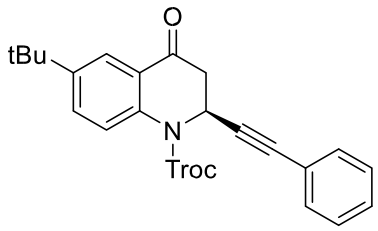

2,2,2-trichloroethyl (S)-6-tertbutyl-4-oxo-2-(phenylethynyl)-3,4-dihydroquinoline-1(2H)carboxylate (**2f**): Prepared according to the general procedure, using MTBE, BOX ligand, quinolone (66.1 mg, 0.20 mmol) and phenyl acetylene (0.26 mmol). **2f** was isolated as a white solid, 32% yield. R_f = 0.57 (4:1, Hexanes:EtOAc), $[\alpha]^{23}_D$ = +90.7 (c = 0.9, $CHCl_3$ ^{1}H NMR (500 MHz, Chloroform-*d*) δ 8.08 (d, *J* = 2.5 Hz, 1H), 7.84 (d, *J* = 8.7 Hz, 1H), 7.63 (dd, *J* =

8.8, 2.5 Hz, 1H), 7.29 – 7.16 (m, 5H), 6.10 (dd, *J* = 5.6, 2.1 Hz, 1H), 5.13 (d, *J* = 11.9 Hz, 1H), 4.77 (d, *J* = 12.0 Hz, 1H), 3.17 (dd, *J* = 17.1, 5.6 Hz, 1H), 3.01 (dd, *J* = 17.1, 2.1 Hz, 1H), 1.05 (s, 9H). ^{13}C NMR (126 MHz, $CDCl_3$) δ 191.98, 151.67, 148.47, 138.03, 132.16, 131.97, 128.87, 128.32, 124.68, 124.09, 123.76, 121.89, 95.03, 85.28, 85.24, 75.91, 47.81, 44.74, 34.78, 31.28. Chiral HPLC: 97.1:2.8 e.r., 95% ee, Chiralcel OD-H column (2% iPrOH/Hexanes, 1 mL/min, 254 nm); t_R (minor) = 8.6 min, t_R (major) = 10.5 min.

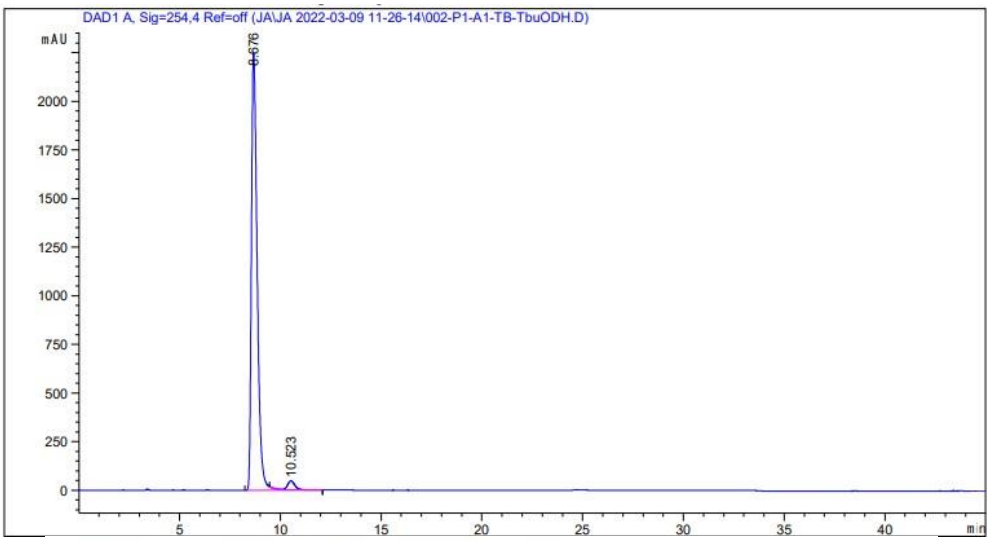

Signal 1: DAD1 A, Sig=254,4 Ref=off

Peak #	RetTime [min]	Type	Width [min]	Area [mAU*s]	Height [mAU]	Area %
1	8.676	BV R	0.3069	4.48000e4	2244.31299	97.1331
2	10.523	VB E	0.4098	1322.25867	47.94098	2.8669
Totals :				4.61223e4	2292.25397	

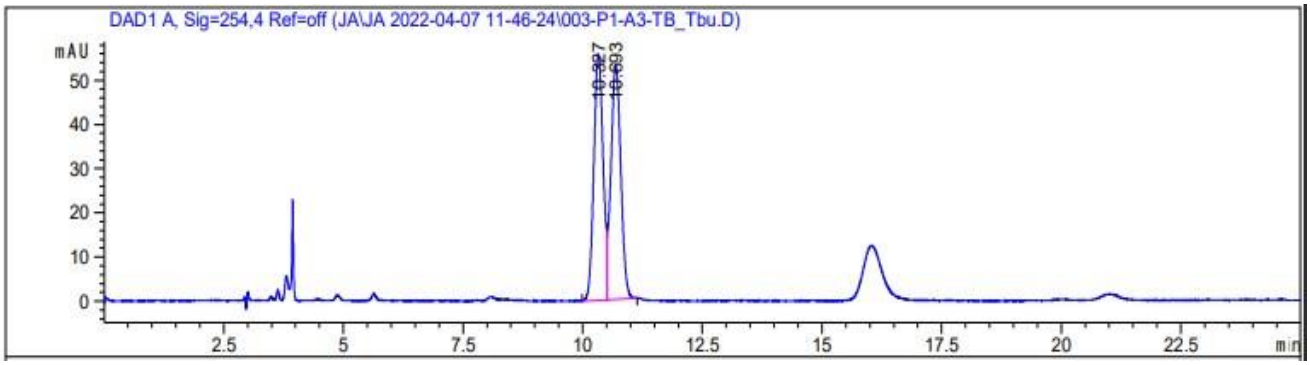

Signal 1: DAD1 A, Sig=254,4 Ref=off

Peak #	RetTime [min]	Type	Width [min]	Area [mAU*s]	Height [mAU]	Area %
1	10.327	BV	0.2041	747.22968	55.68189	49.5754
2	10.693	VV R	0.2086	760.02899	52.92068	50.4246
Totals :				1507.25867	108.60258	

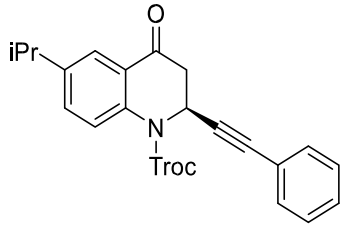

2,2,2-trichloroethyl (S)-6-isopropyl-4-oxo-2-(phenylethynyl)-3,4-dihydroquinoline-1(2H)carboxylate (**2g**): Prepared according to the general procedure, using MTBE, BOX ligand, quinolone (66.1 mg, 0.20 mmol) and phenyl acetylene (0.26 mmol). **2g** was isolated as a white solid, 44% yield. R_f = 0.52 (4:1, Hexanes:EtOAc), $[\alpha]^{23}_D$ = +90.7 (c = 0.9, $CHCl_3$ ^{1}H NMR (500 MHz, Chloroform-*d*) δ 7.92 (d, *J* = 2.3 Hz, 1H), 7.82 (d, *J* = 8.6 Hz, 1H), 7.46 (dd, *J* =

8.7, 2.3 Hz, 1H), 7.30 – 7.15 (m, 5H), 6.10 (dd, *J* = 5.6, 2.1 Hz, 1H), 5.13 (d, *J* = 11.9 Hz, 1H), 4.76 (d, *J* = 11.9 Hz, 1H), 3.17 (dd, *J* = 17.2, 5.6 Hz, 1H), 3.04 – 2.90 (m, 2H), 1.28 (d, *J* = 1.5 Hz, 3H), 1.27 (d, *J* = 1.5 Hz, 3H).
^{13}C NMR (126 MHz, $CDCl_3$) δ 191.98, 151.67, 146.13, 138.29, 133.21, 131.96, 128.88,

128.32, 125.07, 124.74, 124.46, 121.86, 95.02, 85.30, 85.20, 75.91, 47.83, 44.76, 33.67, 23.88, 23.80.
Chiral HPLC: 94.6:5.3 e.r., 90% ee, Chiralcel OD-H column (2% iPrOH/Hexanes, 1 mL/min, 254 nm); t_R (minor) = 10.7 min, t_R (major) = 14.6 min.

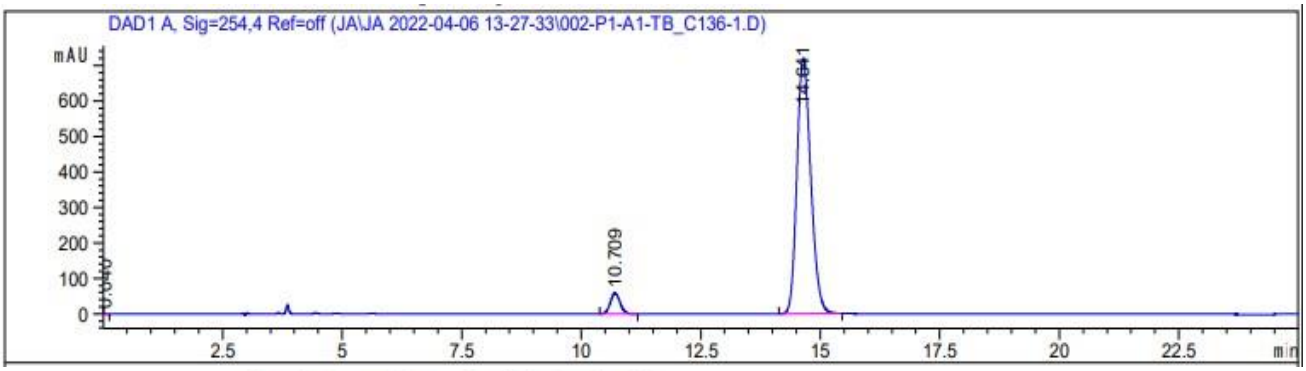

Signal 1: DAD1 A, Sig=254,4 Ref=off

Peak #	RetTime [min]	Type	Width [min]	Area [mAU*s]	Height [mAU]	Area %
1	0.040	BV	0.0661	5.42445	1.14769	0.0353
2	10.709	BV R	0.2204	821.75262	58.68016	5.3529
3	14.641	BB	0.3123	1.45242e4	720.04004	94.6117
Totals :				1.53514e4	779.86790	

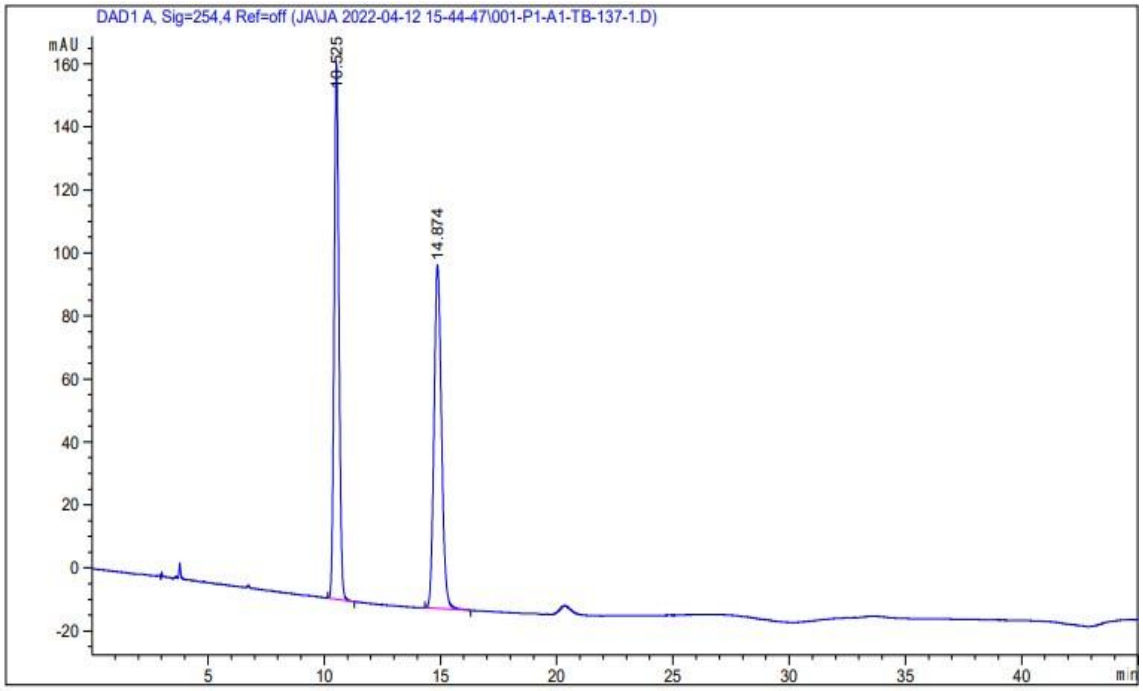

Signal 1: DAD1 A, Sig=254,4 Ref=off

Peak #	RetTime [min]	Type	Width [min]	Area [mAU*s]	Height [mAU]	Area %
1	10.525	BB	0.2238	2443.81885	169.92342	50.1279
2	14.874	BB	0.3463	2431.34985	108.97121	49.8721
Totals :				4875.16870	278.89463	

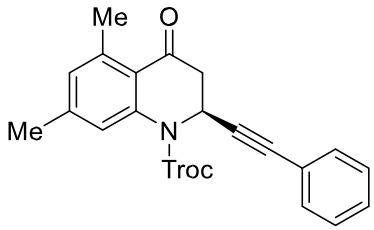

2,2,2-trichloroethyl (S)-5,7-dimethyl-4-oxo-2-(phenylethynyl)-3,4-dihydroquinoline1(2H)-carboxylate (**2h**): Prepared according to the general procedure, using MTBE, BOX ligand, quinolone (66.1 mg, 0.20 mmol) and phenyl acetylene (0.26 mmol). **2h** was isolated as a white solid, 27% yield. R_f = 0.54 (4:1, Hexanes:EtOAc), $[\alpha]^{23}_D$ = +90.7 (c = 0.9, $CHCl_3$ ^{1}H NMR (500 MHz, Chloroform-*d*) δ 7.45 (s, 1H), 7.30 – 7.16 (m, 7H), 6.94 – 6.90 (m, 1H), 6.02 (dd, *J* = 6.0, 1.7 Hz, 1H), 5.16 (d, *J* = 11.9 Hz, 1H), 4.66 (d, *J* = 11.9 Hz, 1H), 3.16 (dd, *J* = 17.5, 5.9 Hz, 1H), 2.95 (dd, *J* = 17.4, 1.8 Hz, 1H), 2.65 (s, 3H), 2.36 (s, 3H).

^{13}C NMR (126 MHz, $CDCl_3$) δ 193.17, 151.82, 144.04, 141.77, 141.19, 131.94, 130.87, 128.81, 128.33, 124.30, 122.33, 122.00, 95.08, 85.52, 85.08, 75.92, 47.35, 46.27, 23.21, 21.86. Chiral HPLC: 96.0:3.9 e.r., 92% ee, Chiralcel OD-H column (2% iPrOH/Hexanes, 1 mL/min, 254 nm); t_R (minor) = 7.2 min, t_R (major) = 14.3 min.

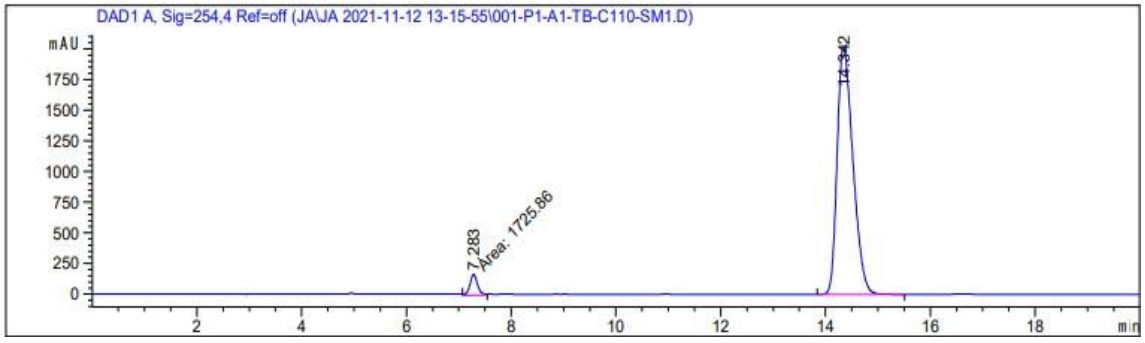

Signal 1: DAD1 A, Sig=254,4 Ref=off

Peak #	RetTime [min]	Type	Width [min]	Area [mAU*s]	Height [mAU]	Area %
1	7.283	MM	0.1707	1725.86011	168.51526	3.9439
2	14.342	BB	0.3232	4.20344e4	2016.80688	96.0561
Totals :				4.37603e4	2185.32214	

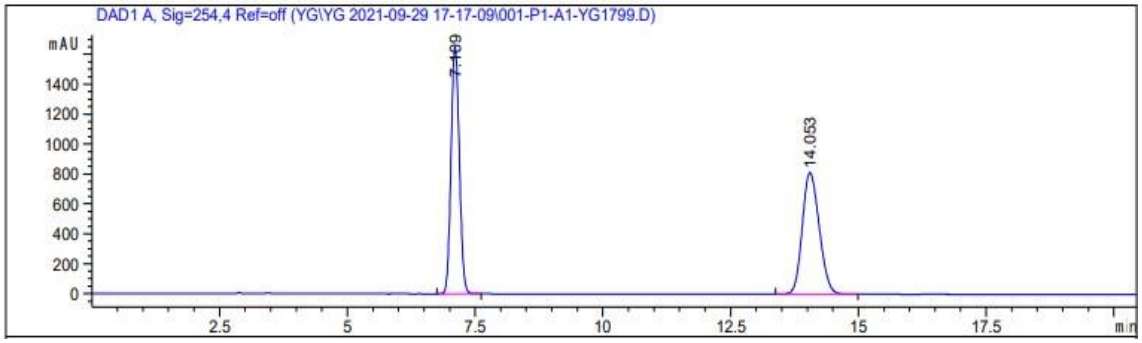

Signal 1: DAD1 A, Sig=254,4 Ref=off

Peak #	RetTime [min]	Type	Width [min]	Area [mAU*s]	Height [mAU]	Area %
1	7.109	BB	0.1777	1.86201e4	1649.82666	49.8559
2	14.053	BB	0.3611	1.87278e4	811.94574	50.1441
Totals :				3.73479e4	2461.77240	

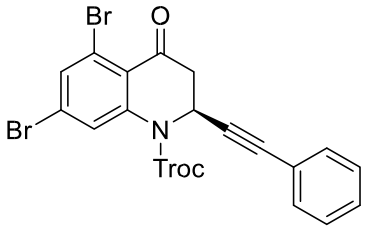

2,2,2-trichloroethyl (S)-5,7-dibromo-4-oxo-2-(phenylethynyl)-3,4-dihydroquinoline1(2H)-carboxylate (**2i**): Prepared according to the general procedure, using MTBE, BOX ligand, quinolone (66.1 mg, 0.20 mmol) and phenyl acetylene (0.26 mmol). **2i** was isolated as a white solid, 53% yield. R_f = 0.51 (4:1, Hexanes:EtOAc), $[\alpha]^{23}_D$ = +90.7 (c = 0.9, $CHCl_3$ ^{1}H NMR (500 MHz, Chloroform-*d*) δ 7.99 (d, *J* = 1.8 Hz, 1H), 7.75 (d, *J* = 1.9 Hz, 1H), 7.31 (ddt, *J* = 8.0, 5.9, 1.9 Hz, 1H), 7.28 – 7.20 (m, 4H), 6.03 (dd, *J* = 6.0, 1.8 Hz, 1H), 5.13 (d, *J* = 11.8 Hz, 1H), 4.71 (d, *J* = 11.8 Hz, 1H), 3.21 (dd, *J* = 17.8, 6.0 Hz, 1H), 3.07 (dd, *J* = 17.8, 1.8 Hz, 1H).

^{13}C NMR (126 MHz, $CDCl_3$) δ 189.46, 151.22, 142.62, 135.69, 132.02, 129.21, 128.46, 128.26, 127.82, 123.24, 122.55, 121.39, 94.62, 86.31, 84.34, 76.19, 47.14, 45.81.

. Chiral HPLC: 97.8:2.1 e.r., 96% ee, Chiralcel OD-H column (2% iPrOH/Hexanes, 1 mL/min, 254 nm); t_R (minor) = 8.1 min, t_R (major) = 15.9 min.

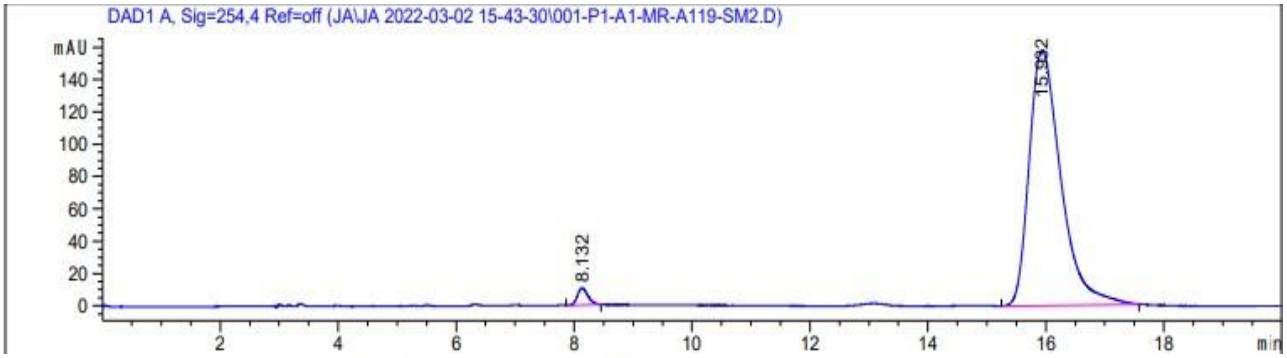

Signal 1: DAD1 A, Sig=254,4 Ref=off

Peak #	RetTime [min]	Type	Width [min]	Area [mAU*s]	Height [mAU]	Area %
1	8.132	BB	0.1643	129.18802	10.37176	2.1449
2	15.932	VB R	0.5046	5893.93457	157.87329	97.8551
Totals :				6023.12259	168.24505	

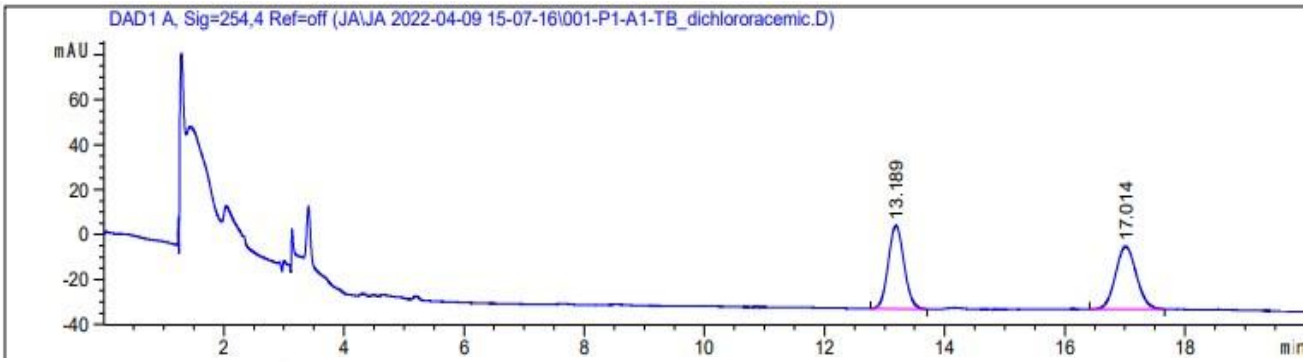

Signal 1: DAD1 A, Sig=254,4 Ref=off

Peak #	RetTime [min]	Type	Width [min]	Area [mAU*s]	Height [mAU]	Area %
1	13.189	BB	0.2614	677.38165	37.11715	50.0010
2	17.014	BB	0.3023	677.35480	27.99102	49.9990
Totals :				1354.73645	65.10817	

Appendix 6: ^{1}H NMR and ^{13}C NMR spectra

Appendix 6A: Phenylacetylene Substitutions

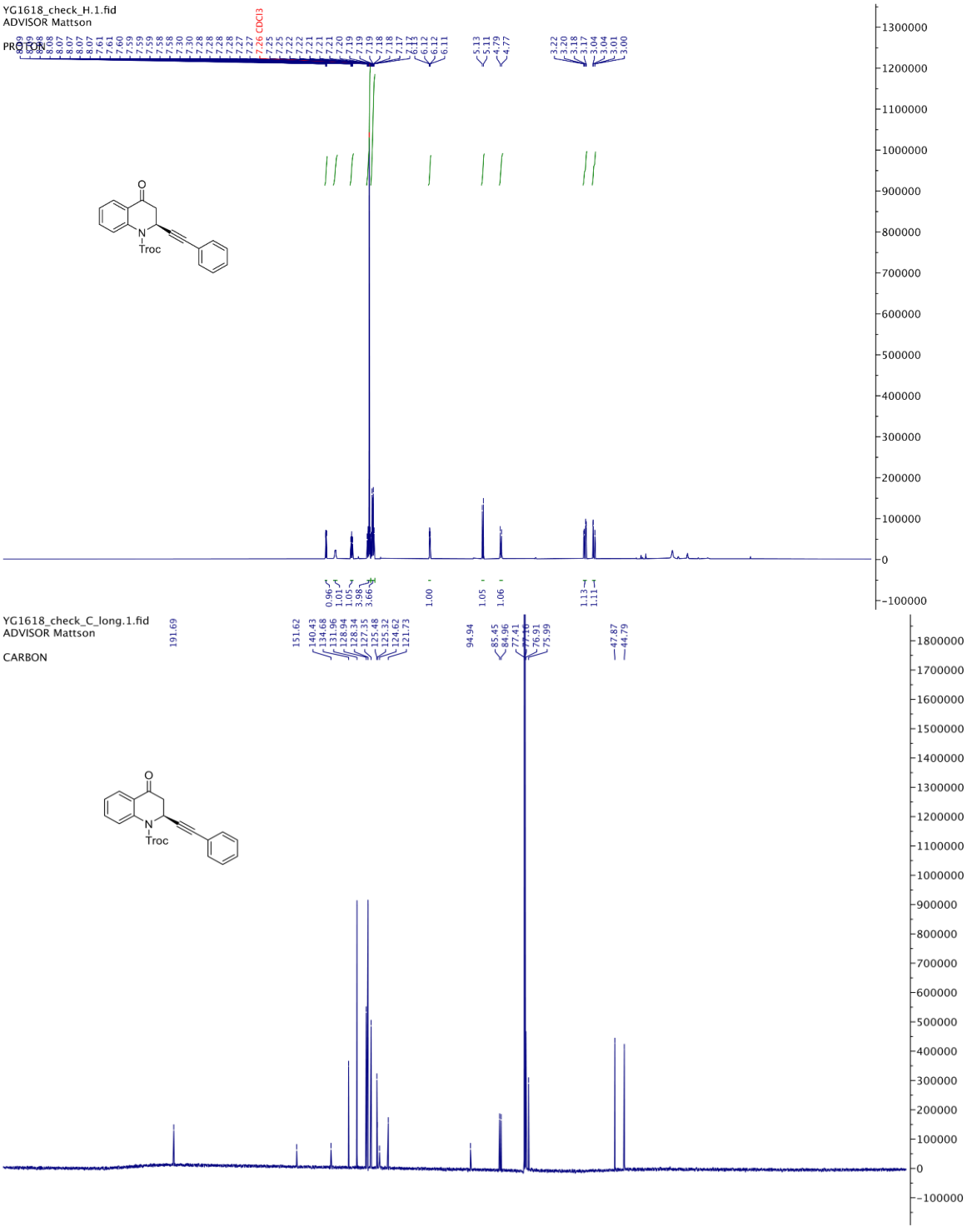

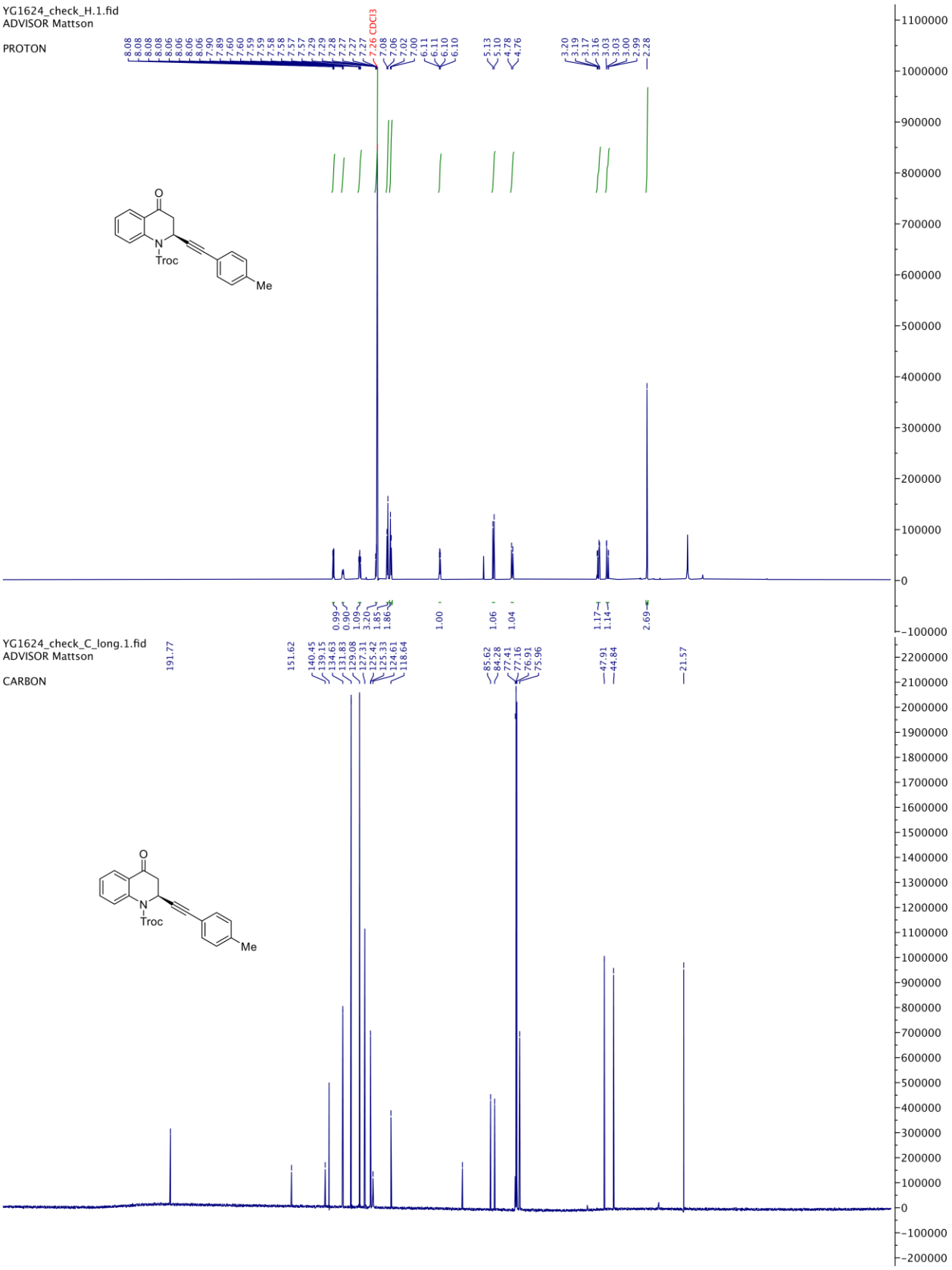
YG1624_check_H.1.fid
ADVISOR Mattson
PROTON
8.08 8.08 8.08 8.06 8.06 8.06 8.06 7.90 7.89 7.60 7.60 7.59 7.59 7.58 7.58 7.57 7.57 7.29 7.28 7.27 7.27 7.27 7.26 CDCl3 7.08 7.06 7.02 7.00 6.11 6.11 6.10 6.10 5.13 5.10 4.78 4.76 3.20 3.19 3.17 3.16 3.03 3.03 3.00 2.99 2.28
O
N
Troc
Me
1100000 1000000 900000 800000 700000 600000 500000 400000 300000 200000 100000 0 -100000
0.99 0.90 1.09 3.20 1.85 1.86 1.00 1.06 1.04 1.17 1.14 2.69
YG1624_check_C_long.1.fid
ADVISOR Mattson
CARBON
191.77 151.62 140.45 139.15 134.63 131.83 129.08 127.31 125.42 125.33 124.61 118.64 85.62 84.28 77.41 77.16 76.91 75.96 47.91 44.84 21.57
O
N
Troc
Me
2200000 2100000 2000000 1900000 1800000 1700000 1600000 1500000 1400000 1300000 1200000 1100000 1000000 900000 800000 700000 600000 500000 400000 300000 200000 100000 0 -100000 -200000

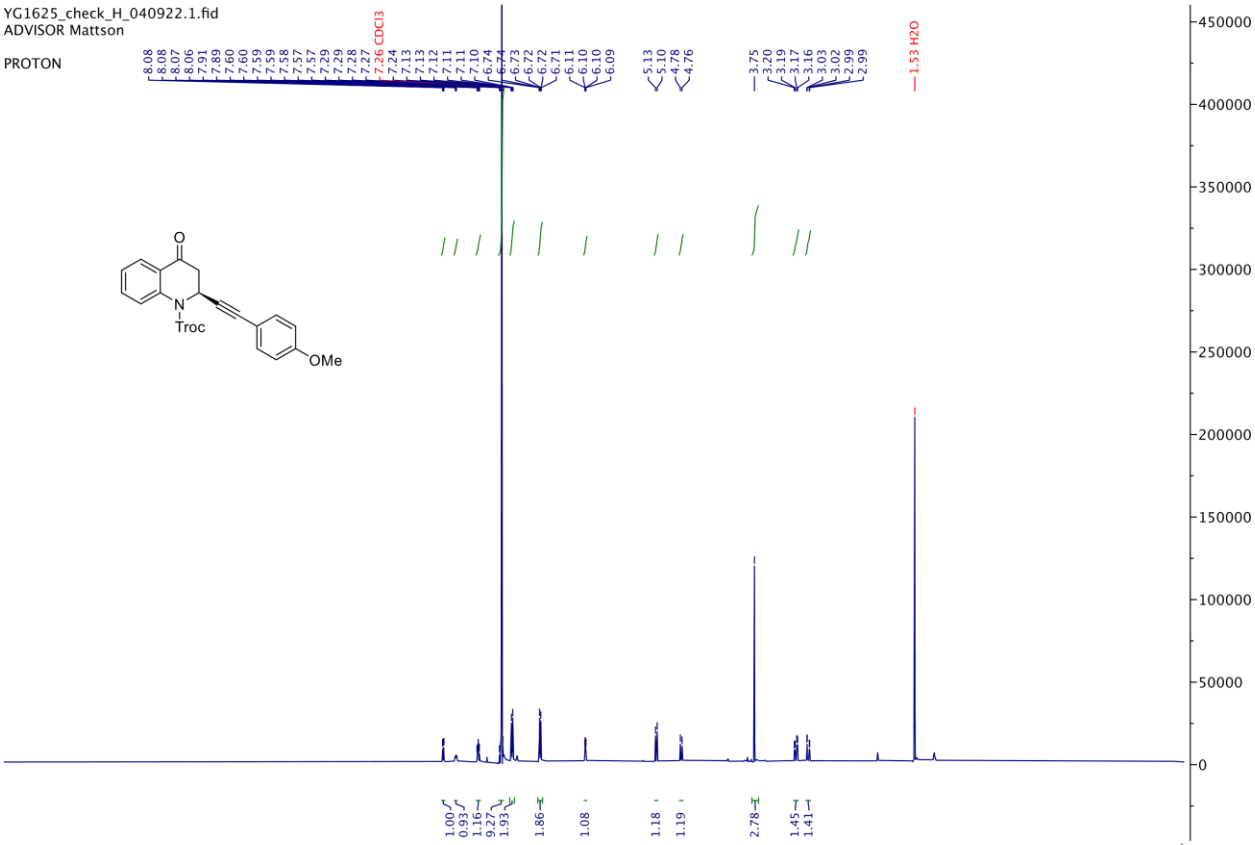
YG1625_check_H_040922.1.fid
ADVISOR Mattson
PROTON
8.08 8.08 8.07 8.06 7.91 7.89 7.60 7.60 7.59 7.59 7.58 7.57 7.57 7.29 7.29 7.28 7.27 7.26 CDCl3 7.24 7.13 7.12 7.11 7.10 6.74 6.73 6.72 6.72 6.71 6.11 6.10 6.10 6.09 5.13 5.10 4.78 4.76 3.75 3.20 3.19 3.17 3.16 3.03 3.02 2.99 2.99 1.53 H2O
O
N
Troc
OMe
450000 400000 350000 300000 250000 200000 150000 100000 50000 0
1.00 0.93 1.16 9.27 1.93 1.86 1.08 1.18 1.19 2.78 1.45 1.41

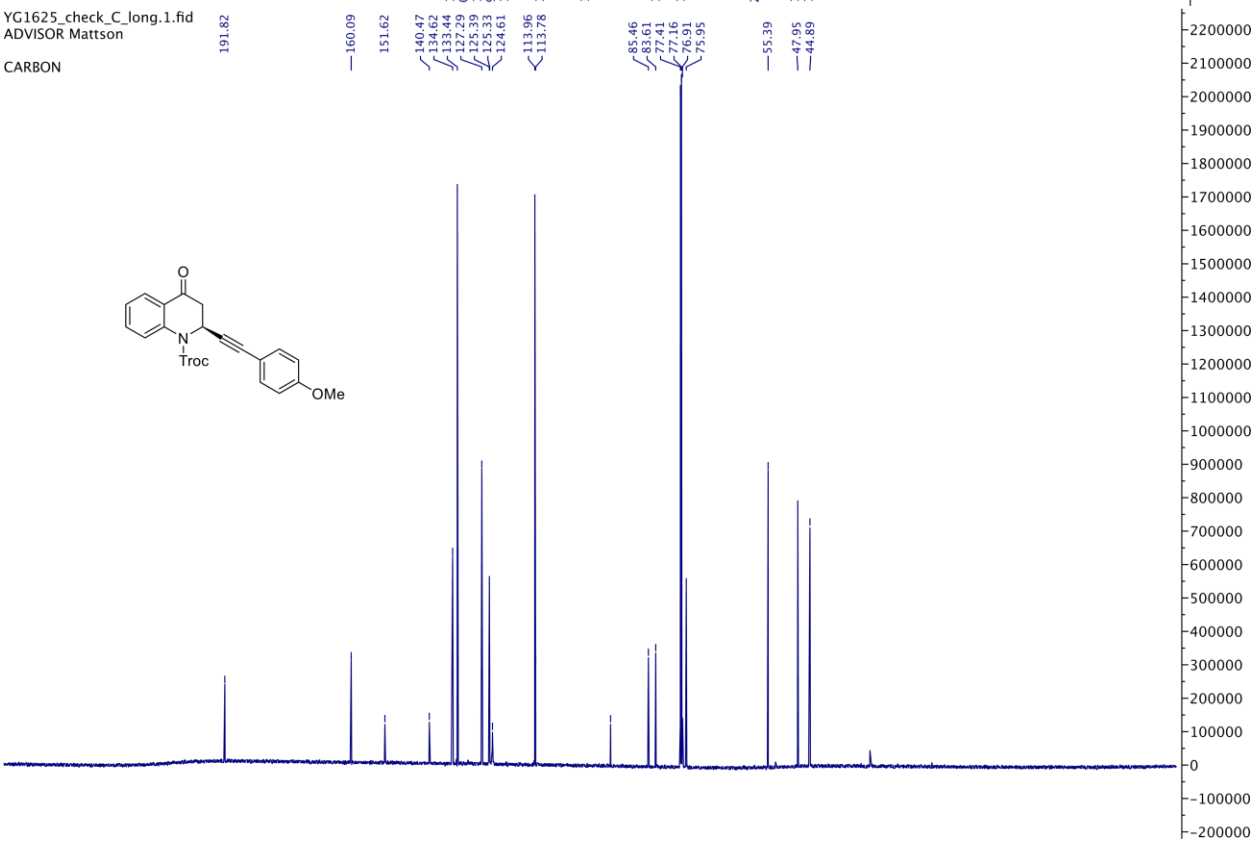
YG1625_check_C_long.1.fid
ADVISOR Mattson
CARBON
191.82 160.09 151.62 140.47 134.62 133.44 127.29 125.39 125.33 124.61 113.96 113.78 85.46 83.61 77.41 77.16 76.91 75.95 55.39 47.95 44.89
O
N
Troc
OMe
2200000 2100000 2000000 1900000 1800000 1700000 1600000 1500000 1400000 1300000 1200000 1100000 1000000 900000 800000 700000 600000 500000 400000 300000 200000 100000 0 -100000 -200000


YG1917_check_H.1.fid
ADVISOR Mattson
PROTON
7.26 CDCl3
1.54 H2O
Troc
tBu
YG1917_check_H.1.fid
ADVISOR Mattson
PROTON
7.26 CDCl3
1.54 H2O
Troc
tBu

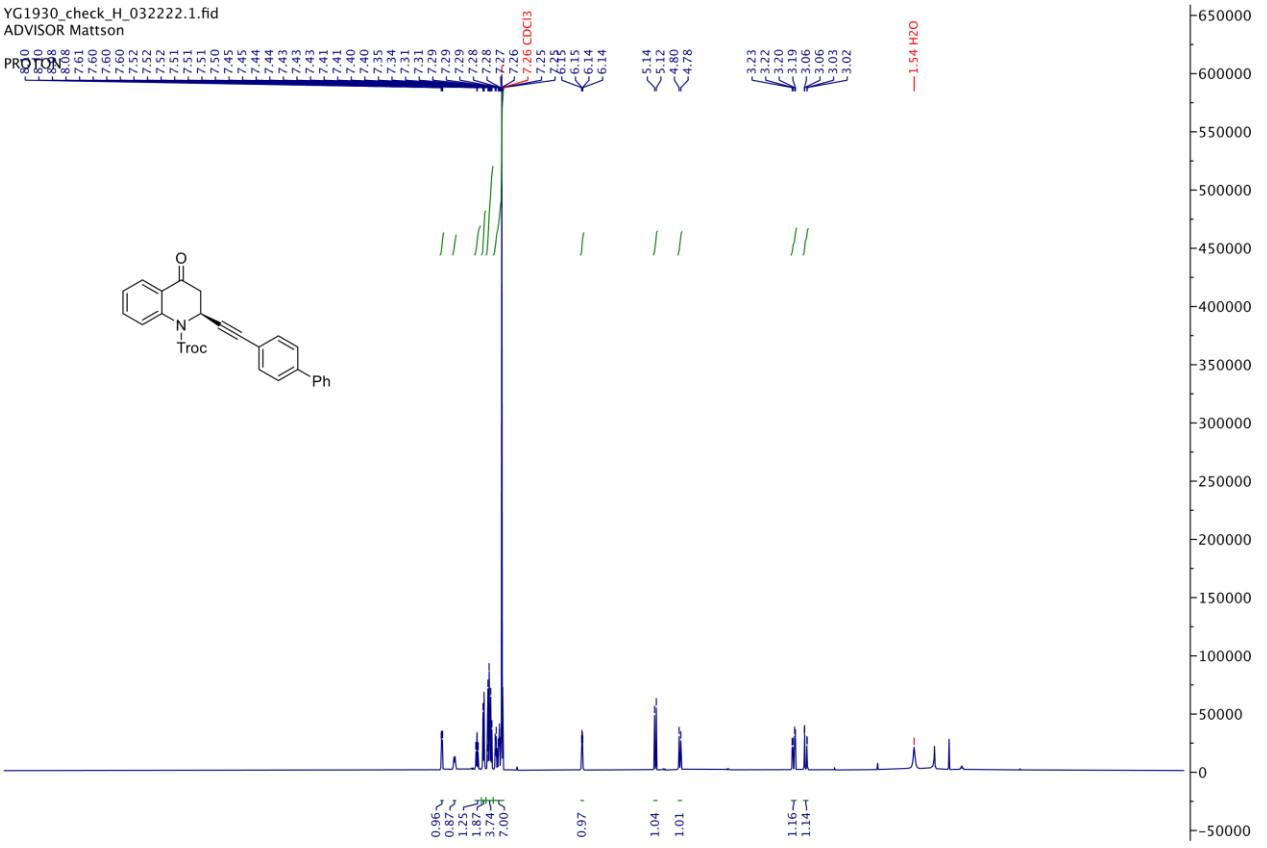
YG1930_check_H_032222.1.fid
ADVISOR Mattson
PROTON
7.26 CDCl3
1.54 H2O
Troc
Ph

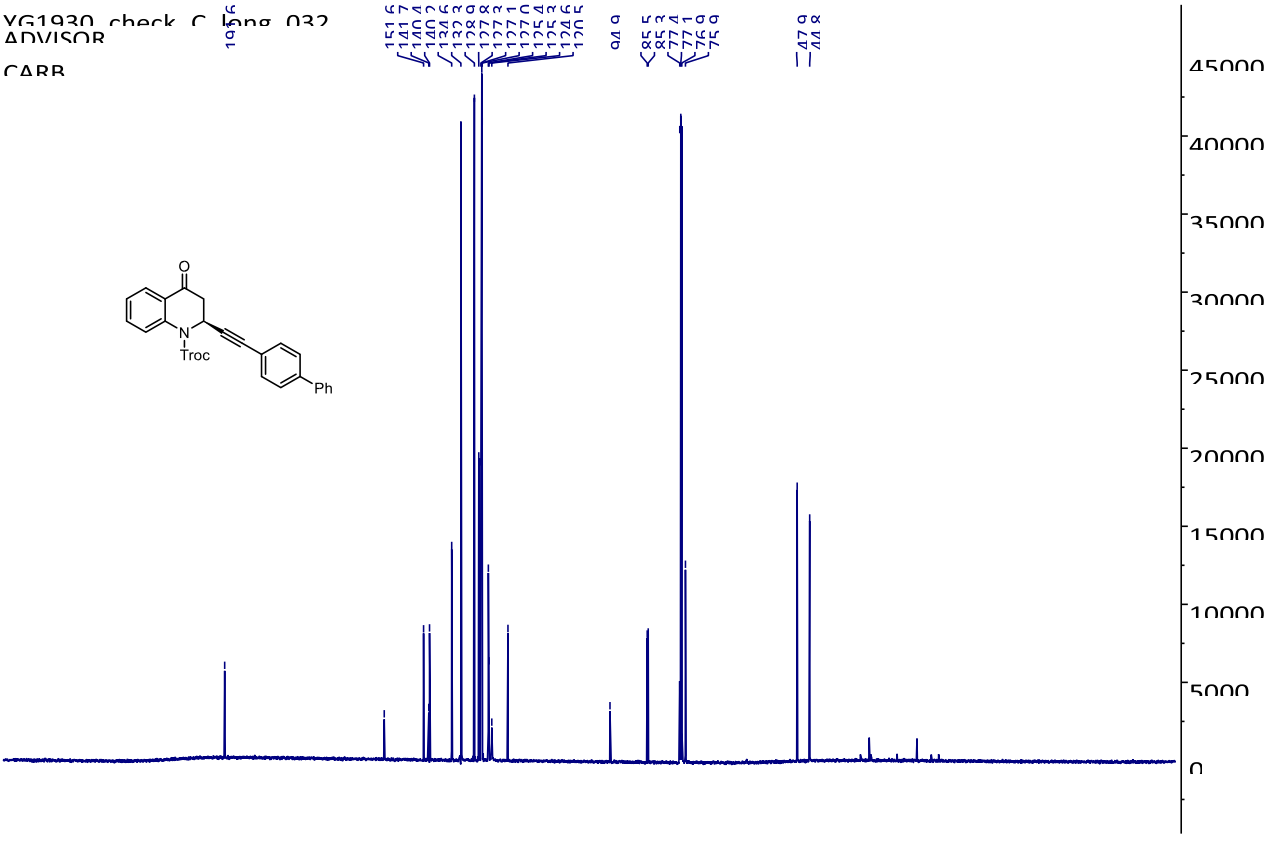
Troc
Ph

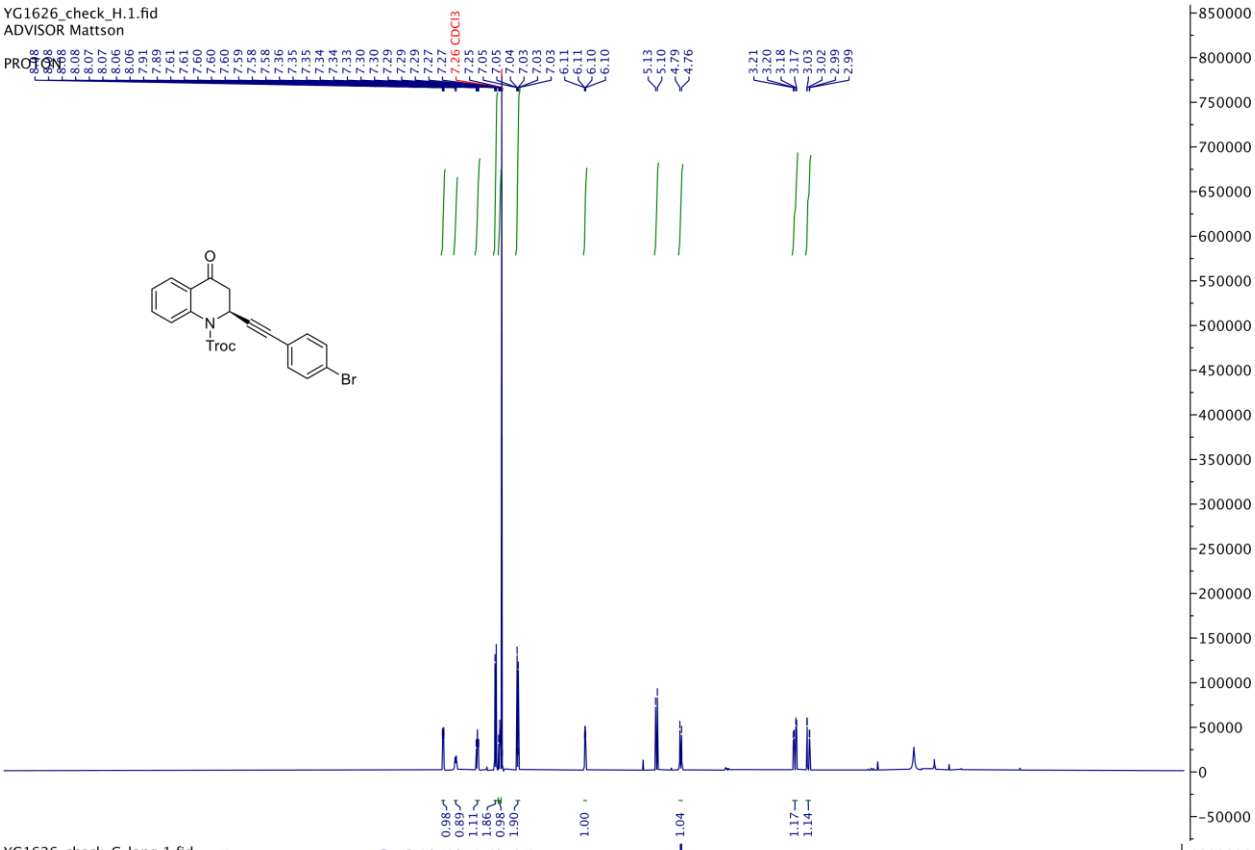
YG1626_check_H.1.fid
ADVISOR Mattson
PROTON
CDCl3
Troc
Br

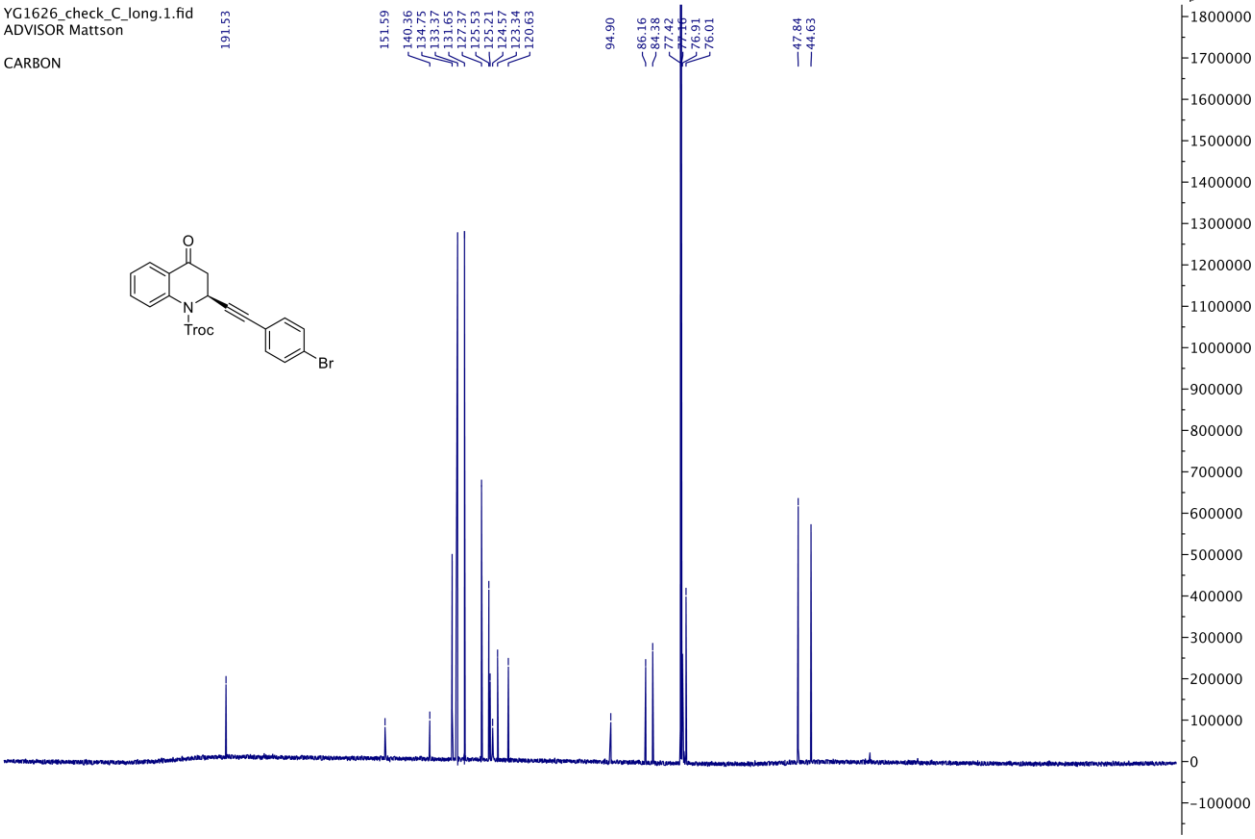
YG1626_check_C_long.1.fid
ADVISOR Mattson
CARBON
Troc
Br

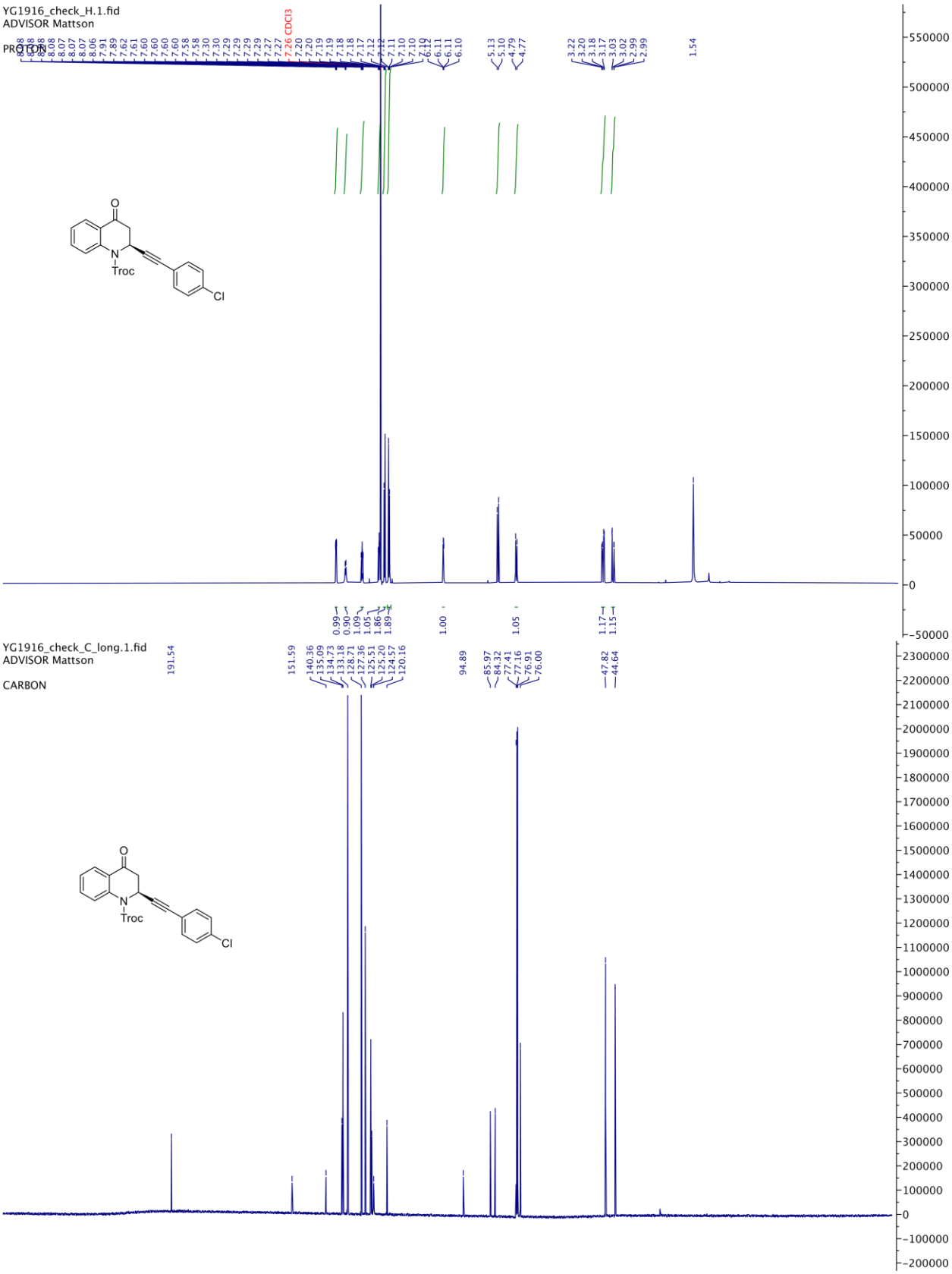
YG1916_check_H.1.fid
ADVISOR Mattson
PROTON
7.26 CDCl3
Troc
Cl
YG1916_check_C_long.1.fid
ADVISOR Mattson
CARBON
Troc
Cl

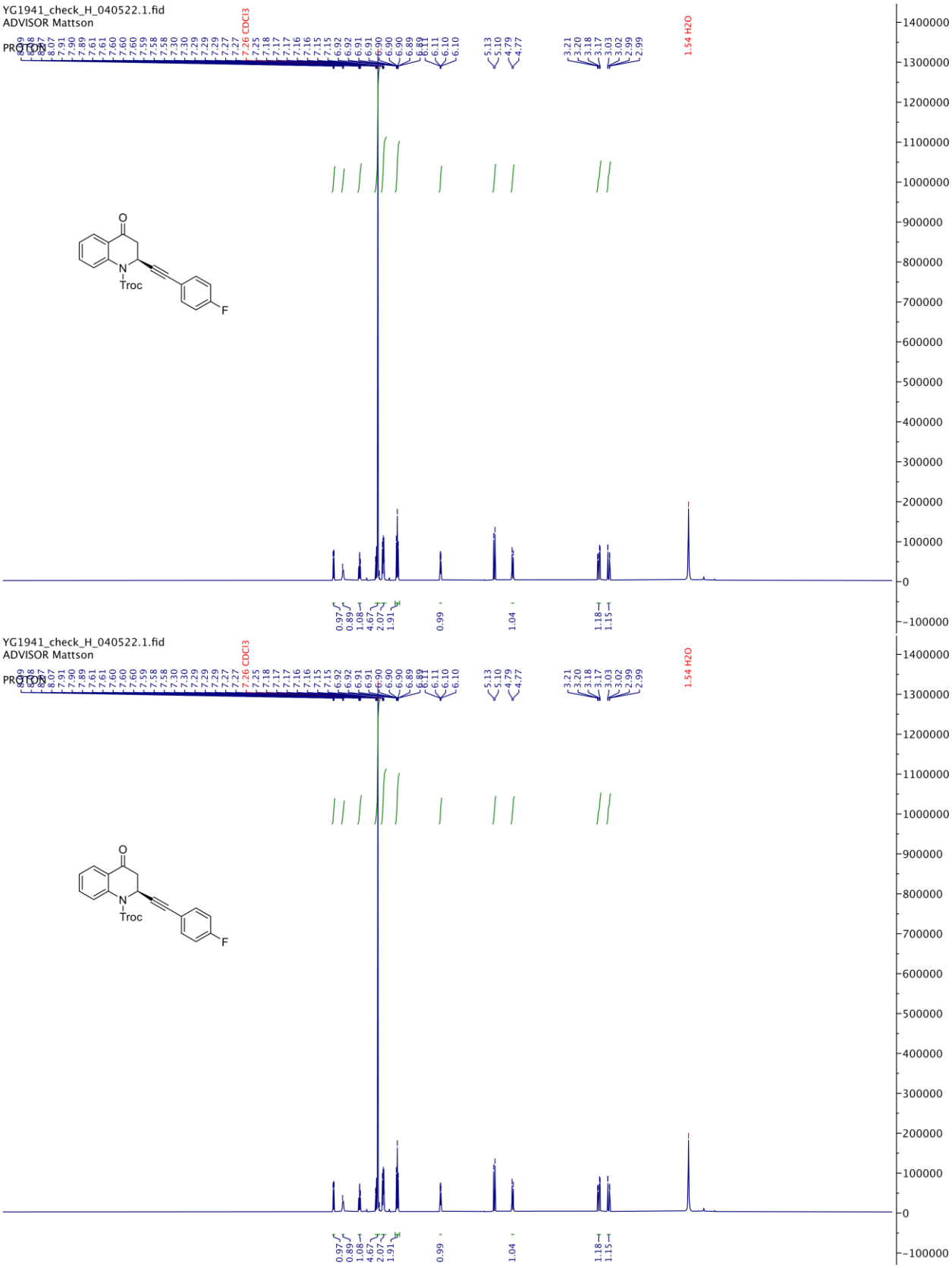
YG1941_check_H_040522.1.fid
ADVISOR Mattson
PROTON
7.26 CDCl3
1.54 H2O
O
N
Troc
F
0.97
0.89
1.08
4.67
2.07
1.91
0.99
1.04
1.18
1.15

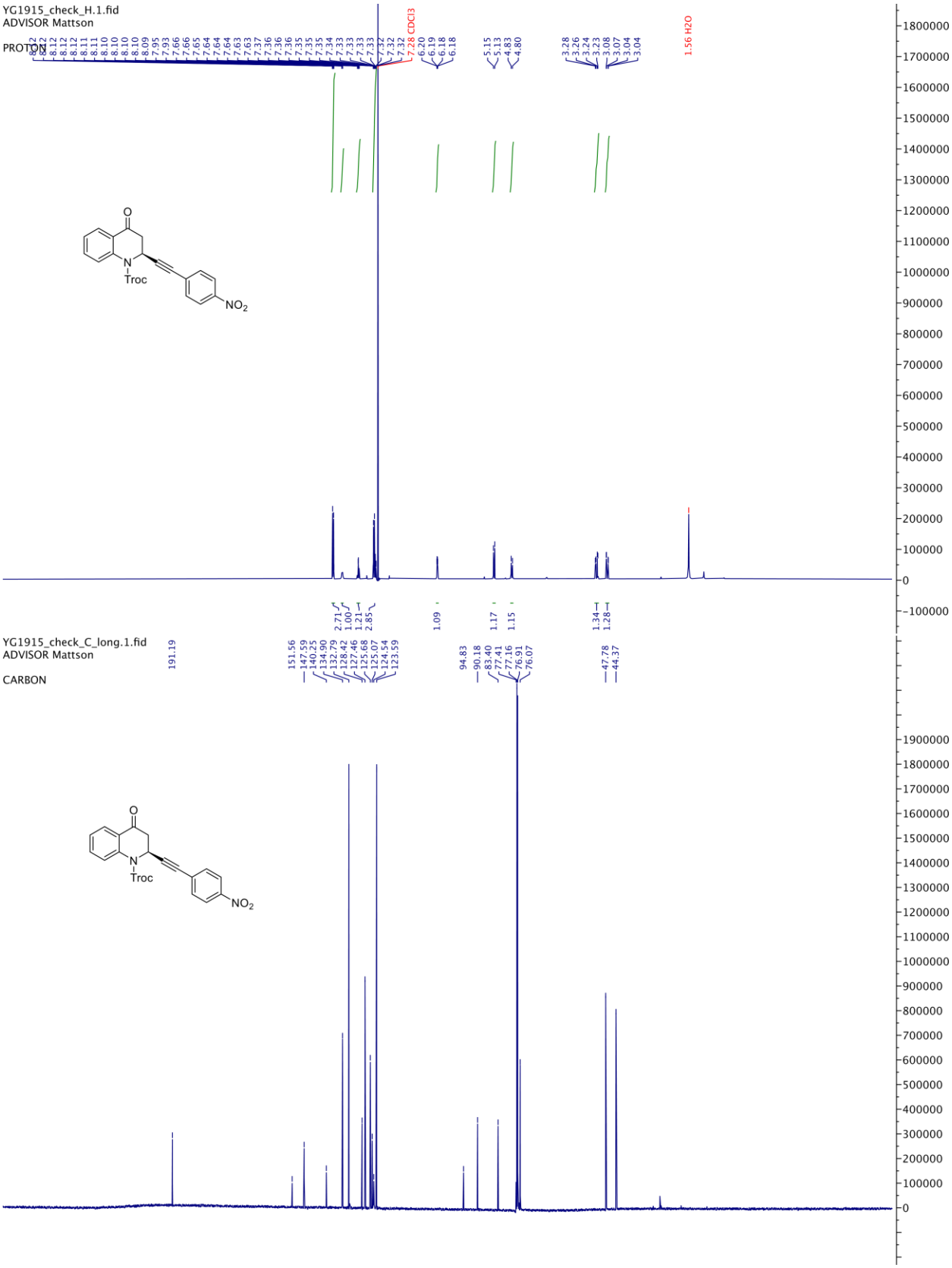
YG1915_check_H.1.fid
ADVISOR Mattson
PROTON
7.28 CDCl3
1.56 H2O
Troc
NO2
YG1915_check_C_long.1.fid
ADVISOR Mattson
CARBON
Troc
NO2

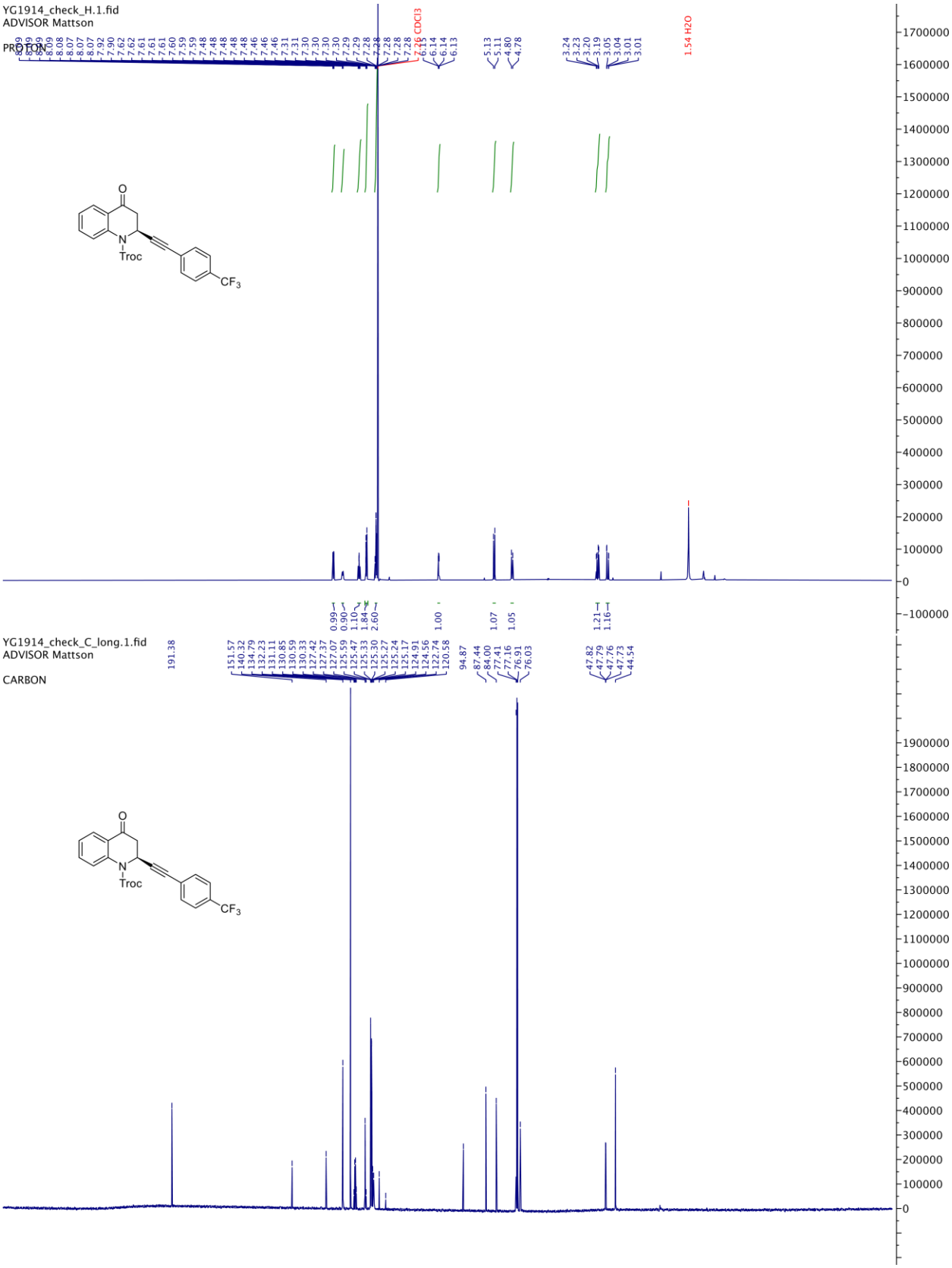
YG1914_check_H.1.fid
ADVISOR Mattson
PROTON
7.26 CDCl3
1.54 H2O
YG1914_check_C_long.1.fid
ADVISOR Mattson
CARBON
Troc
CF3

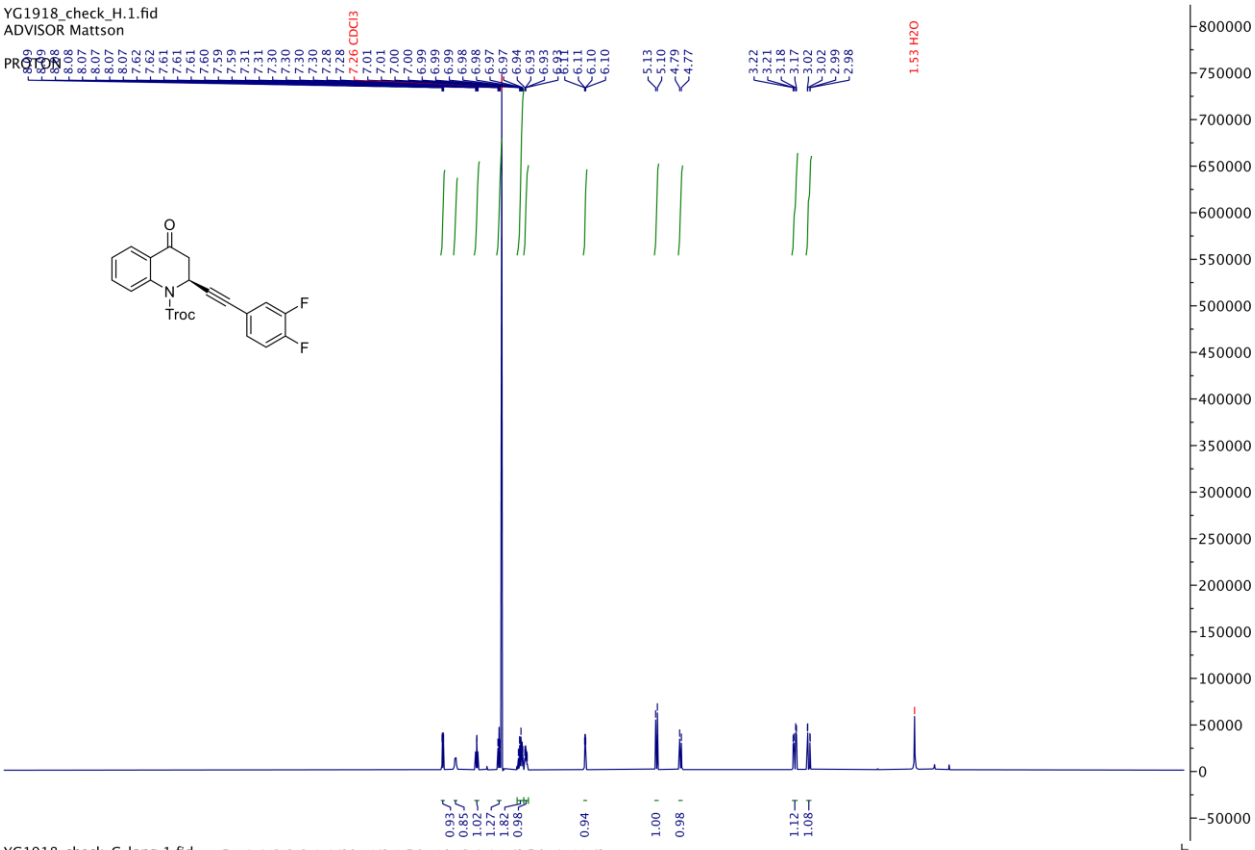
YG1918_check_H.1.fid
ADVISOR Mattson
PROTON
7.26 CDCl3
1.53 H2O
Troc
F
F

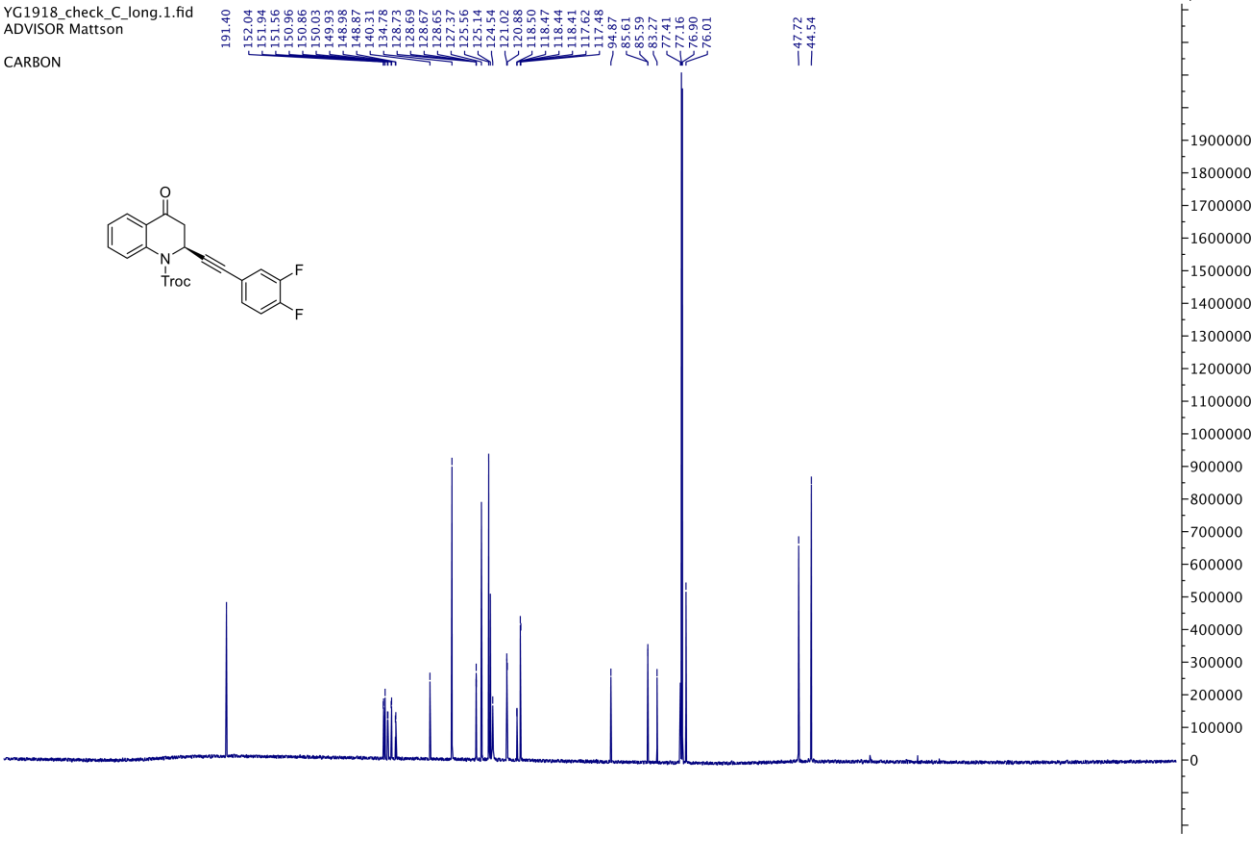
YG1918_check_C_long.1.fid
ADVISOR Mattson
CARBON
Troc
F
F

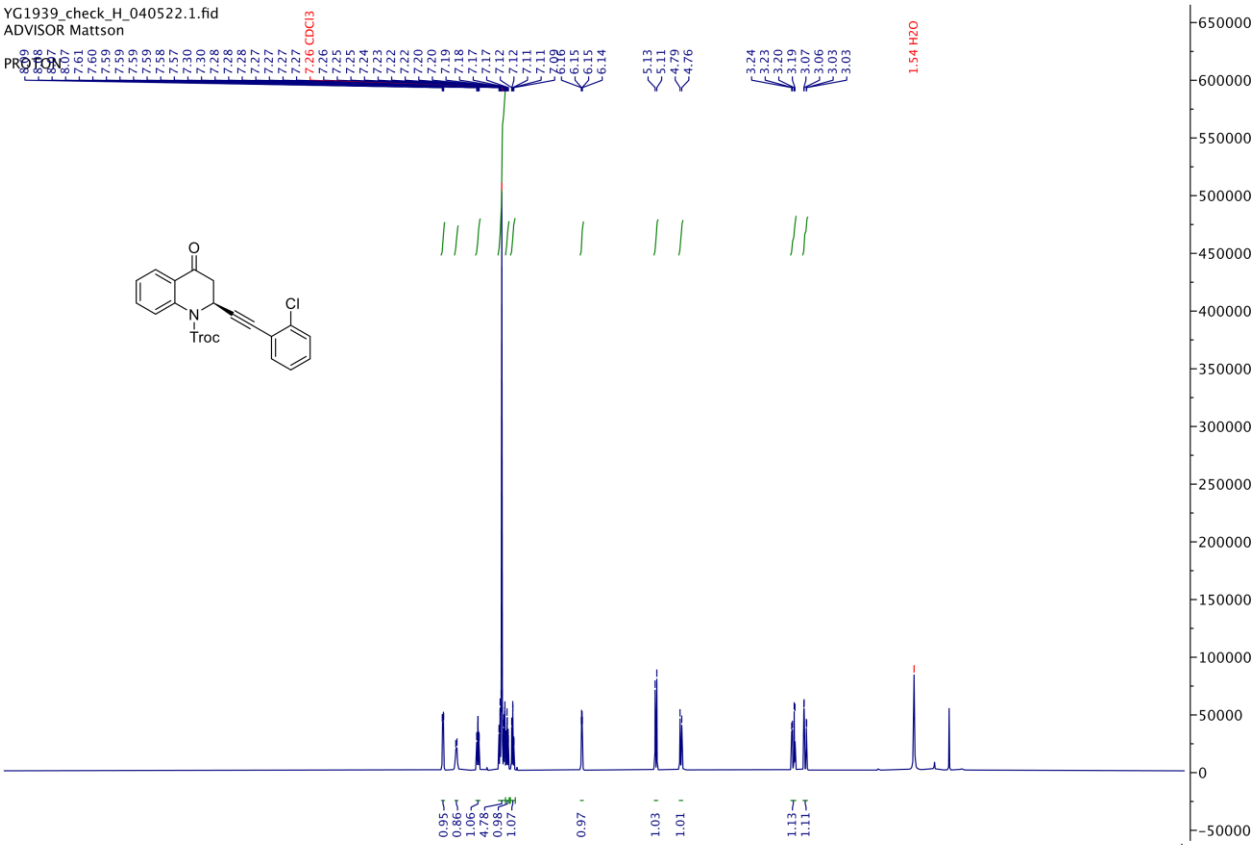
YG1939_check_H_040522.1.fid
ADVISOR Mattson
PROTON
7.26 CDCl3
1.54 H2O
O
N
Troc
Cl

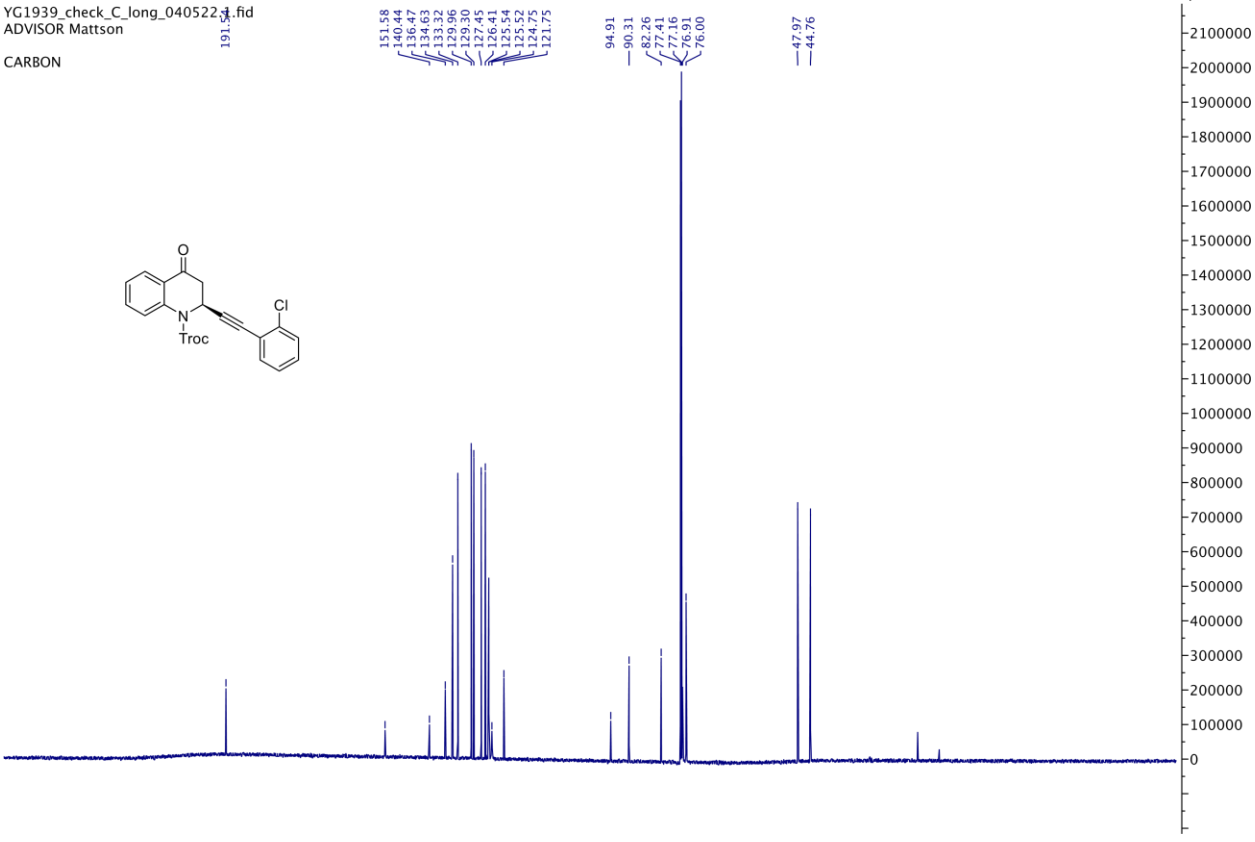
YG1939_check_C_long_040522.1.fid
ADVISOR Mattson
CARBON
O
N
Troc
Cl

Appendix 6B: Quinolone Substitutions

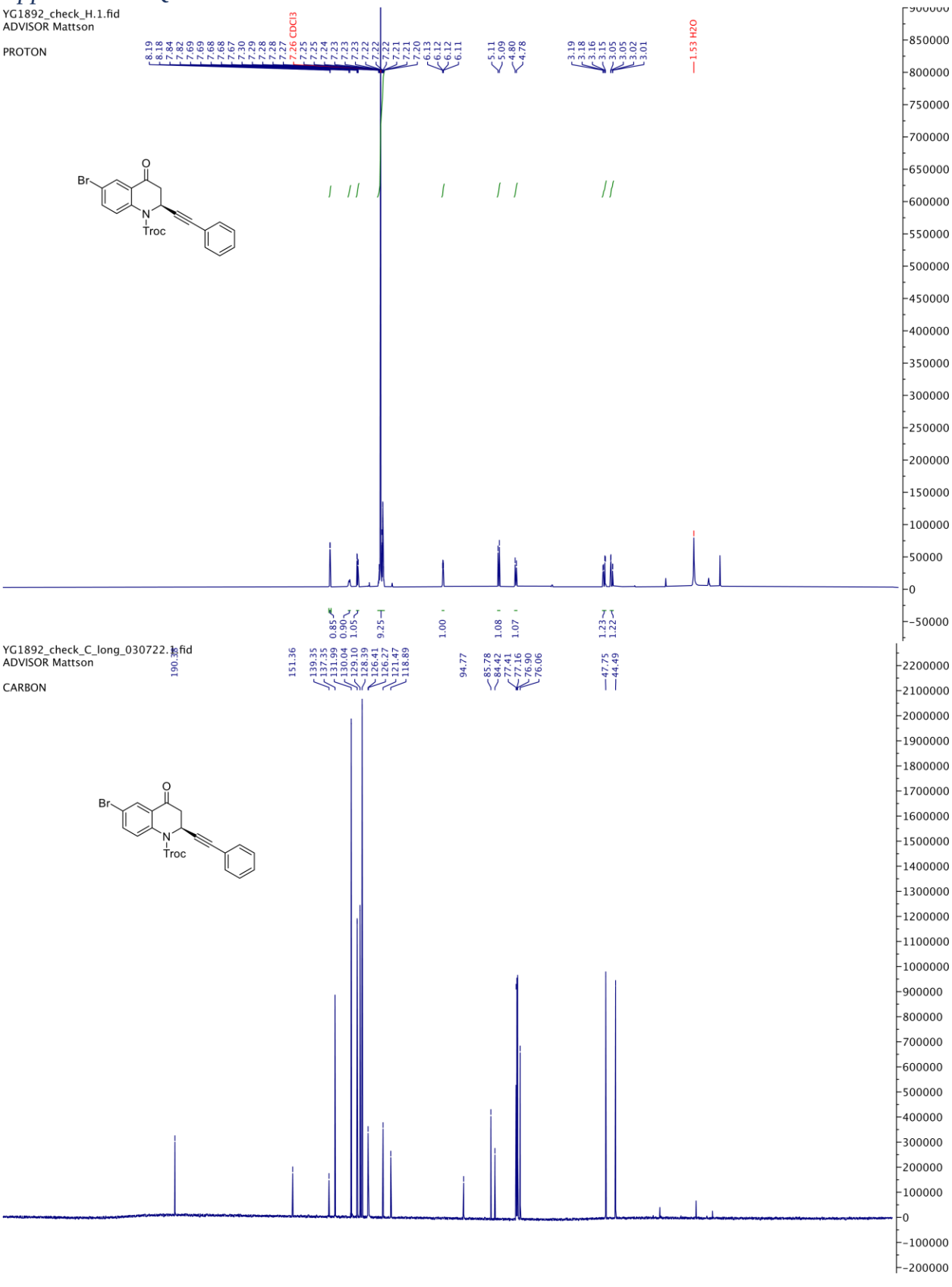

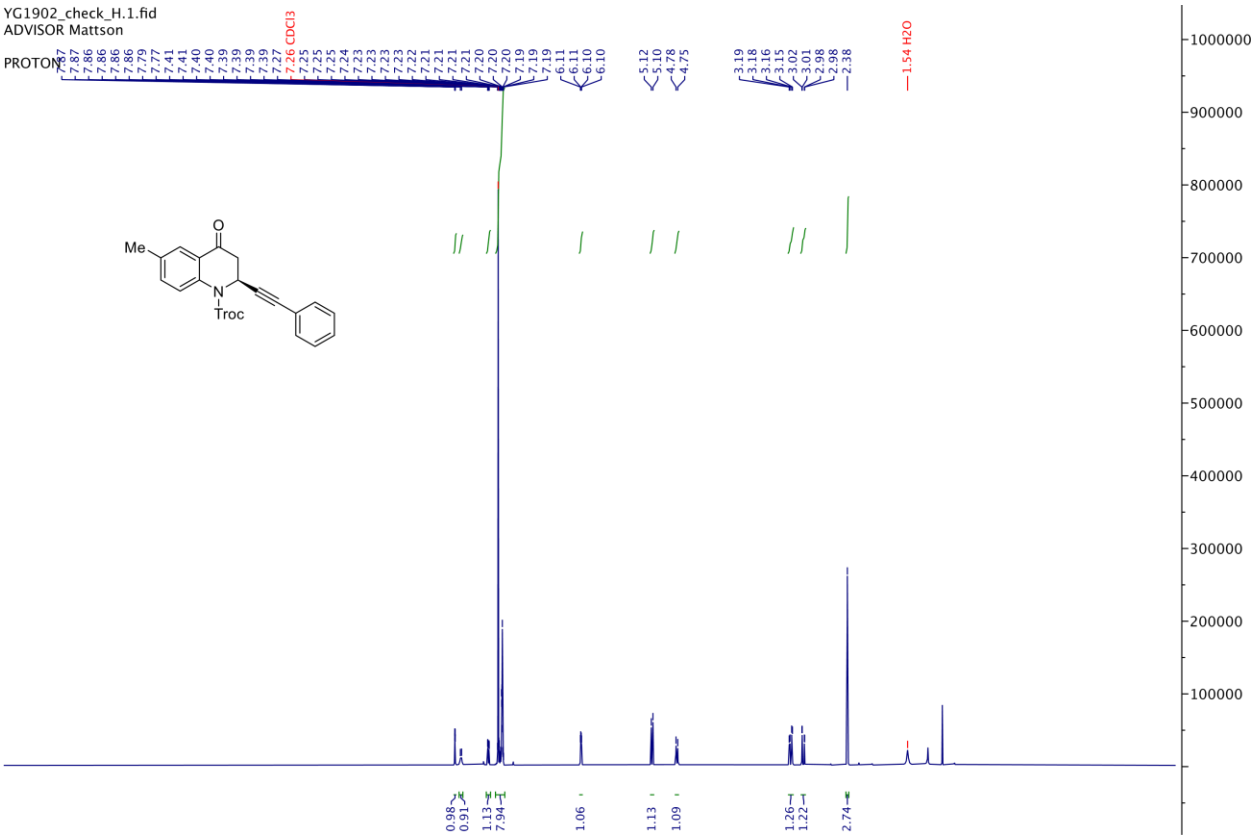
YG1902_check_H.1.fid
ADVISOR Mattson
PROTON
Me
N
Troc
1000000
900000
800000
700000
600000
500000
400000
300000
200000
100000

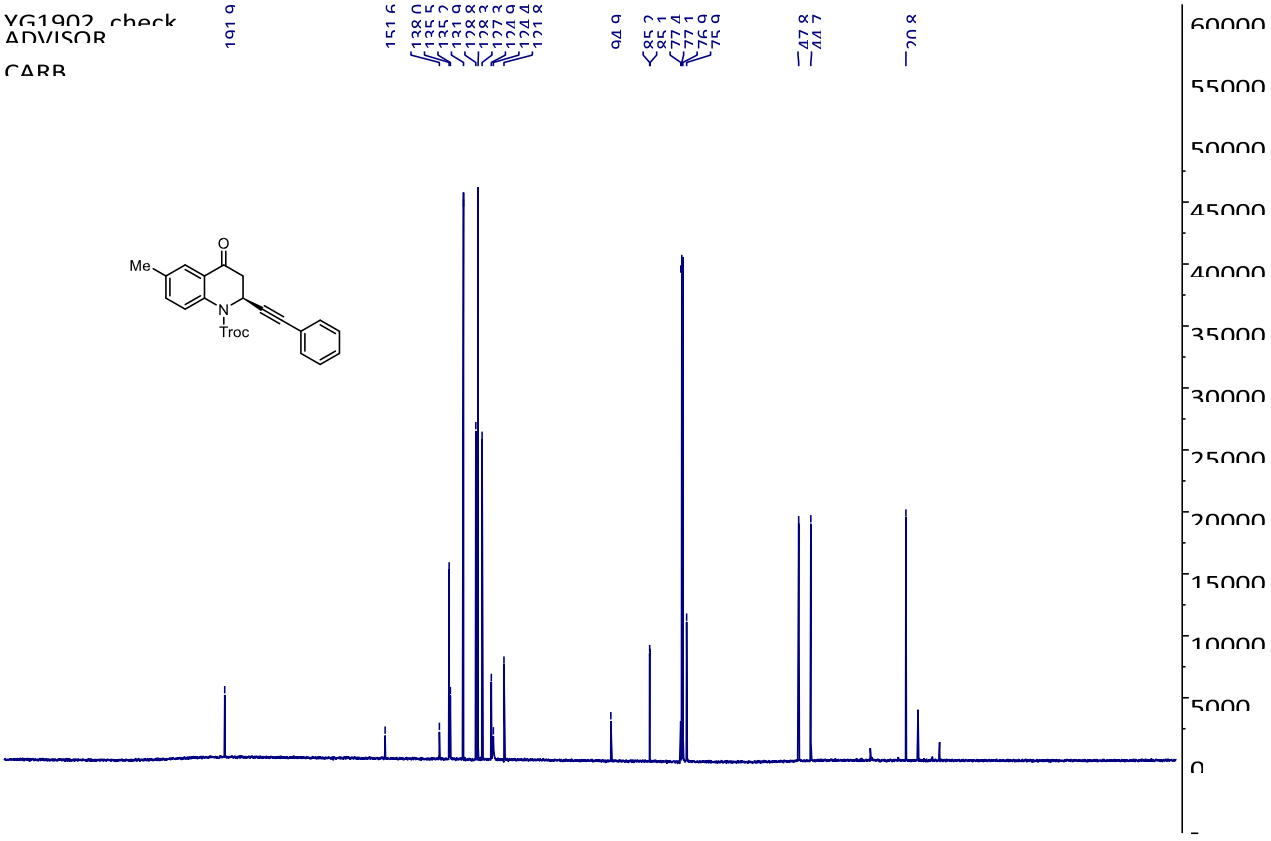
Me
N
Troc
60000
55000
50000
45000
40000
35000
30000
25000
20000
15000
10000
5000
0

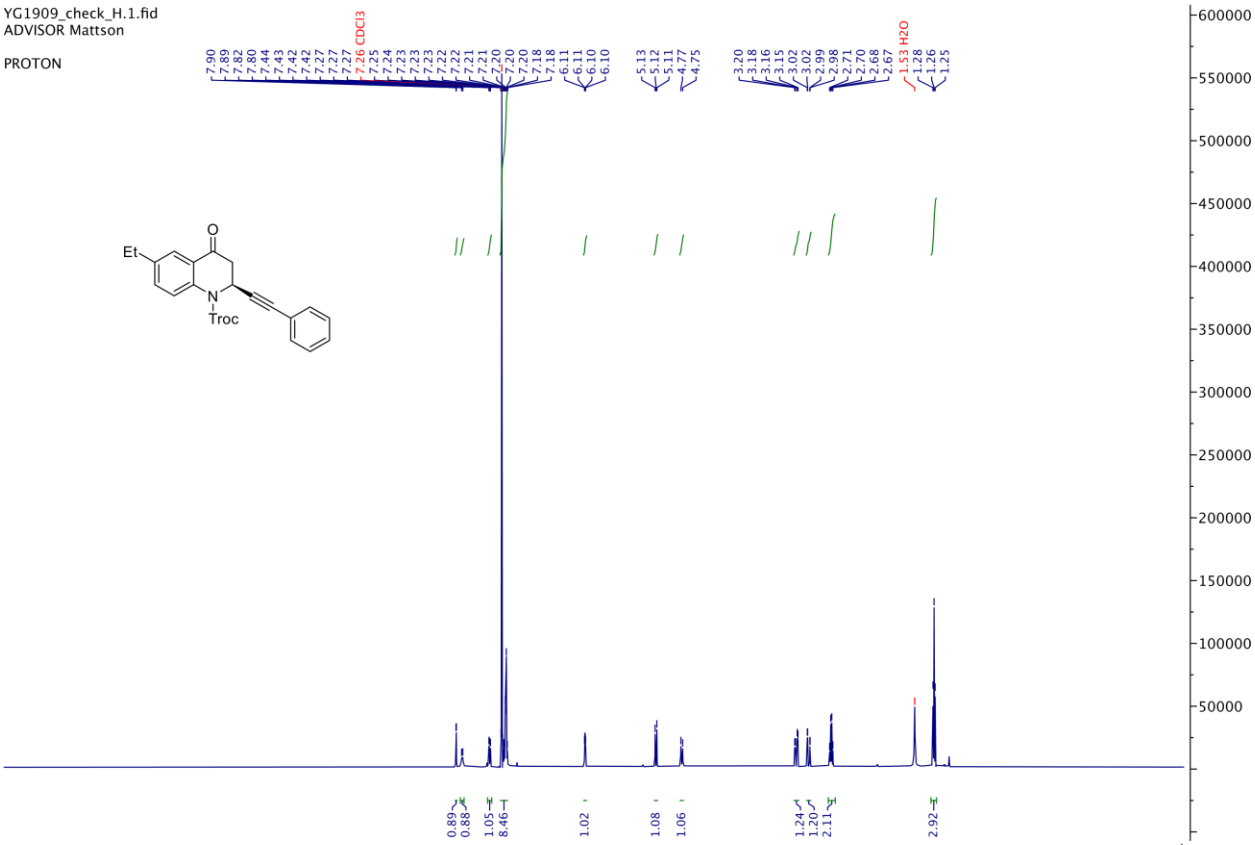
YG1909_check_H.1.fid
ADVISOR Mattson
PROTON
7.90 7.89 7.82 7.80 7.44 7.43 7.42 7.42 7.27 7.27 7.27 7.26 CDCl3 7.25 7.24 7.23 7.23 7.23 7.22 7.22 7.21 7.21 7.20 7.20 7.20 7.18 7.18 6.11 6.11 6.10 6.10
5.13 5.12 5.11 4.77 4.75
3.20 3.18 3.16 3.15 3.02 3.02 2.99 2.98 2.71 2.70 2.68 2.67
1.53 H2O
1.28 1.26 1.25
0.89 0.88 1.05 8.46 1.02 1.08 1.06 1.24 1.20 2.11 2.92
Et
O
N
Troc
600000 550000 500000 450000 400000 350000 300000 250000 200000 150000 100000 50000

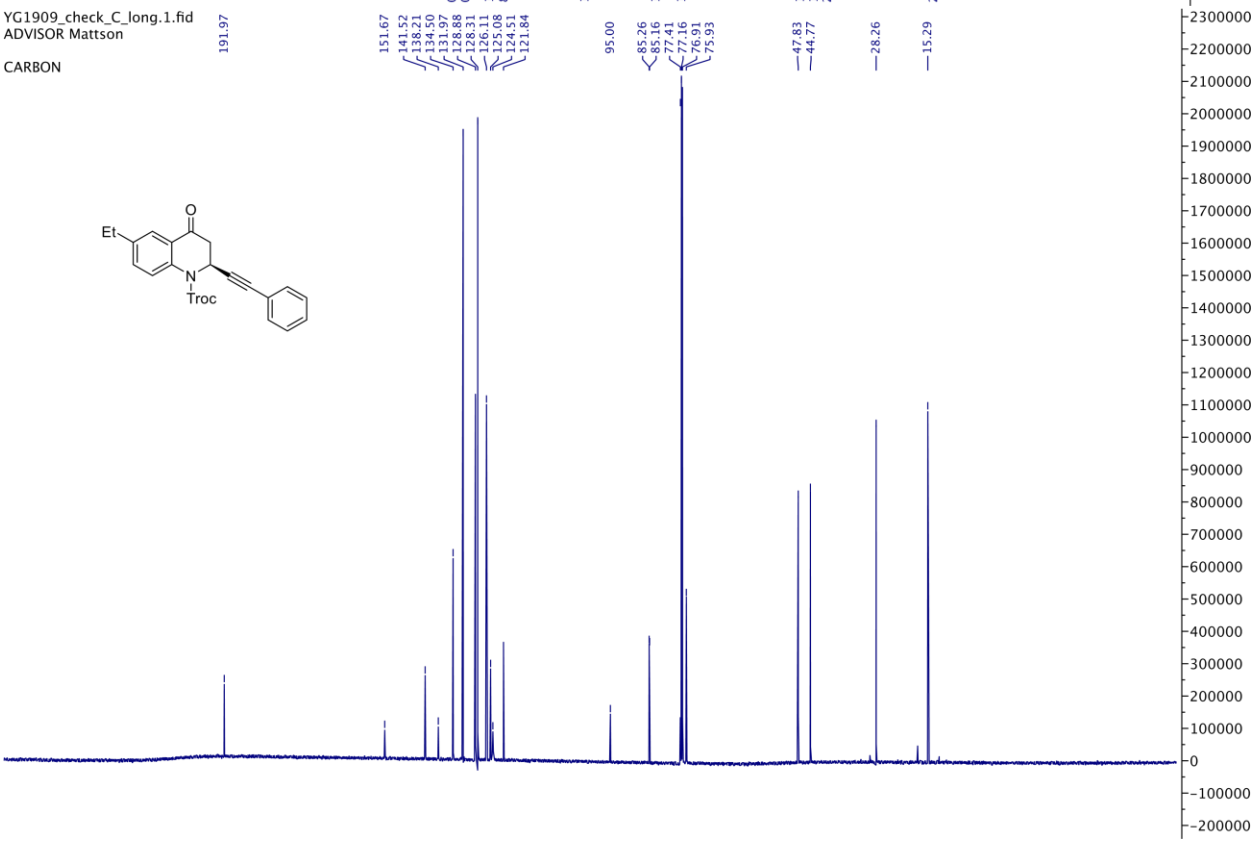
YG1909_check_C_long.1.fid
ADVISOR Mattson
CARBON
191.97
151.67 141.52 138.21 134.50 131.97 128.88 128.31 126.11 125.08 124.51 121.84
95.00
85.26 85.16 77.41 77.16 76.91 75.93
47.83 44.77
28.26
15.29
Et
O
N
Troc
2300000 2200000 2100000 2000000 1900000 1800000 1700000 1600000 1500000 1400000 1300000 1200000 1100000 1000000 900000 800000 700000 600000 500000 400000 300000 200000 100000 0 -100000 -200000

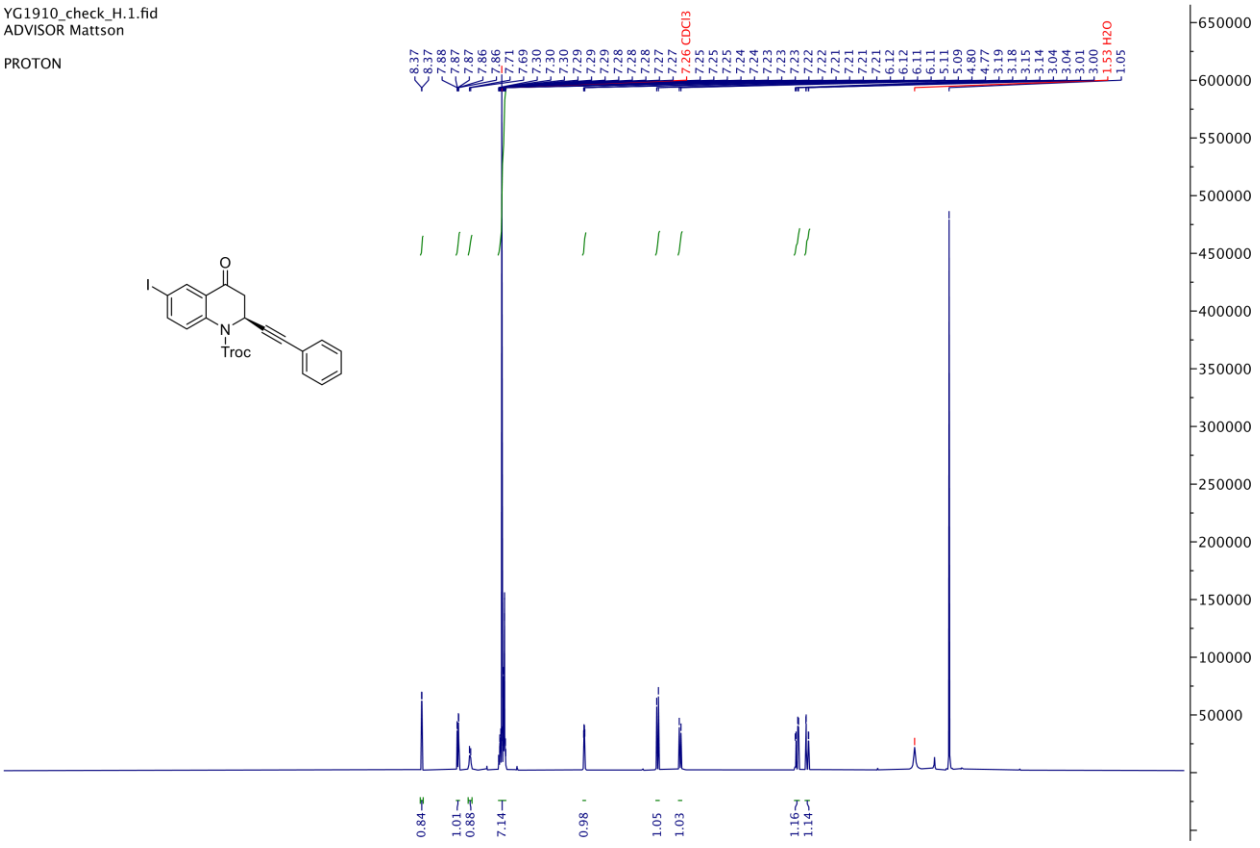
YG1910_check_H.1.fid
ADVISOR Mattson
PROTON
O
I
N
Troc
650000
600000
550000
500000
450000
400000
350000
300000
250000
200000
150000
100000
50000

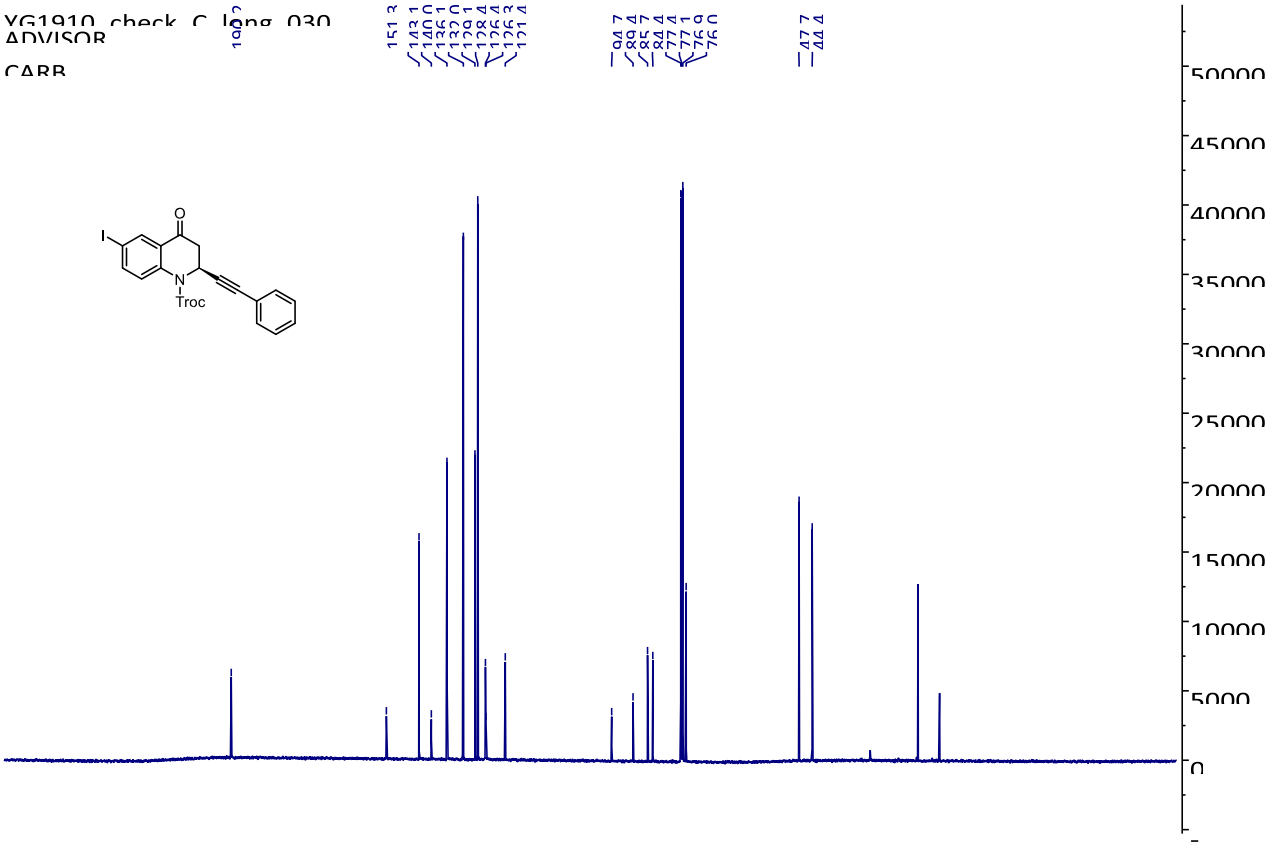
CARB
O
I
N
Troc
50000
45000
40000
35000
30000
25000
20000
15000
10000
5000
0

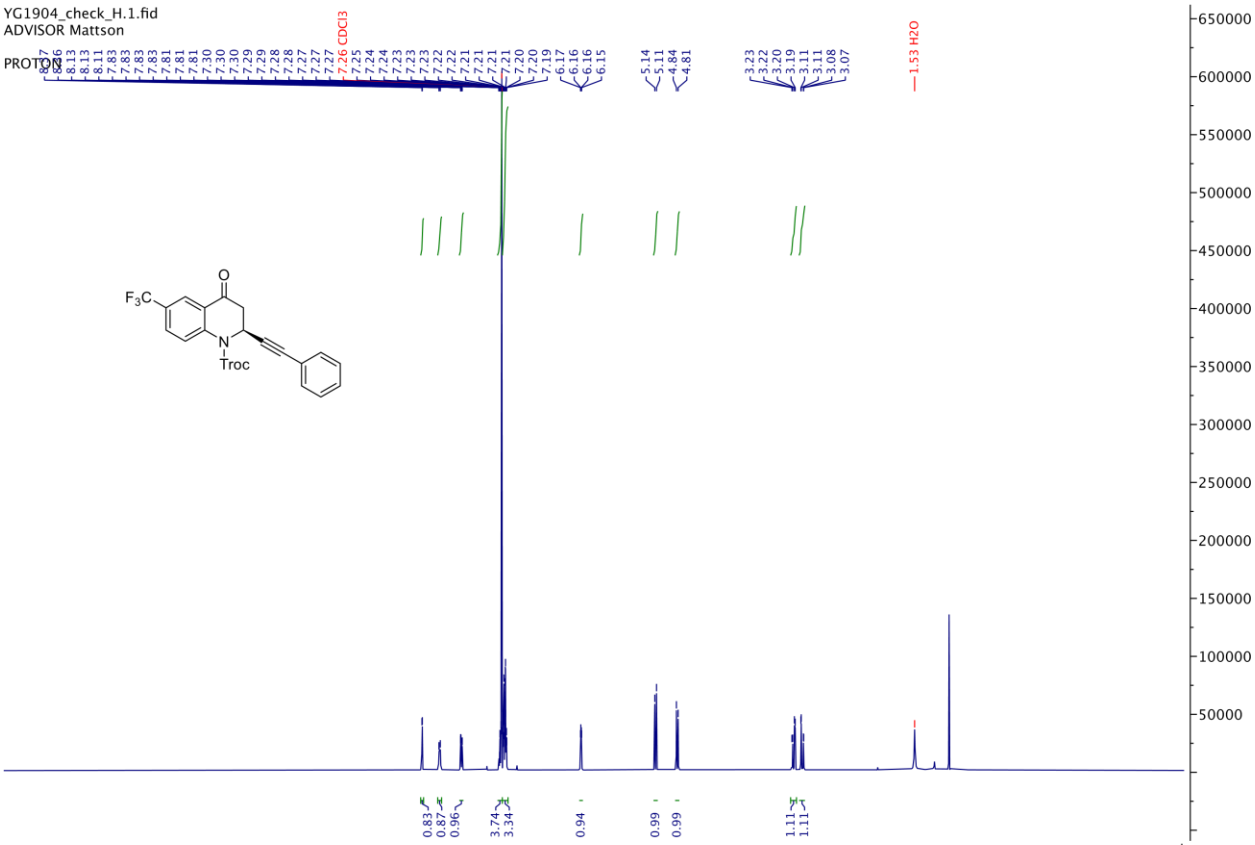
YG1904_check_H.1.fid
ADVISOR Mattson
PROTON
7.26 CDCl3
1.53 H2O
F3C
O
N
Troc

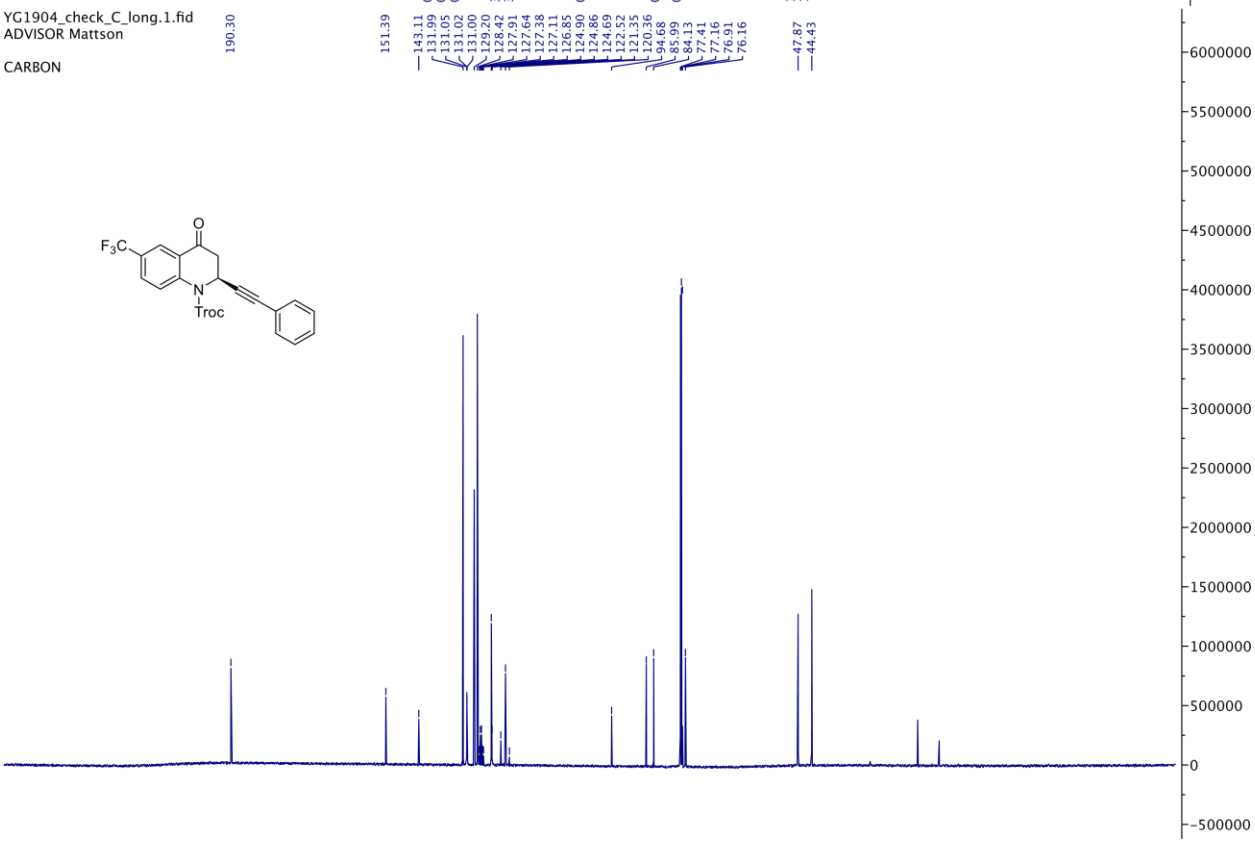
YG1904_check_C_long.1.fid
ADVISOR Mattson
CARBON
F3C
O
N
Troc

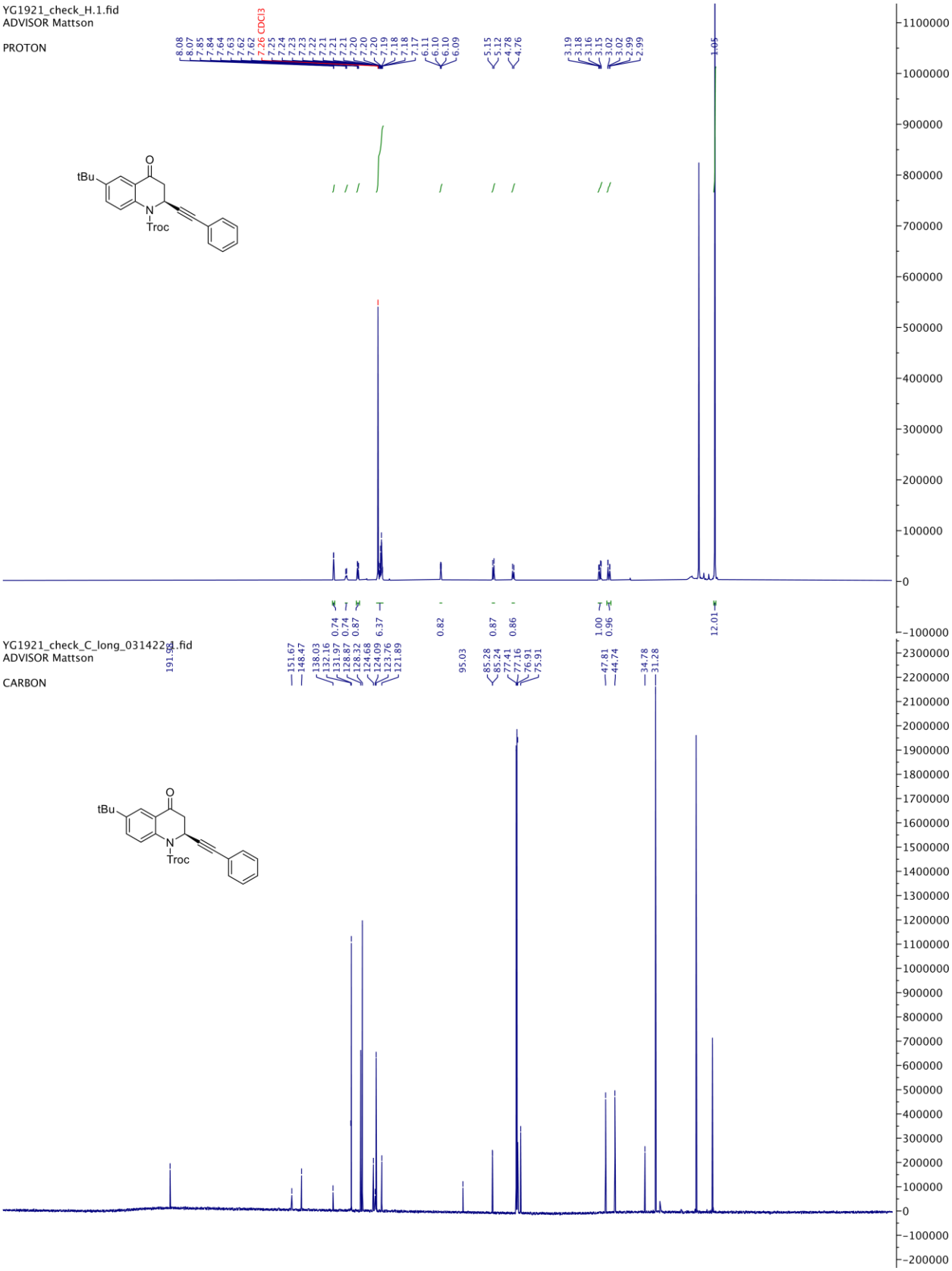
YG1921_check_H.1.fid
ADVISOR Mattson
PROTON
8.08
8.07
7.85
7.84
7.64
7.63
7.62
7.62
7.26 CDCl3
7.25
7.24
7.23
7.23
7.22
7.21
7.21
7.20
7.20
7.19
7.18
7.18
7.17
6.11
6.10
6.10
6.09
5.15
5.12
4.78
4.76
3.19
3.18
3.16
3.15
3.02
3.02
2.99
2.99
1.05
tBu
O
N
Troc
0.74
0.74
0.87
6.37
0.82
0.87
0.86
1.00
0.96
12.01
YG1921_check_C_long_031422a1.fid
ADVISOR Mattson
CARBON
191.92
151.67
148.47
138.03
132.16
131.97
128.87
128.32
124.68
124.09
123.76
121.89
95.03
85.28
85.24
77.41
77.16
76.91
75.91
47.81
44.74
34.78
31.28
tBu
O
N
Troc

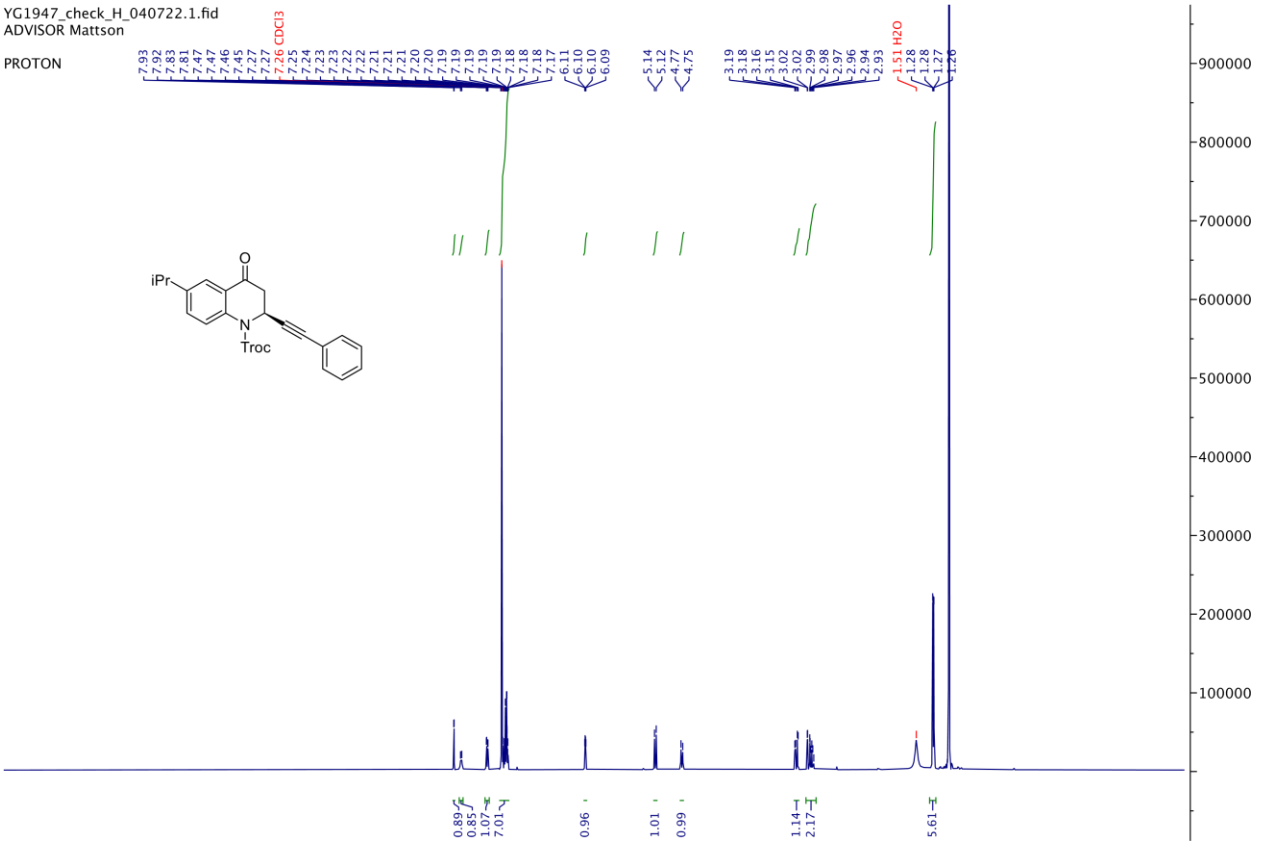
YG1947_check_H_040722.1.fid
ADVISOR Mattson
PROTON
7.26 CDCl3
1.51 H2O
iPr
N
Troc
O

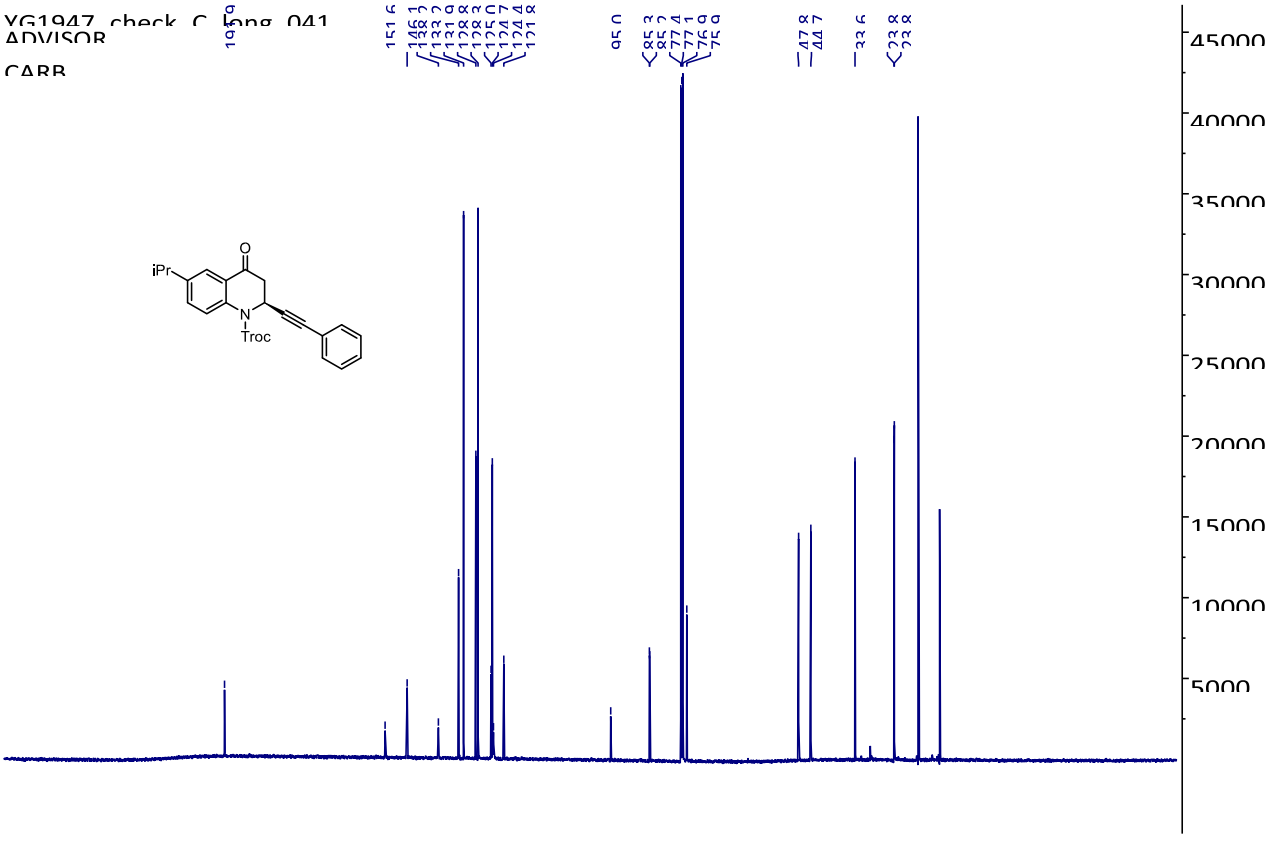
ADVISOR
CARB
iPr
N
Troc
O

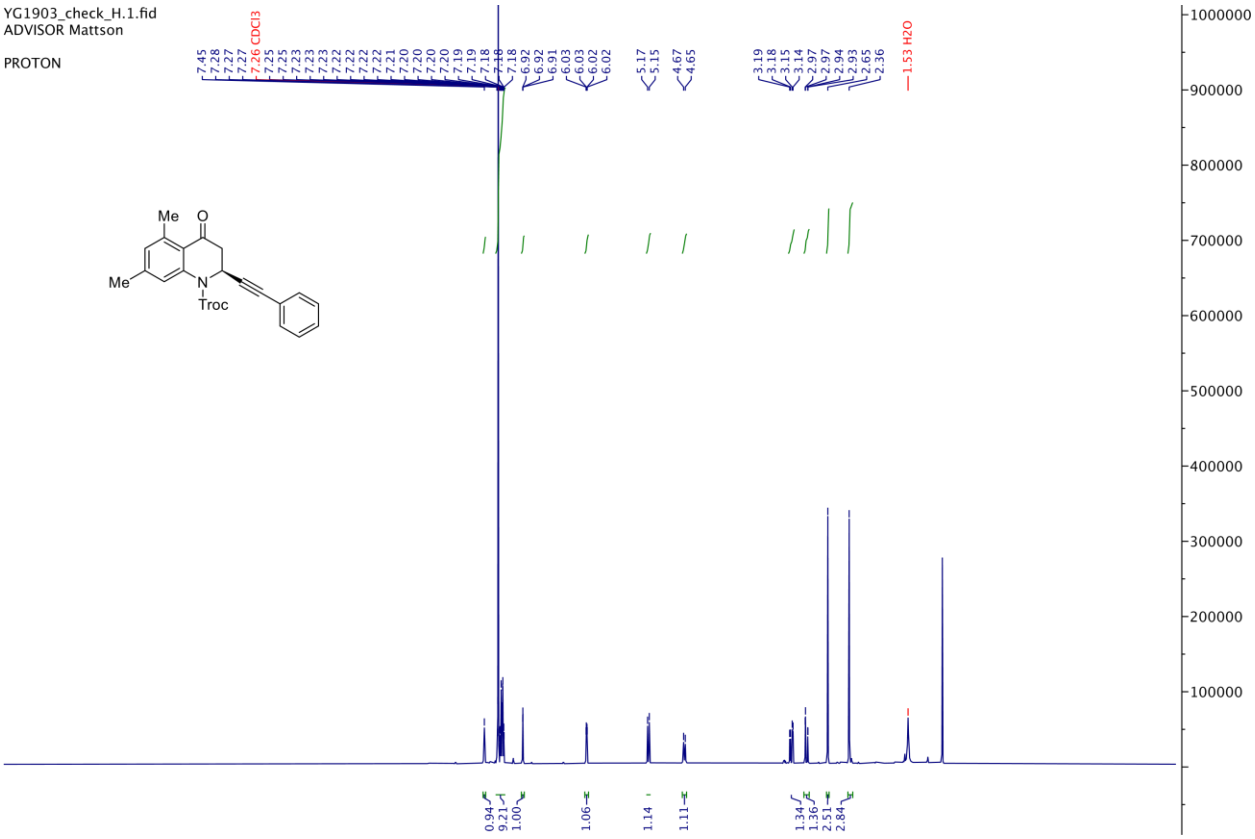
YG1903_check_H.1.fid
ADVISOR Mattson
PROTON
7.26 CDCl3
1.53 H2O
Me
O
Me
N
Troc

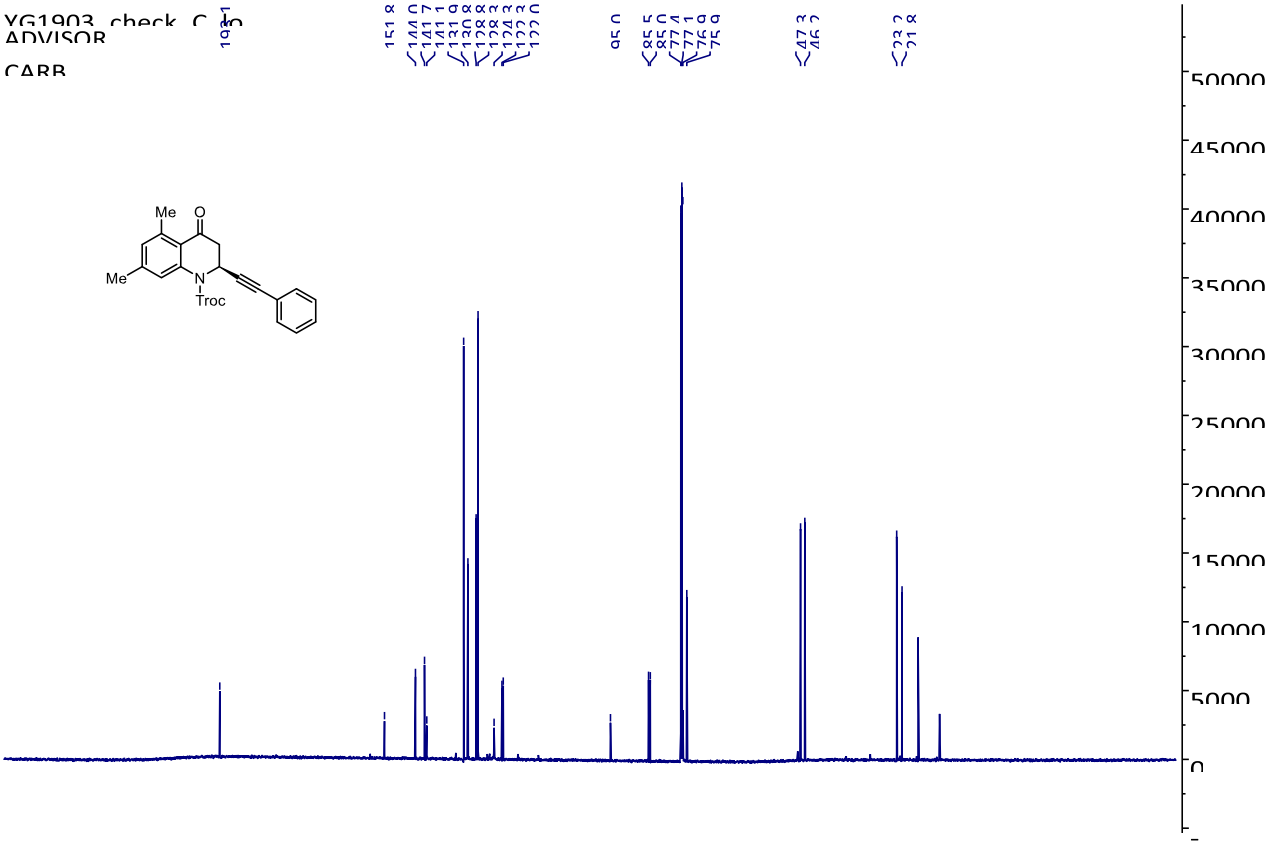
ADVISOR
CARB
Me
O
Me
N
Troc

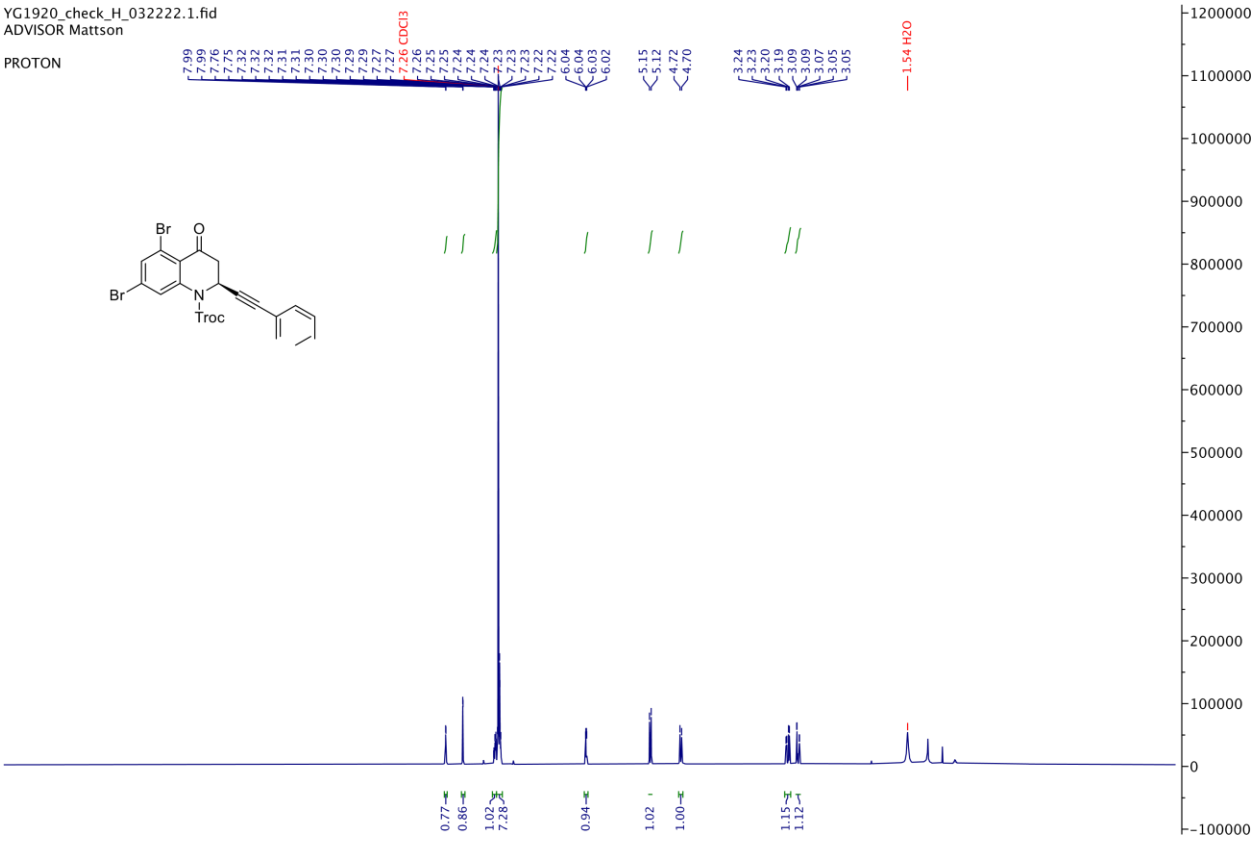
YG1920_check_H_032222.1.fid
ADVISOR Mattson
PROTON
7.26 CDCl3
1.54 H2O
Br
O
Br
N
Troc

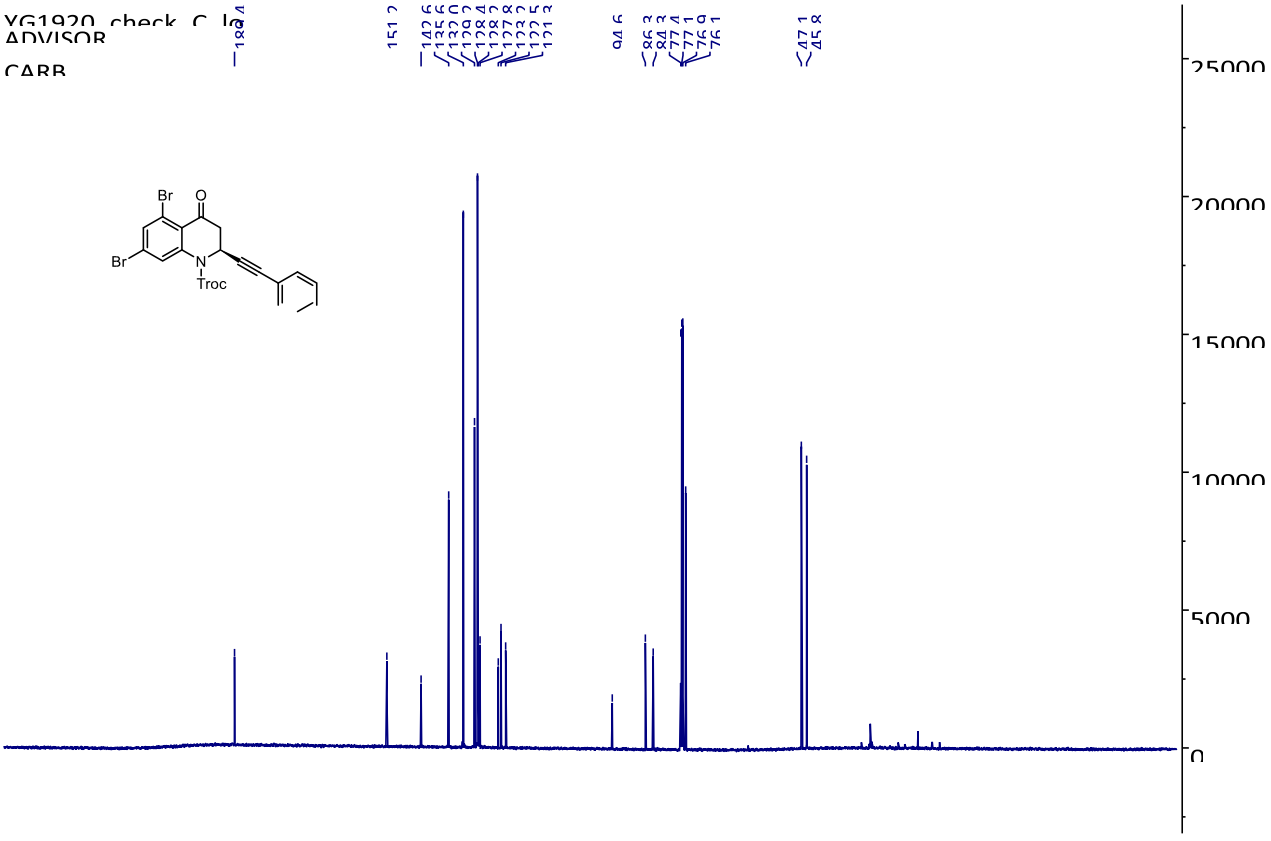
ADVISOR
Br
O
Br
N
Troc

Appendices References

1. Guan, Y.; Attard, J. W.; Mattson, A. E. *Chem.Eur. J.* 2020, *26*, 1742–1747

2. Tarui, S. Kondo, K. Sato, M. Omote, H. Minami, Y. Miwa, A. Ando, *Tetrahedron* 2013, *69*, 1559–1565.

3. Denmark, S. E.; Stiff, C. M. *J. Org. Chem.* 2000, *65*, 5875–5878.

4. Burguete, M. I.; Fraile, J. M.; García, J. I.; García-Verdugo, E.; Luis, S. V.; Mayoral, J. A. *Org. Lett.* 2000, 2, *24*, 3905–3908

5. Hao, E.-J.; Fu, D.-D.; Wang, D.-C.; Zhang, T.; Qu, G.-R.; Li, G.-X.; Lan, Y.; Guo, H.-M. *Org. Chem. Front.* 2019, *6*, 863–867.

6. Denmark, S. E.; Nakajima, N.; Nicaise, O. J.-C.; Faucher, A.-M.; Edwards, J. P. *J. Org. Chem.* 1995, *60*, 4884–4892.

7. Fu, N.; Song, L.; Liu, J.; Shen, Y.; Siu, J. C.; Lin, S. *J. Am. Chem. Soc.* 2019, *141*, 14480−14485.

8. Nolin, K. A.; Ahn, R. W.; Kobayashi, Y.; Kennedy-Smith, J. J.; Toste, F. D. *Chem. Eur. J.* 2010, *16*, 9555−9562.

9. Xiong, H.; Xu, H.; Liao, S.; Xie, Z.; Tang, Y. *J. Am. Chem. Soc.* 2013, *135*, 7851−7854.